

Energy Efficient Operation of Vessels

Analysis of Potential Hybrid Solutions with Li-Ion
Battery System

SET3901: Master Sustainable Energy Technology
Sankarshan Durgaprasad

Delft University of Technology



Energy Efficient Operation of Vessels

Analysis of Potential Hybrid Solutions with
Li-Ion Battery System

by

Sankarshan Durgaprasad

Student Name	Student Number
S Durgaprasad	5459931

Thesis Promoter: Prof. Dr. ir. Marjan Popov
Daily Supervisor: Dr. ir. Aleksandra Lekić
Company Supervisor: ir. Zoran Malbasić
Project Duration: December, 2022 - July, 2023
Faculty: Electrical Engineering, Mathematics and Computer Science, Delft

Preface

I am delighted to present this master thesis, the culmination of my studies in Sustainable Energy Technology at TU Delft. The program has provided a remarkable platform for young energy enthusiasts like myself, fostering a deep understanding of systems integration of Hybrid Power Systems. I express my gratitude to Alewijnse Netherlands for the internship opportunity and support in completing my thesis. Working on real vessels with practical business cases has been an invaluable experience. I thank ir. Zoran Malbasić for his exceptional supervision, expertise in Hybrid Systems, and Power Systems in vessels. I highly recommend Alewijnse as a study destination. I also appreciate Micha Habermehl (Team Lead Hybrid Solutions) for facilitating this collaboration. At TU Delft, I am indebted to Dr.ir Aleksandra Lekić and Prof. Dr. Ir. Marjan Popov for their invaluable guidance. Their supervision and support have been invaluable in exploring my research questions. I extend my deepest appreciation to my family for their unwavering support. This thesis represents countless hours of research, analysis, and reflection. I hope the findings contribute to the field of sustainable energy technology, inspiring further research and innovation in the integration of Hybrid Power Systems. May this work pave the way to a more sustainable and resilient energy future.

Sankarshan Durgaprasad
Delft, July 2023

Summary

This Master Thesis is conducted in collaboration with Alewijnse, a leading maritime systems integrator in the Netherlands. The thesis aims to identify the optimal and cost-effective method of incorporating battery energy storage systems (BESS) into both new and existing DP-2 vessels, as well as DP-3 vessels. The objective is to determine the most efficient battery size and technology, establish the ideal time frame for return on investment, and design a power generation schedule that is ideal for the DP-2 cable laying vessel's power system.

The primary objectives of this research are to optimize the battery system, ensure effective energy system operation, and establish a strong business case. Specifically, the study explores the feasibility of retrofitting a DP-2 vessel that operates in the North Sea and Taiwan with a battery system to create a hybrid system.

To determine the optimal sizing of the battery energy storage system, 12 different battery solutions from two European battery suppliers considering three different fuel price scenarios are analyzed. These solutions encompass a variety of battery technologies, such as High Power or High Energy Li-ion batteries, or a combination of both.

The integration of BESS into vessels offers several operational benefits to operators, including the ability to operate diesel engines at higher or more efficient points of operation to maximize their performance. Battery systems can also act as "virtual generators" during dynamic positioning (DP) mode for DP-2 vessels, reducing fuel consumption, lowering diesel engines ON-time, and decreasing maintenance costs.

However, hybridizing vessels involves more than just integrating an optimally sized battery system. The existing power management system (PMS) and energy management system (EMS) must also undergo upgrades to ensure effective operation. To address these challenges, the BOOSTER (Battery Optimization for Optimal Sizing and Throughput Energy Regulation) methodology, is proposed which incorporates the operation of an optimized management system based on fuel prices and the throughput energy cost of the battery system.

Throughout the research process, a series of sub-questions were developed and addressed to aid in answering the primary research question :

Sub question 1:What is the best mathematical model for optimizing the integration of the BESS into the power system of DP-2 vessels?

Sub question 2:How do different operational profiles impact the sizing requirements of the battery energy storage system (BESS)?

Sub question 3:How does including energy throughput costs in the cost function affect the sizing of the BESS, lifetime, and return on investment?

Sub question 4:Can the existing Power Management System (PMS) and Energy Management System (EMS) be extended to incorporate optimal scheduling of the diesel engine generators and integration of the BESS?

Overall, this research provides valuable insights into developing a methodology for efficient, cost-effective integration of BESS into DP-2 vessels, promoting sustainable energy solutions in the maritime industry.

Contents

Preface	i
Summary	ii
Nomenclature	viii
1 Introduction	1
1.1 Alewijnse B.V Netherlands	2
1.2 Industrial and scientific relevance of this research	3
1.2.1 Research objectives and questions	3
1.3 Report overview	3
2 Literature Review	4
2.1 History of power system in vessels	4
2.2 A systems engineering approach to the IPS (electrical)	6
2.2.1 Electrical power generation system	8
2.2.2 Electrical Power Distribution System	9
2.2.3 Electrical power conversion system	10
2.2.4 Electrical consumers	11
2.2.5 Battery energy storage system	12
2.2.6 Hybrid vessel management systems	14
2.3 Optimum management of vessel power and energy management system	15
2.3.1 Global Planning	15
2.3.2 Marine PMS/EMS Optimisation in Literature	15
2.4 Battery system	18
2.4.1 Battery capacity: high power, and high energy operation	18
2.4.2 Battery longevity	18
2.4.3 Battery technology	23
2.5 Optimal sizing of battery system	25
2.6 Battery Degradation in Optimisation	29
2.7 Optimization of the operation of isolated industrial DG's	31
3 Cable Laying Vessel System	34
3.1 Current system	34
3.2 Hybrid system requested	36
3.3 Proposed BESS sizing and optimal scheduling solution	37
3.3.1 Solution space and key performance matrix	40
4 Data Analysis of Load Profile	42
4.1 Taiwan Sea load profile analysis	42
4.2 North Sea load profile analysis	45
5 MILP Optimization	48
5.1 Model considerations	48
5.2 Decision variables and constants	48
5.3 Objective function	49
5.3.1 FOC cost function	49
5.3.2 Start up cost function	49
5.3.3 Battery throughput cost	50
5.4 Constraints	50
5.4.1 Lower bound and upper bound constraints	50
5.4.2 Inequality constraint	51

5.4.3	Equality constraint	52
5.5	Optimization method	53
6	Results and Discussion	55
6.1	Result : No energy throughput costs	55
6.2	Result: Throughput energy costs - Alewijnse BOOSTER - Battery optimization for optimal sizing and throughput energy regulation	60
6.3	Result: Payback time and years of profitability	62
6.4	Discussion : Research question, best battery solution	65
6.4.1	Best battery solution	65
6.4.2	Sub question 1:	65
6.4.3	Sub question 2:	66
6.4.4	Sub question 3:	66
6.4.5	Sub question 4:	68
6.4.6	Limitations and further work	70
	References	72
	A Definitions	77
	B Research Paper	78

List of Figures

1.1	Alewijnse company logo (left), The Black Pearl hybrid yacht integrated by Alewijnse (right)	2
2.1	Timeline in the key historical milestones of power systems in marine vessels [4]	5
2.2	Steam turbine and segregated power system [5]	5
2.3	IPS and hybrid electric drive [5]	6
2.4	Electrical SLD of a Cable-Laying Vessel	7
2.5	Functional objects belonging to electrical power generation system	8
2.6	SFOC curves of DG 1-5	9
2.7	Functional objects belonging to electrical power distribution system	9
2.8	Functional objects belonging to electrical power conversion system	10
2.9	Functional objects belonging to electrical consumers	11
2.10	Functional objects belonging to battery energy storage system	12
2.11	Ragone Plot : comparison of energy storage technologies [17]	13
2.12	Functional objects belonging to PMS, EMS and BMS	14
2.13	Battery usage	19
2.14	Battery technologies comparison [68]	24
2.15	Risk averse ES sizing [79]	28
2.16	Risk averse ES sizing [21]	28
2.17	Number of cycles as a function of DoD	31
2.18	SFOC curve with maintenance curve - DG 1	32
2.19	SFOC curve with maintenance curve - DG 2	33
3.1	Cable Laying Vessel	34
3.2	SFOC for DG 1-5	36
3.3	Cable laying vessel with BESS	37
3.4	Battery Sizing Model	38
3.5	BOOSTER considerations and output	38
3.6	Proposed BESS sizing solution	39
3.7	Visual description of various solutions	41
4.1	8.5 Months Taiwan load profile	43
4.2	DP mode operation (left- port side, right starboard side)	43
4.3	Auto mode (11) (Operation (left- port side, right starboard side)	43
4.4	NC DP 10 (operation (left- port side, right starboard side)	44
4.5	NC DP 01 (operation (left- port side, right starboard side)	44
4.6	9 Months North Sea load profile	45
4.7	DP mode operation (left - port side, right starboard side)	46
4.8	Auto mode operation	46
4.9	Non-critical mode (01) operation	46
4.10	Non-critical mode (10) operation	47
6.1	Optimized Taiwan results	56
6.2	Percentage of fuel savings per scenario - Taiwan	56
6.3	Optimized Taiwan results	57
6.4	Optimized North Sea results	58
6.5	Percentage of fuel savings per scenario - North Sea	58
6.6	Optimized North Sea results	59
6.7	Impact of including the cost of throughput energy costs	61
6.8	Payback period and years of profitability solutions 1-12	62

6.9	Payback period and years of profitability with and without BOOSTER	63
6.10	Pareto front of all possible solutions	65
6.11	Payback period and years of profitability with and without BOOSTER	67
6.12	SFOC of DG-set in case of parallel loading	68
6.13	Solution 7 lifetime and years of profitability as a function of calendar degradation	71

List of Tables

2.1	Essential vs. non-essential functionalities	11
2.2	Classical and heuristic optimization methods	15
2.3	Summary of optimization methods	17
2.4	Cycle aging of NMC and LFP	21
2.5	List of available batteries in the European maritime industry	22
2.6	Available maritime battery technologies	23
2.7	Review of certain battery sizing methodologies for vessels	27
2.8	Review of existing battery degradation modeling	30
2.9	Coefficient values	32
3.1	Diesel Generator Ratings	34
3.2	Notations based on Bus Tie breakers	35
3.3	Modes of operation	35
3.4	SFOC coefficients	35
3.5	MILP Coefficients for Generator 1-5	35
3.6	Battery solution space	41
4.1	Taiwan DG loading	44
4.2	Event analysis: power	44
4.3	Event analysis: energy	45
4.4	North Sea DG loading	47
4.5	Event analysis : power	47
4.6	Event analysis : energy	47
5.1	Mathematical modelling notations	49
5.2	Parallel loading	52
5.3	Variable limits and constant values	53
5.4	Fuel price per scenario	54
6.1	Taiwan result - no energy throughput cost	55
6.2	Taiwan DG - maintenance	57
6.3	Taiwan DG - running time	57
6.4	North Sea Result - no energy throughput cost	57
6.5	North Sea DG - maintenance	59
6.6	North Sea DG - running time	59
6.7	Solutions summarized (Taiwan + North Sea)	60
6.8	Optimised PMS-EMS strategy	61
6.9	Payback period	64
6.10	Years of profitability	64

Nomenclature

Abbreviations

Abbreviation	Definition
BESS	Battery energy storage system
DG	Diesel engine generator
DP	Dynamic positioning
DoD	Depth of discharge
ETC	Energy throughput costs
ESS	Energy storage systems
EMS	Energy management system
GHG	Greenhouse gases
HTS	High-Temperature superconducting motor
ISA	International standard atmosphere
IC	Internal combustion
IPS	Integrated power system
IM	Induction motor
kW	Kilo Watt
kWh	Kilo Watt Hour
MGO	Marine gas oil
MSB	Main switch board
MTBO	Minimum time before
NC	Non critical
PM	Permanent magnet
PMS	Power management system
ROI	Return on investment
RPM	Revolutions per minute
SLD	Single line diagram
SFOC	Specific fuel Oil consumption
SOC	State of charge

1

Introduction

As of 2018, the maritime industry is responsible for 1056 million tonnes of CO_2 in greenhouse gas emissions [1]. Compared to the 962 million tons of CO_2 generated in 2012, this is a 9.3% increase. Shipping emissions as a percentage of all anthropogenic emissions have grown from 2.76% in 2012 to 2.89% in 2018. The aim of the worldwide public to minimize greenhouse gas emissions has a significant impact on the design and operation of transportation infrastructure today. To counteract this, the IMO's Marine Environment Protection Committee (mEPC72) adopted the inaugural IMO plan to minimize GHG emissions from international shipping as a resolution in 2018. This IMO strategy describes a broad vision for decarbonization, GHG reduction targets through 2050, a list of short-, mid-, and long-term actions to accomplish these targets, obstacles to attaining the targets and supportive actions to overcome them, and criteria for future assessment. It will be updated in 2023 and reviewed in 2028 [2]. These strategies aim to,

1. Reduce at least 40% of the carbon intensity by 2030 and 70% by 2050 with respect to the 2008 levels
2. A GHG reduction of 50% by 2050 compared to the levels of 2008
3. Pursue to phase out GHG emissions in line with the Paris agreement temperature goals

Even though there are regulations in place to force marine enterprises to cut their global emissions, attempts to make the industry more sustainable are still centered on improving energy efficiency in an effort to cut costs and increase profits. To take this into account, several technologies have been created [3]. Namely,

1. Ship design : The use of marine engines and power trains with high efficiency is one example of a technical technique to cut fuel usage. The evolution of the integrated power system over time serves as an illustration of the development of power trains.
2. Alternative fuels : Since LNG emits significantly fewer sulphur and nitrogen oxides than traditional fuels, it is the preferred fuel for replacing traditional fuels used in shipping today. However, the bigger storage areas needed for LNG fuels currently prevents their widespread use.
3. Operational measures : Implementing a range of operational techniques can result in an effective and long-lasting decrease in the amount of fuel used by ships and an overall improvement in operational efficiency. High capacity and resource utilization, as well as accurate communication amongst shipping organizations for effective route planning, are some of these. An additional strategy for improving ship efficiency is to shorten port turnaround times.
4. Inclusion of battery energy storage system (BESS): The use of batteries on ships can serve a variety of utilitarian purposes. While batteries can fully power a vessel for a brief period of time or travel, the primary goal is frequently to increase performance and energy efficiency across the board. Batteries can be utilized for a variety of tasks, including spinning reserve, peak shaving, load optimization, instantaneous power, energy harvesting, and backup power.

Along with political uncertainty, there are also economic and technical concerns. Economic uncertainties are linked to fuel and electricity prices that have an impact on investments and operational

measures, whereas technical uncertainties are related to how quickly emerging technologies are evolving. When making judgments about the specifications for both newly built and existing vessels, it is currently crucial to take prospective modifications and developments into account due to the long lifespan of vessels.

The purpose of this project is to create a hybrid system solution based on the load profile of the ship in Taiwan and the North Sea for a Cable-Laying Vessel. The work was done in collaboration with Alewijnse, a leading maritime systems integrator in the Netherlands, for a Master's thesis at the Delft University of Technology. The "Cable Laying Vessel" is designed specifically for the installation of cable lines underwater. However, a Cable Laying Vessel is also utilized as a research vessel to keep track of numerous events in the ocean and sea waters since cable-laying activity does not occur continuously throughout the year. These vessels are equipped with dynamic positioning and tracking technologies, which allow them to precisely locate their location in the middle of the ocean and install the proper underwater cable connections. Cable laying vessels have DP-2 class requirements that ensure redundancy such that no single point of failure in an active system shall cause the system to fail/loss position. The same requirements are valid for DP-3 vessels.

1.1. Alewijnse B.V Netherlands

Alewijnse is an all-round systems integrator that works closely with its customers to provide a comprehensive range of technical solutions. These solutions encompass various areas such as electrical installations, power distribution, generation and propulsion systems, process automation, audio video and IT, safety and security, and navigation and communications.

Alewijnse undertakes numerous electrification and automation projects each year across different sectors including yachting, naval and governmental, dredging, offshore, and industrial. These projects cover a wide range of activities such as new builds, refits, and repair and maintenance tasks. In the industrial segment, Alewijnse specializes in specific areas such as drinking water, geothermal energy, food, and manufacturing.

The primary goal of Alewijnse is to continuously enhance the value for its employees and customers by fostering progress and acting as a technology partner that engages in collaborative thinking from the initial stages to project completion.

By striving to develop and enhance innovative, sustainable, and high-quality electrification and automation solutions, Alewijnse aims to make a significant contribution to the success of projects in the maritime and industrial sectors.



Figure 1.1: Alewijnse company logo (left), The Black Pearl hybrid yacht integrated by Alewijnse (right)

1.2. Industrial and scientific relevance of this research

Alewijnse plans to equip a cable-laying vessel with hybrid technology in response to a customer's request. The aim is to install two energy storage systems on the vessel to reduce the number of active diesel engine generators (DG) required for redundancy during DP mode. Additionally, the DG's operating point is optimized through mixed integer linear programming (MILP). The batteries are sized according to the operational profiles of the cable-laying vessels in Taiwan and the North Sea. As a system integrator, it is beneficial to have a list of solutions that can be compared based on their optimal results. Therefore, twelve different battery energy storage systems are analyzed considering three different fuel price scenarios, and the PMS-EMS is optimized. Then, the best system goes through the BOOSTER, where the optimum PMS-EMS management considers the energy throughput costs of the battery and the fuel price during its operation. The results are presented and discussed.

1.2.1. Research objectives and questions

The goal of this master's thesis research is to address the following questions,

What is the most effective methodology for determining the ideal battery size, technology, and accurate return on investment timeframe while considering battery degradation? How can we create an optimal power generation schedule for the cable laying vessel's power system?

The **primary research question** that this thesis seeks to address is:

What is the most suitable methodology for integrating battery energy storage systems (BESS) into existing and new-build DP-2 vessels in the most cost-effective manner?

The following sub-research questions have been developed to help address the primary research question:

Sub question 1: What is the best mathematical model for optimizing the integration of the BESS into the power system of DP-2 vessels?

Sub question 2: How do different operational profiles impact the sizing requirements of the battery energy storage system (BESS)?

Sub question 3: How does including energy throughput costs in the cost function affect the sizing of the BESS, lifetime, and return on investment?

Sub question 4: Can the existing Power Management System (PMS) and Energy Management System (EMS) be extended to incorporate optimal scheduling of the diesel engine generators and integration of the BESS?

1.3. Report overview

This report is structured as follows:

- **Chapter 2:** Provides the review of literature and current trends. The focus of this chapter is primarily on the history, optimal management of the vessel's management system, battery system optimization, degradation of the battery system, and the maintenance costs associated with the DG system.
- **Chapter 3:** Explains the vessel system that the project is addressing and the potential solution space.
- **Chapter 4:** Data analysis of load profile investigates the load profiles for different operational conditions for the North Sea and Taiwan.
- **Chapter 5:** Formulation of the MILP problem.
- **Chapter 6:** Produces the results and answers the research questions posed.

2

Literature Review

The objective of this chapter is to present a comprehensive literature review on the topic of electrical power systems in vessels. It begins by discussing the background and importance of power systems in maritime operations in Section 2.1. A systems engineering approach to various components that comprise an integrated power system, their functions, and how they work together for efficient and reliable power supply is described in Section 2.2. The focus then shifts to the planning and optimizing vessel PMS through global optimization techniques in Section 2.3. The current battery systems available in the European maritime industry are discussed in Section 2.4, which serves as a solution space for the optimization problem. The various optimization techniques used to determine the optimal battery size for maritime vessels and their advantages and limitations are discussed in Section 2.5. The degradation of battery systems cannot be ignored in optimal battery sizing, and the literature on incorporating battery degradation into the optimization process is reviewed in Section 2.6. Finally, the optimization of the operation of diesel engine generators concerning maintenance is discussed in Section 2.7.

2.1. History of power system in vessels

Vessels can be classified not only based on their functionality but also based on the type of power system they have onboard. The primary propulsion engines, backup generators, and auxiliary systems like lighting, heating, and air conditioning are all powered by a ship's power system. Along with maintaining, monitoring, and troubleshooting the ship's electrical equipment, the ship's power system also complies with safety and environmental rules.

After German inventor Moritz Hermann Jacobi installed simple battery-powered direct current (DC) motors on test boats in the late 1830s, the first known attempt to employ electricity on a vessel is thought to have occurred. The most recent development includes the world's first fully electric battery-powered ferry for cars and passengers in 2015. Additionally, in 2015 wireless power transfer was in function [4]. Figure 2.1 shows the key milestones in the development of the power system in the maritime industry.

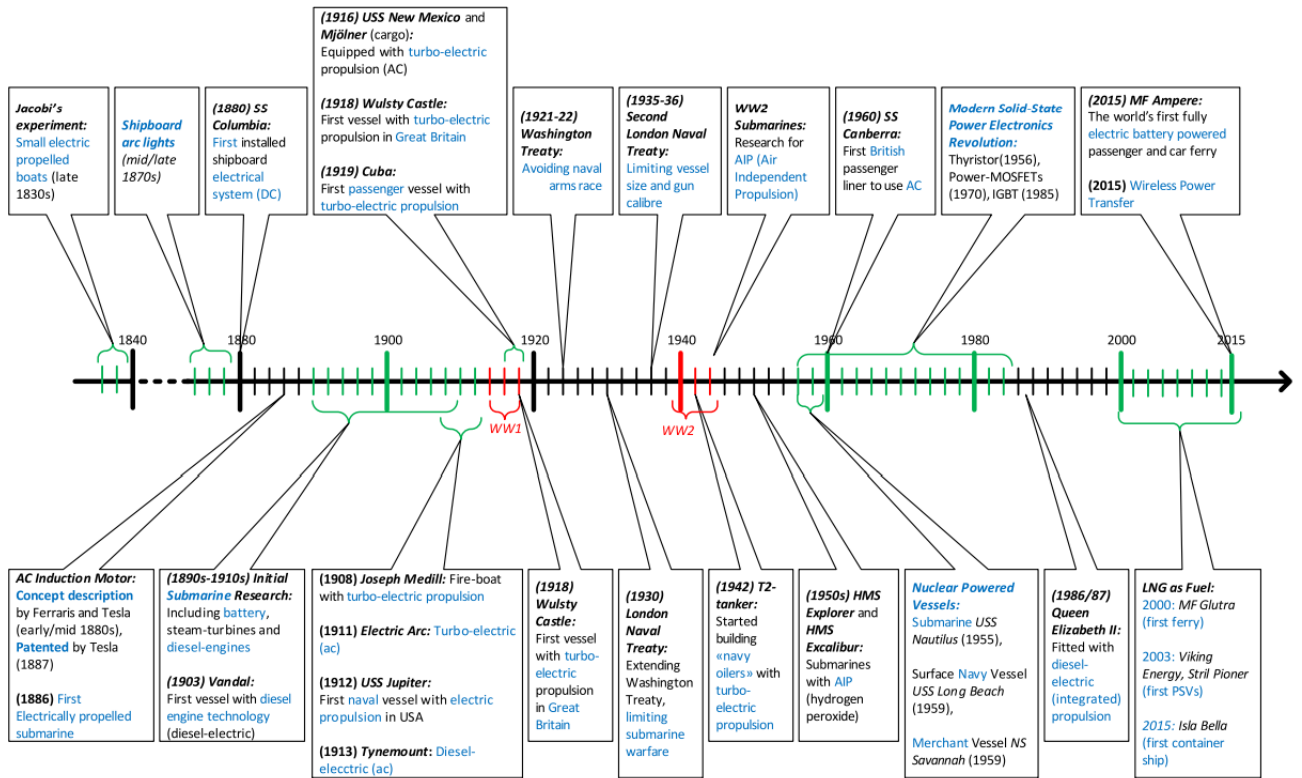


Figure 2.1: Timeline in the key historical milestones of power systems in marine vessels [4]

A brief discussion on electric ships past, present, and future has been presented in [5]. In the past, ships used steam turbines instead of internal combustion engines for better power, smaller engines, and lower maintenance costs. [6]. As a result, there was more room on board for cargo, passengers, and fuel. Ship propulsion and power systems substantially transformed with the switch from steam engines to internal combustion (IC) engines. Greater fuel efficiency, quick start-up times, and lower labor needs are the benefits of IC engines. The demand for a sizable generating plant to power electrical loads and a high-power propulsion plant, resulted in a segregated power system, the drawbacks are discussed in [5]. Figure 2.2 illustrates the schematic of these two systems.

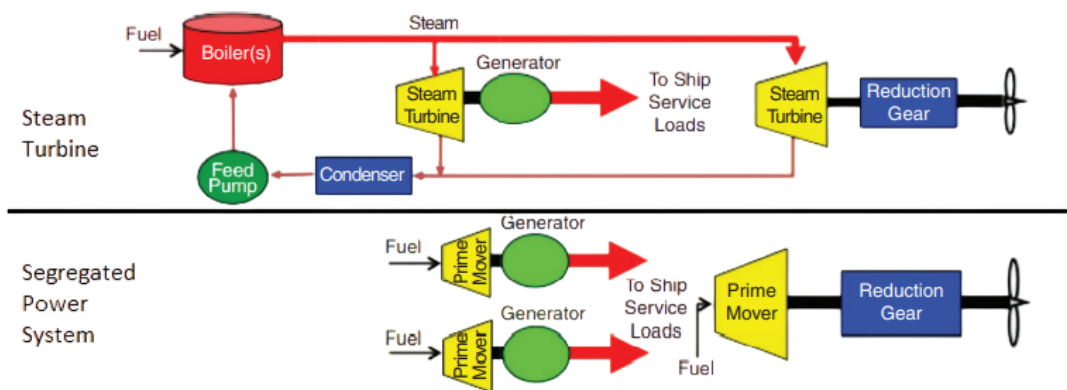


Figure 2.2: Steam turbine and segregated power system [5]

Since the advent of huge multi-megawatt motor drives in the late 1980s, electric power production, everyday service loads, electric propulsion, high-energy weaponry, and high-power sensing devices have all been handled by a new integrated power system (IPS). To supply electrical loads and propulsion

with a single set of generators, variable frequency drives were developed. This is seen in figure 2.3. Compared to traditional ship mechanical propulsion systems, the IPS has lower noise, higher survivability, fewer prime movers, reduced fuel consumption, and enhanced overall arrangement convenience [7]. A technical and financial analysis of a mechanical driveline and IPS for DD-21 Vessel is presented in [8], indicating a reduction of \$12.8 million in ship acquisition cost and a 24% reduction in fuel costs compared to a comparable mechanical driveline.

Electrical power generating system, electrical power distribution system, electrical power conversion system, electric propulsion system, energy storage system (ESS), and power management system (PMS) are examples of common IPS subsystems.

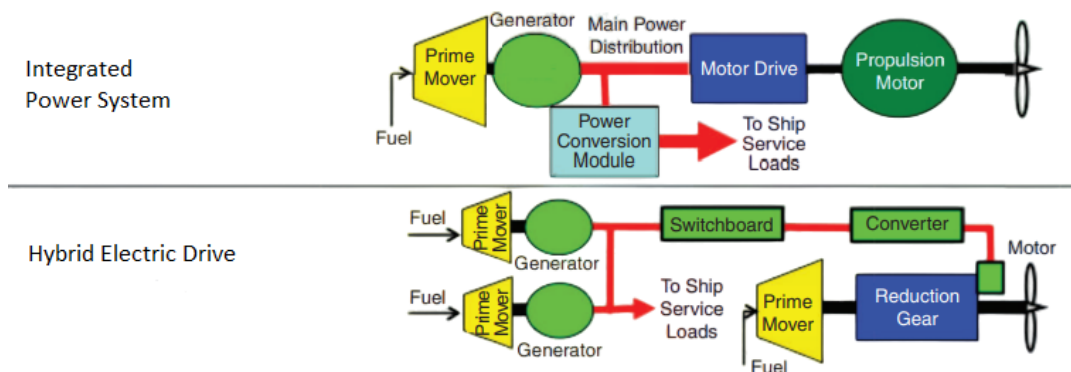


Figure 2.3: IPS and hybrid electric drive [5]

The hybrid plant is a variant of the IPS concept, often known as the power take-in/power take-off design. The same motor used for mechanical propulsion may also power electrical loads in this hybrid system, which blends mechanical and electric propulsion methods. This is seen in figure 2.3.

2.2. A systems engineering approach to the IPS (electrical)

A functional object is an element of a larger system that carries out a certain task or function in systems engineering. It may also be known as a "system component," "system part," or "system element". Similarly, "subsystem" or "module" are terms used to describe a collection of functional items or parts that operate together to accomplish a certain function or goal. A subsystem or module is a group of useful things intended to communicate with one another and collectively contribute to the general operation and behavior of the bigger system [9].

The different IPS subsystems and functional components are covered in this section. An IPS example is used in figure 2.4 to help with system understanding. Electrical power plants with DG's are divided into different power buses (3 in the case of figure 2.4) to accommodate varying operational profiles and power demands. This enables safer and smarter operation of these ships during critical operations. Such ships are called Dynamically Positioned (DP) Vessels, which are involved in operations deemed "safety critical" and are subjected to large variations in loads acting on the vessel, including waves, wind, ocean currents, ice, etc.

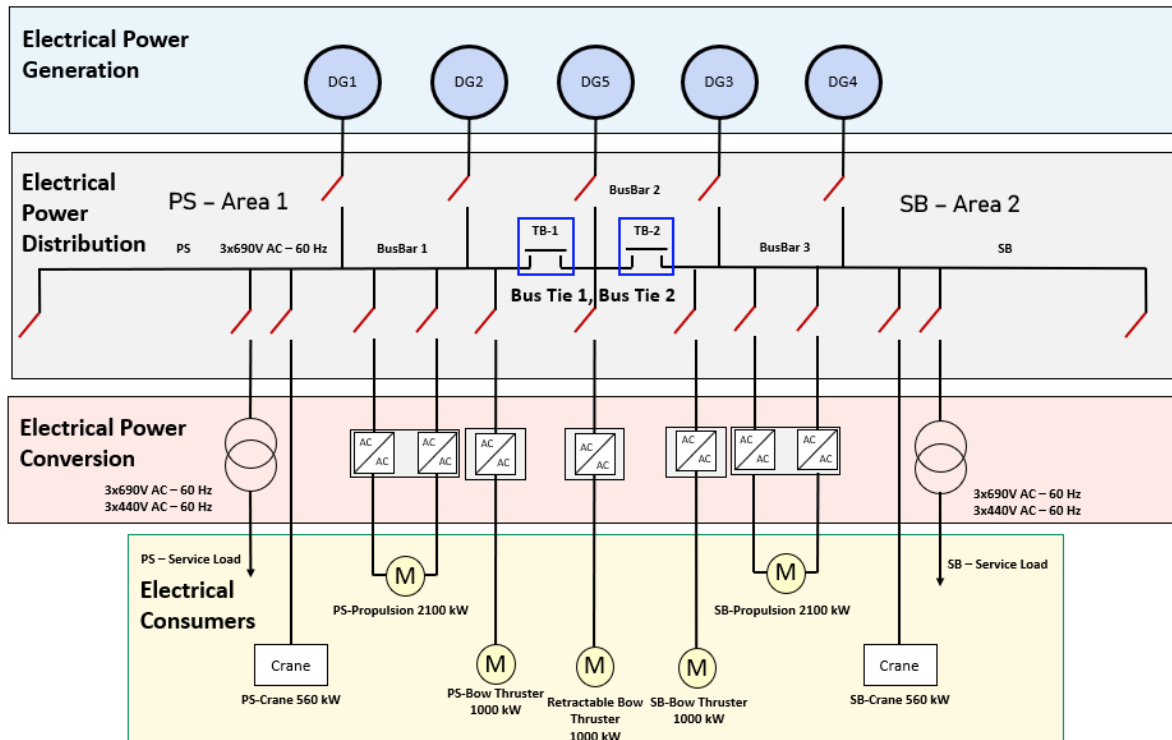


Figure 2.4: Electrical SLD of a Cable-Laying Vessel

The single line diagram (SLD) belongs to a cable-laying vessel. The IPS is divided into five subsystems with various functional objects for this discussion. These are:

1. Electrical power generation system
2. Electrical power distribution system
3. Electrical power conversion system
4. Battery energy storage system
5. Electrical consumers

In addition to this, there are three other management "subsystems" or "modules" in the scope of discussion. These are:

1. Power management system
2. Energy management system
3. Battery management system

A comparison between the technical characteristics between a first-generation IPS and a second-generation IPS is made in [7]. According to this characterization, the above SLD represents a first-generation IPS due to the lack of battery energy storage and AC distribution systems.

2.2.1. Electrical power generation system

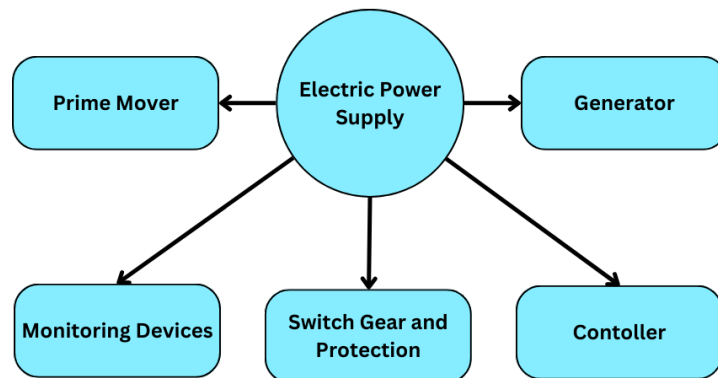


Figure 2.5: Functional objects belonging to electrical power generation system

The electrical power generation system consists of several generators propelled by a diesel engine as the prime mover, see figure 2.5. Diesel engines use heavy fuel oil (HFO) or diesel and are practical for medium- to high-speed vessels, while gas engines are better for high-speed ships. The system includes monitoring tools, switchgear, protection, and other components. The vessels must have a consistent source of power, thus numerous power production units—typically diesel engines—are used to improve the system’s overall functionality, flexibility, and efficiency. The ideal fuel usage factor for a diesel engine is 40%. This suggests that the remaining energy is wasted as heat or exhaust. [10].

Diesel Engines today can be broadly classified into three categories:

1. Operation cycle - Two-stroke or Four-stroke engine
2. Speed -
 - (a) Slow speed (0 to 300 rpm) - The most powerful engines are two-stroke and low-speed engines
 - (b) Medium speed (300-1000 rpm) - Modern engines with four-stroke cycles have a maximum operating speed of 500 rpm
 - (c) High speed (1000 rpm +)
3. Construction - Trunk, opposed-piston, or cross-head

The most common large diesel engines are two-stroke, low speed and cross-head engines.

The specific fuel oil consumption (SFOC) is the metric that best characterizes the quality of the engines. This index indicates the least fuel an engine consumes per kW per hour, kg, or L per kWh. A diesel engine’s actual fuel consumption depends on the load it is under and is not constant. Most engines are built and engineered to use no more than 80% of their rated power in fuel oil [11]. Figure 2.6 shows the specific fuel consumption of the five Diesel Engine Generators of figure 2.4. The fuel used by the DE is Marine Gas Oil (MGO).

The SFOC of a diesel engine can be represented as a second-order polynomial [12]. This is of the form

$$f(p) = (a \times p^2) + (b \times p) + c, \quad (2.1)$$

where $a, b,$ and c are constants. Polyfit function on MATLAB can be used to return the coefficients for a polynomial $p(x)$ of degree n , which is the best-fit [13]. This results in the curves shown in the first

subplots of of figure 2.6.

Alternatively, the SFOC curves can also be modeled based on the L/hr consumption. This can be represented in a linear equation in the form of:

$$f(p) = (a \times p) + (b), \tag{2.2}$$

where a and b are constants, and p is the generated power.

This equation results in the SFOC curves of the bottom three subplots in figure 2.6.

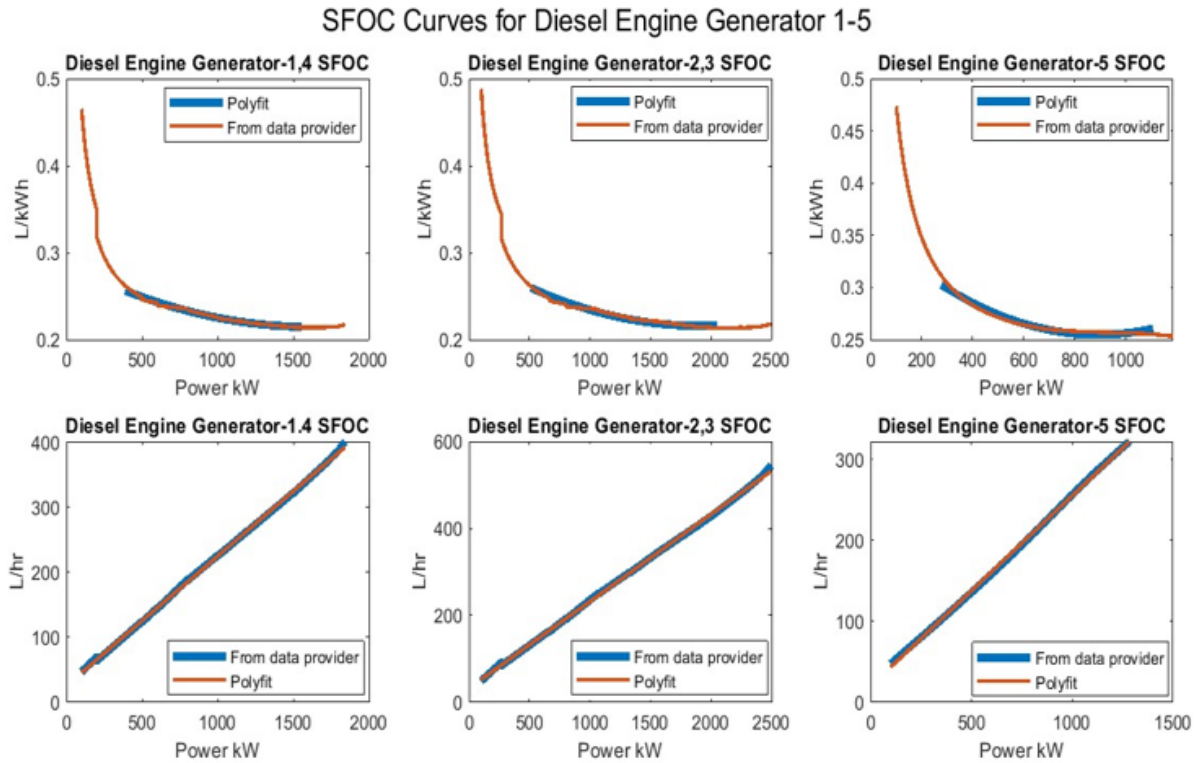


Figure 2.6: SFOC curves of DG 1-5

2.2.2. Electrical Power Distribution System

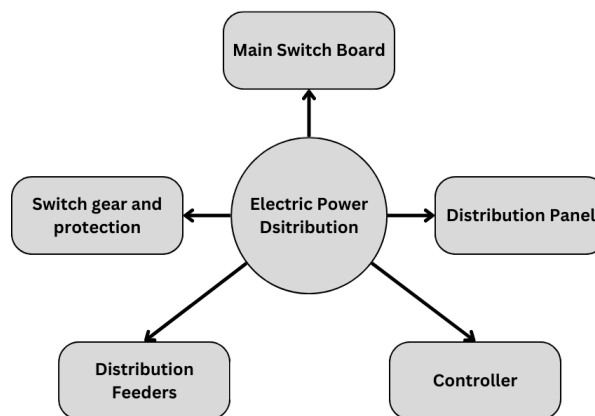


Figure 2.7: Functional objects belonging to electrical power distribution system

The typical electrical power distribution system in a vessel can be categorized into four main parts (see figure 2.7):

1. Switchboard
2. Distribution panel
3. Distribution feeders
4. Switchgear and protection

As per [14], switchboards on ships are responsible for supplying electricity to different locations while ensuring safety regulations. These systems can be categorized as AC or DC switchboards. The study compared a 690 V-AC (LVAC) switchboard and a 1000 V-DC (LVDC) switchboard and found that LVDC switchboards reduced emissions by 9.2% per type of gas and saved 592 tons of fuel annually for the specified operational profile. Moreover, the LVDC architecture decreased weight by 1.1 tons and 3.8 m³. However, the cost of implementation and protection aspects were not discussed.

The main switchboard (MSB) supplies high-power loads, while lower-powered devices may be connected to the distribution board. The distribution panel is responsible for organizing, protecting, and controlling circuits in a particular area or segment of the ship. Distribution feeders deliver electricity from the primary distribution source to various loads or customers within a specific zone or area. To function safely and reliably, switchgear must control, safeguard, and isolate circuit breakers, switches, and other electrical equipment. Relays act as protection devices that detect abnormal power system conditions and take necessary steps to protect the system from potential harm or risks.

2.2.3. Electrical power conversion system

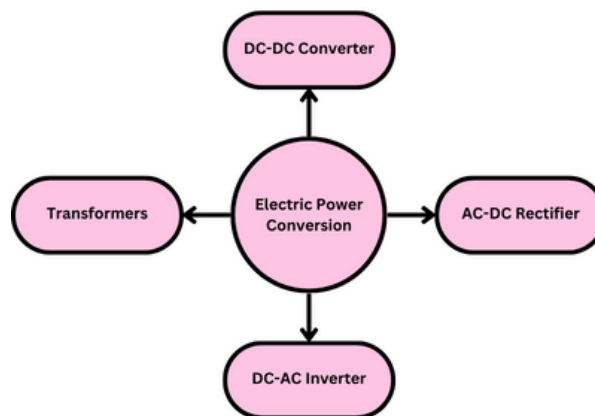


Figure 2.8: Functional objects belonging to electrical power conversion system

The main functional objects of the electrical power conversion system are provided in figure 2.8. Energy conversion, frequency control, and power conditioning are among the many tasks that this system is responsible for. The frequently used converters onboard and for cold ironing are summarised by [10]. These include,

- Current source inverter
- Thyristor rectifier
- Cyclo-converter
- Voltage source inverter
- Single phase converter
- Active front end
- Multilevel inverter

Work [15] presents a thorough analysis of the current onboard and cold ironing power conversion methods available. The categorization is based on the power, switching frequency, voltage, quantity of switches, and soft switching. Each conversion configuration's benefits and drawbacks are also listed. It was discovered that IGBT switches were the most often utilized components in power electronic converters.

A power transformer is crucial to the distribution and conversion systems because it separates various components of the electrical power system and supplies loads with the proper voltage level. In certain ships, it is also employed as a phase-shift transformer to reduce the bulk of current harmonics produced by frequency converters in various loads, such as the propulsion system. Reducing current harmonics helps decrease voltage distortion for generators and other connected loads at the point of common coupling (PCC).

2.2.4. Electrical consumers

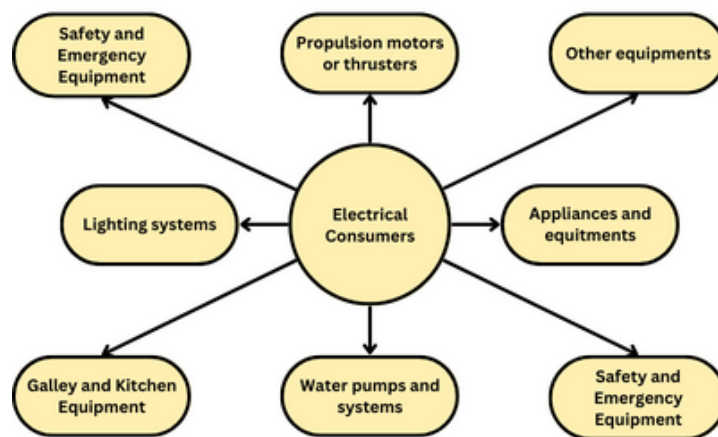


Figure 2.9: Functional objects belonging to electrical consumers

Figure 2.9 provides the functional objects of the electrical consumer system. A wide variety of electrical loads exist, as shown in the figure. These loads can also be divided into service loads and propulsion loads. The most frequent propulsion loads include shaft propulsion, which comes in various power ranges, commercial azimuth thrusters, and cushioned propulsion (1–25 MW) [10]. Service loads include things like lighting, air conditioning, and refrigeration. The most predominant loads in a vessel are the propulsion loads. In addition to this classification, loads can be broken down into essential and non-essential categories; see table 2.1.

Table 2.1: Essential vs. non-essential functionalities

Essential	Non-essential
Alarm	Air conditioning system
Steering gear	Refrigeration
DP System	Purifiers
Navigation system	Some lighting

Certain loads become essential during DP mode due to safety regulations.

The electrical power from the distribution board is converted by converters and transmitted to a propulsion module, such as a motor. A drive based on IGBT or IGCT power electronic modules makes up an electrical device of the first generation of electrical power modules (EPM). An EPM of a later generation

employs permanent magnet (PM) or HTS motors to improve upon the conventional IM. Such motors use SiC power electronic modules or IGBTs as propulsion drivers [7].

2.2.5. Battery energy storage system

As shown in figure 2.10, the BESS is made up of a variety of functional components, including battery modules, a BMS, monitoring tools, and more. Among these components, the battery module is the primary focus of this section.

Utilizing energy storage to increase ship efficiency and lessen environmental effects has become more popular in the maritime industry. The first-generation integrated power system (IPS) depicted in figure 2.4 does not include any BESS, whereas the second-generation incorporates storage technologies.

An overview of state-of-the-art energy storage technologies is presented in [16], where different storage technologies are analyzed, including

1. Battery Storage Technologies
2. Flywheel Technology
3. Supercapacitor Technology
4. Thermal Energy Storage

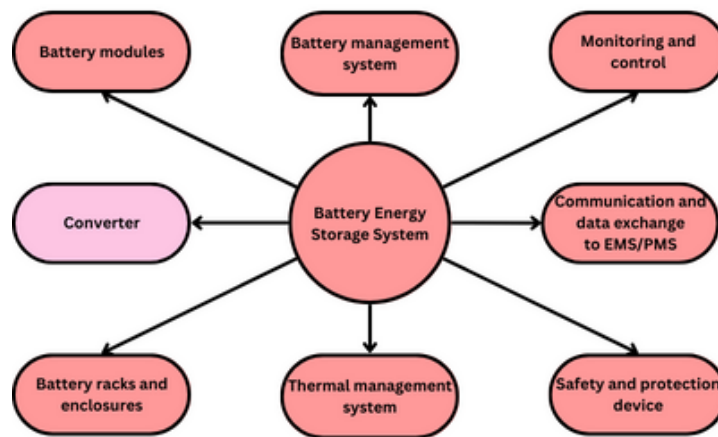


Figure 2.10: Functional objects belonging to battery energy storage system

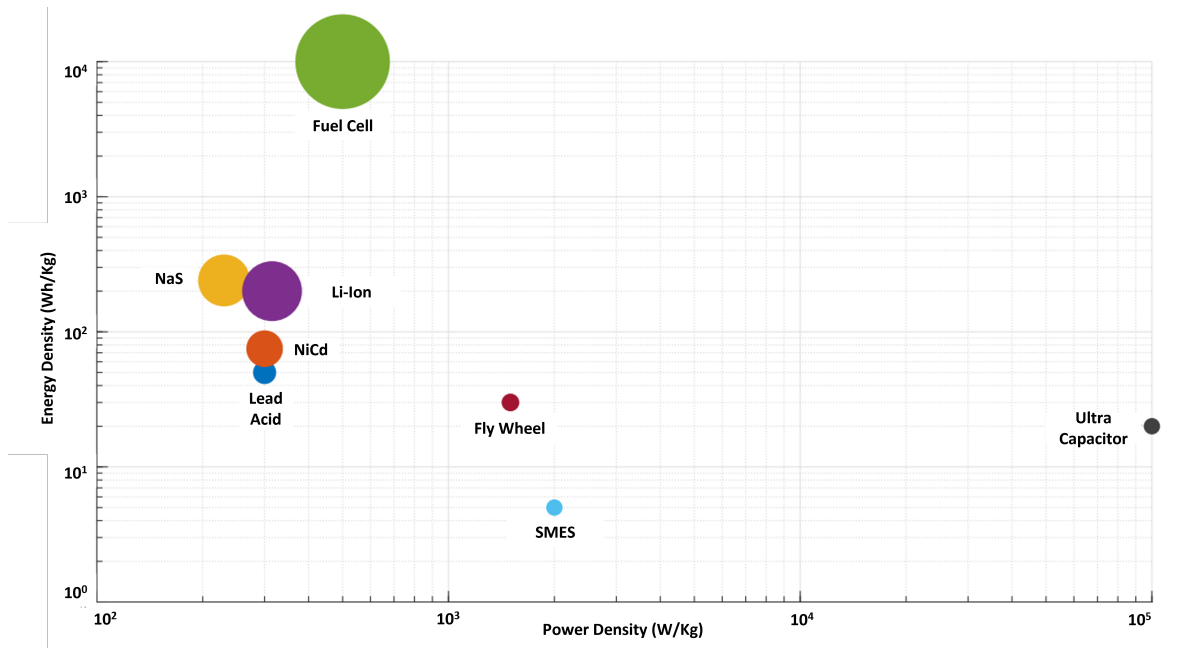


Figure 2.11: Ragone Plot : comparison of energy storage technologies [17]

Flow batteries aside, Lithium-ion batteries are known to have the highest energy density compared to other battery types like Lead-acid, Nickel-based, or Sodium-Sulfur batteries, as detailed in [18]. The maximum gravimetric and volumetric densities are obtained in Nickel Manganese Cobalt Oxide (NMC) and Nickel-Cobalt-Aluminum Oxide (NCA) batteries. When the European Maritime Safety Agency (EMSA) hired DNV GL to do research on electrical storage systems in 2018, it was discovered that Li-ion batteries cost between \$500 (456.61 € as of Monday 3rd July, 2023) and \$1,000 (91.32 € as of Monday 3rd July, 2023) per kWh, not including installation and converter expenses [19].

For a comprehensive review of energy storage systems for vessels, refer to [17]. Figure 2.11 provides a visual representation of various storage technologies energy and power densities, demonstrating that different technologies have complementary advantages. This opens up the potential to combine two storage devices and create more reliable and resilient systems, known as hybrid energy storage systems.

Hybrid energy storage systems, such as battery - ultra capacitor and battery-flywheel systems, are frequently used because of the unique abilities of capacitors and flywheels to absorb high power transients, combined with batteries acting as longer-term energy storage solutions. This information is highlighted in [17]. Additionally, the literature suggests that batteries and fuel cells hold promise. However, hydrogen storage at cryogenic temperatures has not yet reached a maturity level suitable for industry-wide implementation.

2.2.6. Hybrid vessel management systems

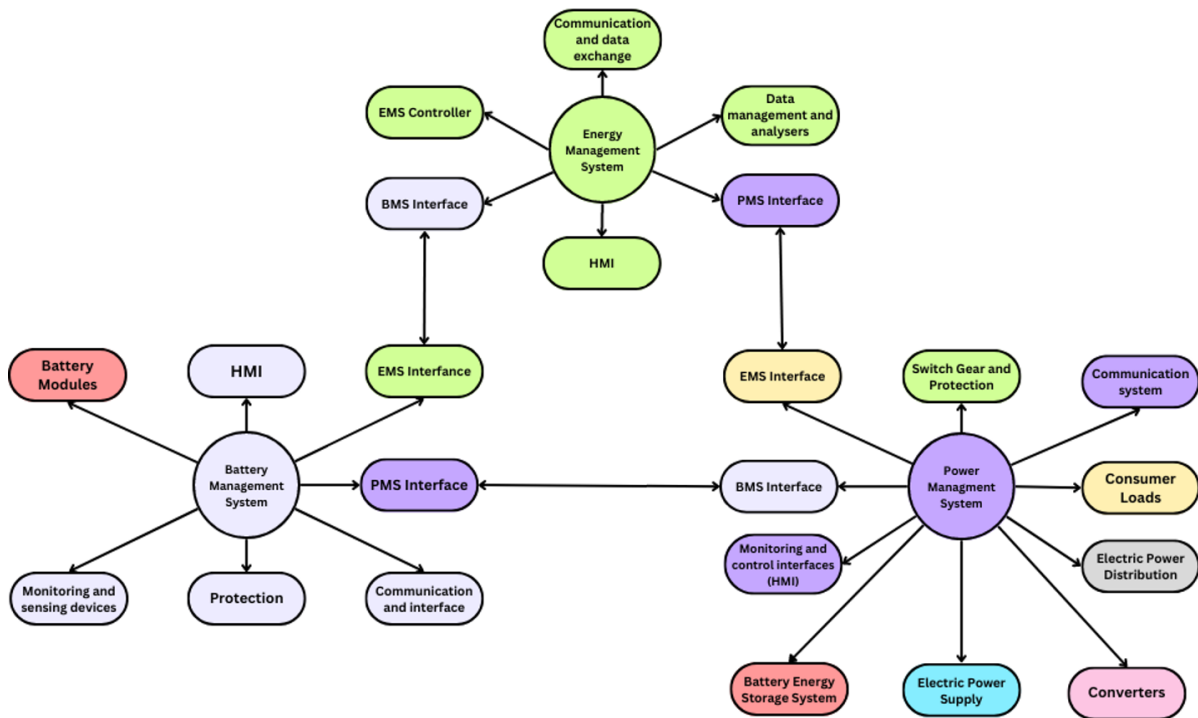


Figure 2.12: Functional objects belonging to PMS, EMS and BMS

Figure 2.12 illustrates the various operational components of the hybrid vessel management systems, including the PMS, EMS, and the BMS. While each system operates independently, they rely on feedback from one another to function effectively.

The primary power management (PMM) module of a first-generation IPS performs tasks including modifying the system's power flow and monitoring and controlling the power system. A second-generation PMM is capable of system analysis, energy storage (ES) management, security management, optimal power flow management, and these features. PMM examples include the PMA300 from Siemens and the PMS800 from ABB.

A ship's energy management system tries to cut energy use and increase overall efficiency. This system aims to minimize energy waste, slash fuel consumption, and lower operating expenses by efficiently monitoring and regulating energy usage across various systems and equipment. It provides real-time monitoring and analysis of data on energy usage, allowing ship operators to identify energy-intensive activities and put preventative measures in place to increase effectiveness. By reducing greenhouse gas emissions and ensuring regulatory compliance, an energy management system also contributes to environmental sustainability. The maritime industry may enhance its reputation as an environmentally responsible sector by increasing its energy efficiency while prioritizing safety and dependability through the early detection of system issues.

2.3. Optimum management of vessel power and energy management system

The PMS, is a set of operations, scheduling algorithms, and control tactics used to effectively distribute power among various energy sources and guarantee a constant supply of electrical power under various load scenarios. Its goal is to build an integrated energy system that is dependable, cost-effective, and efficient. Hybrid vessel power systems are becoming more necessary due to the increased usage of electric ship propulsion, giving PMS a platform to evaluate ships' economic and environmental performance. However, the added complexity makes it challenging to research and implement.

Rule-based and optimization-based approaches are categories of the PMS/EMS research already done [20]. Rule-based PMS/EMS relies on human judgment, predefined goals, and priorities, but optimization approaches are becoming increasingly common since they can produce more effective results.

2.3.1. Global Planning

From [21], it is clear that a vessel's maximum maneuverability demand can lock up to 90% of its available power. DG's are typically used in conjunction to provide the highest level of dependability. Typically, their points of common coupling are physically apart and include separate circuit breakers. See figure 2.4. Running DG's at low loads for reliability often results in inefficiency because the operation points tend to be above medium load. See figure 2.6. This leads to increased fuel consumption and costs.

The effectiveness and dependability of maritime vessels can be increased using an onboard BESS. The BESS may function as a versatile tool in the system design, enabling improved fuel efficiency while yet retaining dependability. In the case that one of the online generators fails, the BESS can temporarily supply electricity until another generation can be synchronized to take its place. This enables a more effective operation plan for the engine generators without compromising dependability.

The authors of [22] have categorised global planning as shown in Table 2.2.

Table 2.2: Classical and heuristic optimization methods

Method	Type	Reviewed
Classical Optimization	Dynamic Programming	Yes
	Linear Programming (LP)	Yes
	Non-Linear Optimization (NLP)	Yes
	Mixed Integer Non Linear Programming (MINLP)	Yes
	Interval Optimization	Yes
	Branch and Bound	Yes
	Adaptive Multi Clustering Algorithm	No
Heuristic Methods	Genetic Algorithm and NSGA-II	Yes
	PSO	Yes
	Improved Sine Cosine Algorithm	Yes
	Whale Optimization, Salp Optimization, Differential evolution, Grey Wolf Optimization	No

2.3.2. Marine PMS/EMS Optimisation in Literature

1. **LP:** The authors of [23] chose load-dependent start tables by optimizing a cost function based on fuel usage, the vessel's load profile, and the likelihood of blackouts. In contrast to the majority of prior publications, the authors present comprehensive requirements for the safe functioning of the DG's in DP mode. Battery system optimization is not carried out. Another example of LP can be observed in [24].
2. **NLP:** In [25], a power flow technique is applied to optimize the vessels EMS using BESS. The work focuses on the system's active and reactive power restrictions. Additionally, when AC loads

are present, converter restrictions are also considered. Unlike most other papers, [25] splits the operational load profile into various operating modes, including DP mode.

3. **MILP:** An optimized decision-based model for determining diesel-electric machinery in the conceptual stage ship design is presented in [26]. The Branch and Bound technique (BAB) is used to tackle the MILP problem of designing the objective function to determine the ideal size of the DG. The issue was resolved for various operating states, including the harbor, transit (supply and towing), DP (standby low and high), anchor handling, and condition for pulling bollards. This provides information on the methods used to determine the ideal diesel engine size, which may also be expanded for BESS. The BAB technique further linearizes the optimization issue by using SFOC values between two adjacent locations and weight variables to get a linear approximation of the engine load. The Authors of [27] also perform MILP-based optimization for a DP vessel, considering different battery sizes, interest rates, and splitting operational profiles.
4. **MINLP:** Research on the efficient planning and operation of a ship, as well as determining the appropriate battery size needed, has been studied by [28]. The cost function created is based on a mixed integer nonlinear programming issue and is designed to reach an optimal operation. An ESS is considered for this system. A two-step multi-objective management model has been devised in [29]. To meet the needs of the high power and energy requirements, hybrid energy storage system (HESS) is utilized. The initial phase of management optimizes the DG and HESS's financial dispatch. Solving a MO-MINLP is required in this phase. In the second stage, the high-power and energy needs of the HESS are divided, and the storage system's lifespan is maximized. To balance the load demand and use the battery as a spinning reserve, this is accomplished by constantly switching the high-power storage system between charging and discharging modes. The depth of discharge, maximum charge, and discharge power limitations are addressed as an NLP optimization in the second stage.
5. **Dynamic Programming:** Dynamic programming was used by the authors of [30] to achieve fuel savings through generator, speed, and distance traveled optimization. Economic dispatch is carried out using the Lagrange technique. This approach does not require an ESS because propulsion motors are used to optimize the DG. For example, signals are sent to the propulsion motors to enhance production and to absorb more power if the DG's are not operating at their best. In the case of DG's running at higher operation points, the opposite is done. In [30] the optimal power is reached by varying the ship's speed. However, this work also involves the inclusion of a BESS. A multi-objective mathematical programming (MOMP) model is formulated in [31] to obtain the optimized energy dispatch scheme while the emissions, energy balance, and technical constraints are taken into account.
6. **Particle Swarm Optimization:** Similar to [28] PSO is used to optimise the objective function in [32]. Economic and pollution optimization for cruise ferries with PV panels is performed due to the repetitive nature of voyages between ports, data is used to predict future loads. Due to the repetitive nature of voyages between ports, data is used to predict future loads more easily. Fuel consumption is analyzed for equal load sharing in DC and AC architectures for an OSV load profile in [33]. The authors use PSO to solve the non-linearity of the specific fuel consumption (SFC). For more accurate SFC curves, the SFC function is divided into different generator loading ranges, and each range is piece-wise polynomials with a SFC polynomial equation. The PSO algorithm was first proposed by Kennedy and Eberhart in [34]. The OSV comprises equally sized generators. Three cases are presented, the first two compare DC and AC networks with equal loading of generators, and case three uses PSO for load sharing among DG. Since the generators share the load unequally and unit commitment is unnecessary, it is easier to model the PSO algorithm. For the given load profile, a total of 152 tons of fuel was saved annually with a DC network and 307 tons with the PSO algorithm. The authors do not consider the costs incurred to realize a DC network or a PMS with PSO.
7. **Genetic Algorithm:** The total generation cost during a whole voyage is minimized in [35] using Genetic Algorithm. The system operation, technical generator limits, and unit commitment are

considered throughout the optimization process to determine the ideal generator-rated power. The study does not focus on optimizing the issue-solving methodologies because the purpose was to implement and identify the best solution to size the system and schedule it. Therefore, a genetic algorithm was chosen.

8. **Improved Sine and Cosine Algorithm:** Improved Sine and Cosine Algorithm (SCA) is deployed to solve global optimization for a zero-emission ferry boat based out of Proton-Exchange Membrane Fuel Cell (PEMFC) in [36]. SCA is said to compute more quickly than PSO and GA. The findings of the comparison between the optimal component sizing and the existing configuration show that the suggested strategy is profitable in that it reduces the investment and operating expenses by 2%. Rules-based BESS sizing and SCA-based size were compared. It was found that the proposed method can yield a 2.4% cheaper power scheduling in SCA.
9. **Real Time Optimization:** Global planning techniques may produce the best results, but they can be computationally costly and require much knowledge about the ship's routine. They are, therefore, helpful for early-stage management tasks like planning, sizing, scheduling voyages, and energy dispatch but impractical for real-time power control. On the other hand, real-time optimization (RTO) approaches enable continuous review and modifications based on current information to reduce expenses. The main benefit of RTO is that it allows the system to make real-time, optimal decisions that align with the facts at hand.

Table 2.3: Summary of optimization methods

Method	Type	Reference	Reviewed
Classical Optimization	Dynamic Programming	[31],[30]	Yes
	Linear Programming	[23],[24]	Yes
	Non-Linear Optimization	[25]	Yes
	Mixed Integer Non Linear Programing	[28], [29]	Yes
	Interval Optimization	[37]	Yes
	Branch and Bound	[26]	Yes
Heuristic Methods	Adaptive Multi Clustering Algorithm	N.A	No
	Genetic Algorithm and NSGA-II	[35]	Yes
	PSO	[32],[33],[34]	Yes
	Improved Sine Cosine Algorithm	[36]	Yes
	Whale Optimization, Salp Optimization, Differential evolution, Grey Wolf Optimization	N.A	No

2.4. Battery system

Six key aspects must be considered when choosing a battery for different purposes. These include prices, safety, and physical characteristics like size and weight. Three of these relate to the battery's operating performance, i.e., capacity, power, and lifespan. Each factor's importance in the selection process changes depending on the particular application. When it comes to the maritime industry, the battery's capacity and power rating has a significant impact on the ship's range and speed, while its lifespan and cost determine the expenses related to its installation and usage. Moreover, the safety and size of the battery play a crucial role in deciding its placement and integration within the ship.

2.4.1. Battery capacity: high power, and high energy operation

Battery capacity is the total quantity of energy or electricity produced by electrochemical processes inside the battery and is represented in ampere-hours [38]. Typically, this is expressed in Wh or Ah. The battery's power rating, commonly stated in Watts (W), measures its ability to charge and discharge at high current rates. The capacity of the battery and the power the battery can provide is typically traded off. These batteries can be categorized as high power (HP) or high energy (HE) systems in maritime battery systems. Table 2.5 gives an overview of the available battery systems as of April 2023.

C-rates are used to represent the maximum permitted charge and discharge. The charge rate is the quantity of current that, given an hour to work, can drain a fully charged battery. In [39], HE batteries are classified as longer duration batteries and HP batteries as lower duration batteries. It can be seen in [39] that HE batteries are lower in €/kWh and HP batteries are lower in €/kW.

A HP battery is appropriate for applications that require a lot of power for a brief amount of time, such as starting an engine, since it is designed to deliver high currents in short bursts. HP batteries might not be suitable for deep cycling or other applications that need constant power production over a long period due to their lower energy density. On the other hand, a HE battery is designed to provide power steadily over a longer time, making it ideal for deep cycling applications. They frequently have better energy densities than HP batteries, allowing them to store more energy per unit of weight or space.

2.4.2. Battery longevity

The expected lifetime of a battery is heavily dependent on aging. There are essentially two types of aging.

1. Calendar aging: A battery's capacity and performance naturally deteriorate with time, even if it is not being used. This process is known as calendar aging. The primary reason for this aging process is the battery's internal chemical reactions, which can alter the physical and chemical characteristics of the battery's components
2. Cycle aging: Battery deterioration brought on by charge-discharge cycles is called cycle aging. This depends on the battery's depth of discharge (DoD), the intermediate state of charge, and the rate of charge and discharge

Calendar aging

The design and usage of batteries must consider calendar aging, especially for applications that call for long-term storage or rarely use, such as backup power systems or infrequently used electric cars. As per [40], more than 90% of the vehicle lifetime (personal car) is the parking mode. The role of a battery in a vessel can be slightly different. A battery in a typical DP-2 vessel can be used as a virtual generator. During this period, the battery is not being used and may be subject to calendar aging. In this study, 66 % of the time, the vessel is in DP mode. The authors in [40] study calendar aging in three different ways.

1. Constant SOC, Constant Temperature
2. Fixed SOC, Varying Temperature
3. Varying SOC, Varying Temperature

Maritime batteries are always present in a fixed enclosure. Hence the temperature is constant. In addition, the battery is idle only in DP mode wherein the SOC is fixed to act as a virtual generator for

20 mins. Hence the condition for calendar aging in maritime batteries must be studied under constant SOC and constant temperature conditions. The authors of [41] perform tests for calendar aging with 3 different types of cells, i.e. : NCA, NMC, and LFP cells. The authors chose 16 different SOC levels. This is important as a clear relationship between the capacity fade and SOC levels can be observed. The cells showed greater calendar aging as the storage temperature increased. However, no consistent degradation with the state of charge was detected [41]. Instead, plateau regions were detected covering SoC regions of more than 20-30%. A significant step is observed in capacity curves at 60% SoC for NCA & NMC cells and 70% SoC for LFP cells. The authors of [42] provide a detailed analysis for calendar aging of Li-ion batteries at different environmental temperatures. The data the authors summarise provide the normalized yearly battery degradation as a percentage of its capacity. From this study, a 3% year-on-year battery degradation for LFP and NMC batteries are considered for further calculations in this master thesis. Overall the calendar aging at 25°C for the two types of cells over the period of 9 months are approximately the same. When designing batteries, it is important to consider calendar aging and account for it in the sizing process by adding a non-usable safety margin region , see figure 2.13 or in the lifetime calculation.



Figure 2.13: Battery usage

Cycle Aging

From [43] it was concluded that the tests showed that the cycle aging depended only on the moved charge Q and did not depend on the cycle shape. Hence, aging can be represented as a function of the number of cycles or time (cycles per unit time). This, however, implies that every cycle is equal to the other. Figure 2.17 shows the relationship between the Depth of Discharge (DoD) and the number of life cycles. It can be observed that the cycle life is significantly affected by the DoD. The total useable energy for the 100kWh battery in figure 2.17 at 50% DoD is 1.1 GWh. Whereas, the total usable energy for a 100 kWh battery at 80% DoD is 0.368 GWh. This is 2.989 times smaller than the usable energy at 50% DoD for the same battery size. The authors of [44] investigated the degradation of LFP batteries for temperatures of 25°C and 40°C. The degradation was tested for both cycle aging and calendar aging. It was found that cycle aging contributed as the main source of capacity fading.

The authors of [45] test $LiFePO_4$ batteries for degradation under dissimilar charging and discharging temperatures. It is concluded that there exists a quadratic relationship between degradation and charging temperature and a linear relationship with discharge temperature. Maximum degradation is observed while charging and discharging at +30°C and -5°C, and while charging at 15°C it was found that the degradation was independent of degradation temperature.

Further literature has been consolidated in table 2.4. It can be observed that the C-rate is a major factor for capacity fading in NMC batteries whereas in LFP batteries C-Rate is not a significant factor. This suggests that NMC batteries are best to be used for high-energy applications, whereas the choice of LFP batteries is best for high-power applications.

Table 2.4: Cycle aging of NMC and LFP

Battery	test	C-Rate of tests	Comments	Reference
NMC	Number of batteries - 21 Number of C-rates - 5 Number of voltages - 3	0.5, 0.8, 1, 1.2, 1.5	1C - Critical charging rate 4.2 V - Critical voltage Above critical charging/ voltage degradation increases Battery degrades at 10% - 1.2 C 23% - 1.5 C 7% - 1 C	[46]
NMC	Number of batteries - 12 Number of C-rates - 4	0.7, 2, 4, 6	The lifespan of the battery impacted by higher charging rates Charging >4C, chemical changes are caused in the battery This leads to considerable harm and a decrease in its lifespan.	[47]
LFP	Number of cycles - 4500 Number of C-Rates - 3	4, 1, (Constant V)	3 Stage charging process (CC (at 4C), CC(at 1C), CV(at 3.6V) Performance lost due to capacity fade and not internal resistance of charging Discharge internal resistance is greater than charge internal resistance	[48]
LFP	Number of Batteries - 3 Number of C-rates - 2	1, 4	the capacity reduction (at 4000 cycles) 15% when charged at a rate of 1C 17% when charged at 4C. Reduction in capacity comparable at 4C and 1C for <1000 cycles degradation increases for 4C for >1000 cycles	[49]
LFP	Number of batteries - 200 Number of C-rates - 4 Number of temperature - 5	0.5,2,6,10	DoD >50% reach the designated EoL state earlier Capacity fade due to temperature and DoD >>>C-rate	[50]

Table 2.5: List of available batteries in the European maritime industry

Battery Name	Battery Provider	(kWh)	(Wh/kg) -(Wh/l)	Charge (Cont - Max) (C-rate)	Discharge (Cont - Max) (C-rate)	Number of Cycles	Reference	
High Energy NMC	EST-Floattech	10	NA	0.5	1.0	NA	[51]	
High Power NMC		5.8		2.0	3.0	3.0	NA	[52]
High Energy LFP		10.24		0.5	1.0	0.5	4500 (1C - 80% DoD)	[53]
Orca Energy	Corvus	5.6	77 - 88	3	PSV	NA	[54]	
Blue Whale		43	110 - 130	0.7	1	NA	[55]	
Dolphin Energy		11	177 - 100	0.4	1.1	NA	[56]	
Aries	Aries+ / Aries+ S	8.8	126 - 170	0.6	2 (30s)	4,000 (1C - 100% DoD)	[57]	
Orion+		17.6	130 - 209	0.43	1.3C (30s)	4,000 (1C - 100% DoD)		
Aquarius+		6.9	99 - 142	1	3 (30s)	6,000 (1C - 100% DoD)		
Centaur	EASY Marine	21.5	126 - 201	0.35	1 (30s)	6,000 (1C - 100% DoD)	[58]	
E-LTO ENERGY		23.3	137 - 218	0.35	1 (30s)	4,000(1C - 100% DoD)		
E-LTO POWER		3.1	50 - 66	1	3	6,250 (80% DoD)		
XPand Battery Bank Solution	Echandia	1068 (Bank)	77.4 - NA	0.15 (300s)	0.37 (100s)	50,000 (50% DoD)	[59]	
COBRA		274 (Bank)	57.4	1.45(300s)	2 (100s)	70,000 (50% DoD)		
NOMADA		670 (Bank)	80-60	2	NA	10,000 (1C - 80% DoD)		
NOMIA	Lehmann Marine	94	NA	PSV	PSV	NA	[60]	
SMAR-11N		12.4	138.6 - NA	1	1	3(30s)	[61]	
SMAR-4A		40.4	136 - NA	0.88	0.88	3500 (1C - 100% DoD)	[62]	
XMOD 123E	Spear Power Systems	11.3	111 - 98	3	3	4000 (1C - 100% DoD)	[62]	
XMOD 96P		4.1	74-55	4	4	NA	[63]	
		12.3	185.5 - 230.7	0.3	0.5 (10s)	4000 (0.3 C 80% DoD)	[64]	
	9.6	150 - 181	2	3.9 (10s)	10,000 (1C 80% DoD)			

2.4.3. Battery technology

A comprehensive review of the existing Li-ion battery technologies are studied in [65], [66], [67], and [68]. Tables 2.5-2.6 show the battery technology/chemistry used in certain industrial available batteries as of April 2023. Currently, NMC and LFP are the two most commonly used battery types in the market. However, it seems that the industry is shifting towards favoring LFP batteries over NMC batteries in the near future due to their superior safety features.

Table 2.6: Available maritime battery technologies

Battery name	Battery provider	Battery technology	Reference
High Energy	EST-Floatech	NMC and LFP	[51]
High Power		NMC and LFP	[52]
High Energy		LFP	[51]
Orca Energy	Corvus	NMC	[69]
Blue Whale		LFP	
Dolphin Energy		NMC	
Dolphin Next Gen		LFP	
Aries	Ayk Energy	LFP	[57]
Aries + / Aries + S			
Orion			
Orion +			
Aquarius +			
Cantaur			
Easy Marine	EASy Marine	LFP	[58]
E-LTO Energy	Echandia	LTO	[59]
E-LTO Power		LTO	[59]
XPand Battery Bank Solution	Freudenberg	NMC	[60]
Cobra	Lehmann Marine	LFP	[61]
NOMADA	Super-B	LFP	[62]
NOMIA		LFP	[62]
15 OEM	ZEM Energy	NMC	
9 AKM		NMC	
SMAR-11N	Spear Power Systems	NMC	[63]
SMAR-4A		Nano	
XMOD 123	XALT Energy - Fredenberg	NMC	[64]
XMOD 96			[64]
Green Battery - Energy	Praxis Automation	LFP	[70]
Green Battery - Power			[70]

A detailed comparison of key performance aspects is shown in figure 2.14 and [67]. $LiFePo_4$ (LFP), NMC and LTO batteries will be discussed below. It can be observed that:

1. **Cost:** NMC batteries are the most expensive type of Li-ion batteries under consideration and LTO is the cheapest
2. **Specific Energy:** NMC batteries are shown they have the highest specific energy amongst LFP and LTO batteries. This implies for a required size of the battery in kWh NMC batteries would occupy the least amount of space. LFP and LTO batteries would occupy a similar amount of space
3. **Specific Power:** LFP batteries have the highest possible specific power amongst NMC and LTO. NMC and LTO have similar specific power capabilities
4. **Specific Power:** LFP and LTO batteries are amongst the safest batteries in the industry
5. **Performance and Lifespan:** LTO batteries last long and can charge quickly because of their unique anode material, while LFP batteries have a stable cathode material that makes them safer and allows them to operate at high temperatures without significant degradation

The cost of Li-ion batteries in [71] are shown in terms of cost per 1800-4100 \$/kW (1643.28-3743.03 €/kW as of Monday 3rd July, 2023) and 900-1700 (821.64-1551.99 €/kWh as of Monday 3rd July, 2023).

Since 2011 the price of batteries has significantly become lesser. The price of batteries is forecasted in [72]. It is predicted that the cost of batteries will come down to 71 \$/kWh (64.82 €/kWh as of Monday 3rd July, 2023) in 2050. The cost of BESS can be expressed as in equation (2.3).

$$\text{Total cost (\$/kWh)} = \text{Battery cost (\$/kWh)} + \text{Power electronic cost (\$/kW)} \quad (2.3)$$

The battery operating cost can be included in to cost function in multiple ways. In [73] battery energy storage study assumes that the batteries have a fixed life time. Fixed marginal costs can be considered as done in [74]. Otherwise, piece-wise linear battery degradation costs can also be assumed as shown in [75].

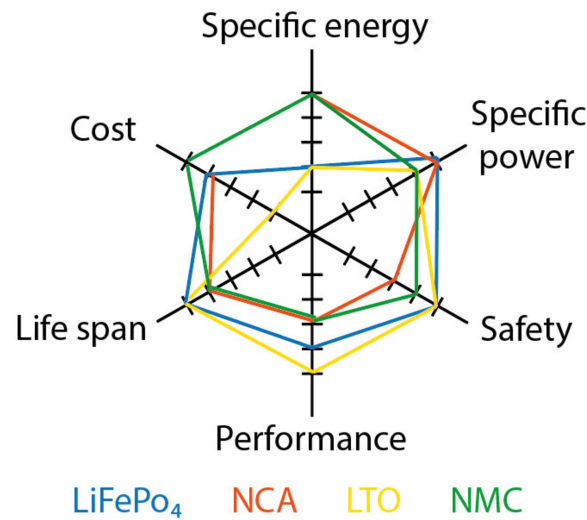


Figure 2.14: Battery technologies comparison [68]

2.5. Optimal sizing of battery system

Energy management systems must consider battery sizing optimally since it may assist to calculate the quantity of energy storage needed to fulfill demand while utilizing renewable energy sources to their fullest potential.

The unit commitment, investment cost, optimization technique, generator power limit, ramp restrictions, and maximum C-rate of batteries are some of the important elements that affect the best battery sizing. Unit commitment is the process of planning the operation of power plants in a way that meets energy demand while ensuring that costs are kept to a minimum. The appropriate sizing is influenced by the batteries investment cost since choosing the battery system's size requires considering the system's total cost of ownership.

Battery sizing optimization techniques might include heuristics, dynamic programming, linear programming, and nonlinear programming. Ramp limitations and generator power restrictions affect battery sizing since they govern how much energy a generator can produce. The load profiles are further crucial for BESS sizing. Predictive journeys may make predicting battery size, cycle, and lifespan simpler.

Due to their predictable load profile, electric ferries are seen as low-hanging fruit when it comes to hybridization. A two-layer optimization is deployed for optimal battery sizing in [76]. The outer layer optimizes battery capacity depending on cost and annual interest rate, while the inner layer offers the best method for cutting fuel usage. However, this activity does not require the generator's unit commitment or starting expenses. The objective function was solved using Fmincon function in MATLAB.

Paper [77] considers three main factors while sizing BESS, survivability, cost, and quality of service. A power system's capacity to continue operating in a damaged state is referred to as its survivability. In a power system, the term "quality of service" describes how consistently the system operates under typical circumstances. The battery is sized according to the peak power requirements, DoD, the short-term interruptible limit of providing power for 5 minutes, and long-term interruptible power for 10 minutes. In this case, the objective functions with the three elements are solved using multiple objective particle swarm optimization (MOPSO). Thoughts like increasing the number of cycles or fuel savings cannot be found in this study. The battery's design is based on a two-step optimization process, with the first stage focused on improving the way the power plant runs. This is referred to as the inner optimization. The outer optimization optimizes the battery size.

The most cost-effective Li-ion battery parameters is found using MATLAB software and programming calculations in [78]. Utilizing the generator at its ideal operating point is the aim. This study, unlike the majority of others, covers converter expenses and battery maintenance costs. It is a nonlinear multi-objective optimization problem since the battery size is optimized using three objective functions. The system's cost is the first objective function, power fluctuations are the second, and battery life lost is the third. These objective functions are solved using a decomposition-based multi-objective differential evolution approach.

The operation of a vessel and the ESS sizing problem is addressed in the same framework in [79], this is covered in the first stage of the proposed risk-averse energy storage sizing method. The second stage addresses the information gap decision that decides the number of modules required to achieve the necessary power and energy, see figure 2.15. This paper emphasizes the need to provide the proper weight of the operational profile, safety, and task sequence. Li-ion batteries, flow batteries, and ultracapacitors are the three different energy storage types for which the findings are provided.

A novel set of formulations to predict the optimal battery size, type of technology, DoD, and replacement year is presented in [80] for a microgrid system. The detailed objective function accounts for investment expenses, generator running costs, and the cost of unsupplied energy. This work considers various factors, including unit commitment, start-up and shut-down costs, ramp restrictions, battery replacement costs, and maintenance expenses, in contrast to other works previously mentioned. The objective function is a CPLEX-solved mixed integer linear programming model. The DoD-based investment costs, operational expenses, cost of supply loss, and battery size are finally presented.

Operational safety conditions (based on N-1 safety) and minimum generator operation is the proposed design procedure to arrive at the BESS power capacity in [21]. The first step involves considering safety standards and pre-determining the number of required online generators for each operating mode. The second phase is figuring out the investment cost and fuel savings. The results are presented for several selected battery sizes as a function of the yearly fuel savings and payback period. Due to the military nature of the ship's operation, the selected BESS is expected to be 60g/Wh, 1800 \$/kWh (1643.28 €/kWh as of Monday 3rd July, 2023), and have a C-rate of 4C. However, regularly available battery systems cannot accomplish this. The algorithm is shown in figure 2.16.

Interval optimization method has been used in [37] to find the optimal size of the ESS and power system scheduling. When the ship is moving at full speed, the peak load is between 1611 - 1969 kW, and when it is at anchor, the off-peak load is between 450 - 550 kW. For all combinations of peak and off-peak load within these periods, the range of potential total power consumption is computed using interval arithmetic. This method allows for the calculation of battery size.

Rule-based IEEE standard calculates the BESS sizing in [20]. This method is simple, fast, and effective to calculate the required battery sizing for the necessary safety conditions. However, this standard does not optimize the battery sizing and is a relatively old standard.

Table 2.7: Review of certain battery sizing methodologies for vessels

Reference	Method of optimization	Features covered	Features missing
[76]	Double Layer Optimization	Generator: Power Limit Cost Function: Fuel Savings, Battery Cost, Startup Cost Penalty factor	Maintenance Cost, Power Electronic Cost
[77]	MO-Particle Swarm Optimization	Cost Function: Power Electronic Cost, Battery Cost	Fuel Savings, Maintenance Cost Generator Limits (Max and Ramp) Penalty factor
[78]	MO Differential Evolution Algorithm	Generator: Power Limit, Cost Function: Fuel Savings, Power Electronic, Maintenance Cost, Battery Cost	Start-up Cost, Ramp Rate, Unit commitment, Penalty factor
[79]	SCA	Generator: Power Limit, Ramp Rate Cost Function: Fuel savings, battery cost	Power electronic cost, Maintenance Cost Penalty factor
[80]	MILP	Generator: Power Limit, Startup Cost, Ramp Rate Cost function: Power electronic cost, Start-up cost Battery Maintenance cost, Battery Cost	Fuel Savings, Penalty factor
[21]	No information	Cost function: Battery cost, fuel savings, weight of system	Not much information
[37]	Interval Optimization	Generator: Power Limit, Ramp Rate Cost function: Fuel savings, Maintenance Cost, Battery Cost	Start-up Cost, Power Electronic Cost
[20]	Rule Based IEEE Standard	Cost function : Fuel Efficiency	Power electronic, Maintenance, Battery Cost start-up cost, ramp rate
[28]	MINLP	Generator: Power Limit Cost function: Fuel Savings, Startup Cost	Power Electronic, Maintenance cost, Battery Cost, Ramp rate
[30]	MO-MP vs MILP	Generator : Power Limit, Cost Function: Fuel Savings, Power Electronic Cost Battery Cost,	Maintenance cost, Ramp Rate, Start up, Penalty factor

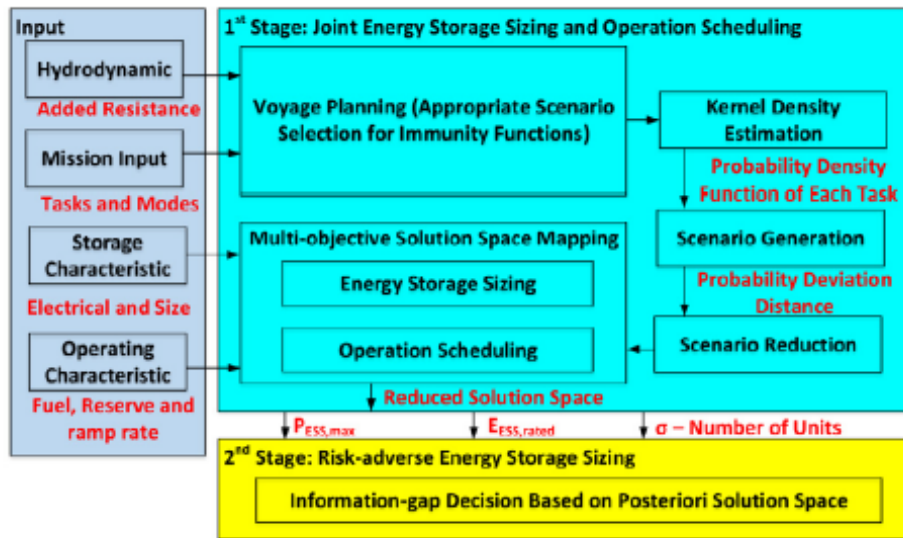


Figure 2.15: Risk-averse ES sizing [79]

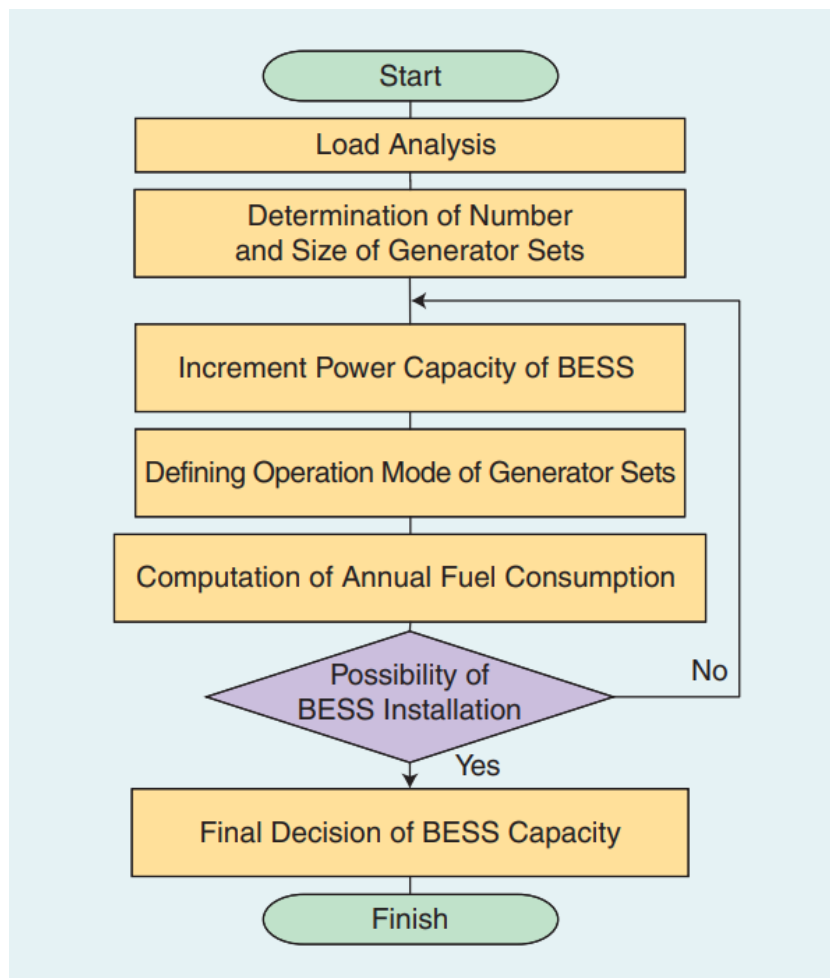


Figure 2.16: Risk-averse ES sizing [21]

2.6. Battery Degradation in Optimisation

Battery degradation must be taken into consideration for the optimization model to accurately depict the behavior of battery systems in real-world applications. The phrase "battery degradation" refers to the gradual loss of battery capacity over time as a result of factors including usage, temperature, and cycling.

The authors of [81] discuss the multi-objective optimization of cost, energy consumption, and battery degradation for fuel-cell battery hybrid electric vehicles (FC HEVs). The work suggests power-matching algorithms that consider system cost, energy efficiency, and battery deterioration and are optimized by the particle swarm optimization (PSO) algorithm. Two hybrid systems are suggested based on the change in the degree of hybridization (DOH). The ideal hybridization levels of the hybrid powertrain are discovered under four sets of weighting variables. The price per kWh for batteries with high energy and power densities considered is around \$137 (€ as of Monday 3rd July, 2023). A semi-empirical battery deterioration model built on the Arrhenius degradation model was selected as the battery degradation model.

An example of a residential PV-Battery microgrid model considering battery degradation as a function of the number of cycles can be found in [82]. However, this is not included in the inner optimization loop. In addition, the discharging current is considered when calculating the weighted number of cycles.

Different types of battery stress modeling have been discussed in [83]. The first approach is to include the objective function's cost per kWh for the entire battery. This strategy minimizes additional operational expenses and the cost per kWh produced by the battery's overall energy output. The second technique mentioned involves adding the battery's deterioration charges to the operational expenses. The energy capacity and the cost per kWh for replacement are compounded by the battery's daily minimum SoC. This strategy lowers the number of smaller cycles while decreasing degradation costs. The third approach mentioned considers the difference between the greatest and lowest value of SoC each day. This effectively lowers the DoD and raises the battery's lifetime throughput, which lowers energy costs.

The authors of [83] criticize the use of constraints in limiting battery degradation. It is important to note that the author discusses linear programming. Constraints can help in locating the best solutions. Other optimization techniques, like MINLP, might be time-consuming. The recommended method in [84] involves using two models that work together in an iterative process to effectively model battery degradation and optimize the operation of photovoltaic systems. Based on a predetermined battery degradation cost, the first model is an economic one that employs optimization for linear programming to identify the best hourly battery consumption profile. The price of battery deterioration is determined by the second model, which considers the battery's load profile and degradation. Up to the point of convergence, these two models are applied repeatedly to find the price per kWh.

A battery degradation-aware optimal power distribution method has been proposed for decentralized energy networks in [85]. With normalized quantification of multi-services profitability, [85] analyzes the best whole-life cycle planning for the BESS. The article considers variables such as battery cycle lifetime and SOH, charging and discharging techniques, the operational environment, and divergence of actual Depth of Discharge (DoD) from rated DoD. The battery's on-site operation's link between the number of cycles and DoD is modeled using empirical data. Furthermore, the BESS's total electrical output throughout its lifespan at the rated discharge depth is considered.

The authors of [80] propose a novel set of formulations to determine the optimal battery energy storage (BES) size, technology, DoD, and replacement year considering its technical characteristics, service life, and capacity degradation to minimize the micro-grid scheduling total cost and improve the precision and economic feasibility of the BES sizing. The battery lifetime/serviceability year is decided on the cycle life or the float life. Where float life, also known as standby life or calendar life, refers to the expected lifespan of a battery system. At the same time, it is maintained in a partially charged or float state without undergoing regular charge-discharge cycles.

A cycle counting algorithm called "rain-flow" is presented in [86] for segregating the charging/discharging curve into two categories: complete cycles and incomplete cycles with an incomplete DoD. Utilizing non-linear equations in the optimal sizing model for BES can result in convergence to a local optimum. A linear regression (LR) method is used to model the system.

Optimal sizing and usage of the battery system are optimized for every time step using Receding Horizon Control (RHC) scheme in [87]. By considering the battery's SOC, which is constrained to avoid deep discharge or overcharging during operation, the optimization model incorporates the linear approximation of battery deterioration per cycle.

A combination of battery degradation as a function of cycles to failure and rain flow algorithm has been implemented in [88]. Other factors affecting the battery life are neglected. Evolutionary algorithms are used to model the system.

Table 2.8: Review of existing battery degradation modeling

Reference	Optimisation	Purpose	Method
[81]	MO-PSO	HEV	Semi-empirical and Arrhenius
[82]	GA	PV-Battery Microgrid	Capacity loss to battery cycling
[83]	LP	Off-Grid Power System	Cost per kWh throughout the battery Daily DoD reduction
[84]	LP	PV-Battery System	Modified Shepherd Equation Active material degradation Corrosion of positive electrode
[85]	MIP	Decentralized Energy Network	Limit charge/discharge cycles
[80]	MINLP	Microgrid	DoD, Float life
[86]	LR	Managing Energy Imbalance	Incomplete and complete DoD
[87]	RHC	Electricity Market Participation	Discharge per cycle
[88]	EA	Windturbine - Battery system	Cycles to Failure

As discussed earlier, electrochemical batteries have a fixed lifetime due to the irreversible changes that take place during the charging and discharging of batteries. This can be seen in figure 2.17. The y-axis represents the number of cycles and the x-axis represents the depth of discharge. Three different batteries have been taken into consideration from two different battery suppliers.

A choice of battery has to be made based on the technical requirements of average C-rate, maximizing the number of cycles for a given depth of discharge. At 20% DoD, batteries of battery supplier 1 provide 85000 cycles, whereas batteries of battery supplier 2 provide a better number of cycles at 50% DoD. This significantly affects the cost per energy throughput of the battery [89].

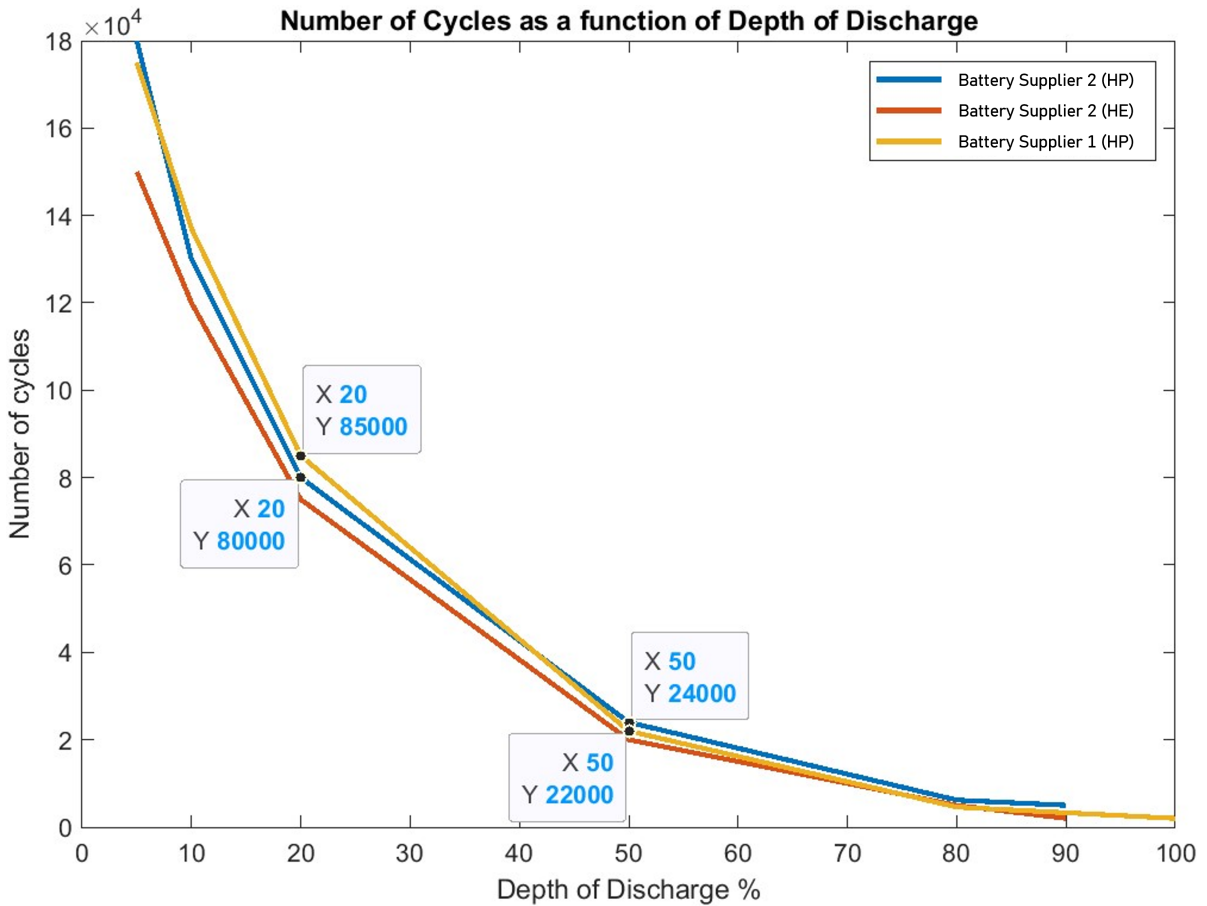


Figure 2.17: Number of cycles as a function of DoD

2.7. Optimization of the operation of isolated industrial DG's

Maintenance costs for fleet owners can sum up to hundreds of thousands of Euros per year. A large part of these costs include the diesel engine generator costs. The authors of [90] show that the maintenance costs of running industrial DG's correspond to 10% of the energy generation costs. Such high maintenance costs arise despite loading the diesel engine generators at a high load factor.

The operational and maintenance costs can be divided into 3 parts as shown in the equation (2.4) below

$$\text{Maintenance Cost} = \text{PMC} + \text{OC} + \text{CMC}, \quad (2.4)$$

where PMC, OC and CMC stand for the preventive maintenance costs, operational costs, and corrective maintenance costs. Corrective maintenance costs can also be called overhaul costs. The preventive maintenance costs depend only on the size of the DG, whereas the operational and corrective maintenance costs depend on the loading of the DG.

Hence, the preventive maintenance costs in an optimization objective function can be neglected as this is fixed irrespective of the load factor. However, the costs can be considered if a choice has to be made based on DG sizing and minimizing the lifetime costs of a DG in a new build. The authors of [90] point out the operational costs are negligible compared to the cumulative maintenance costs. The authors developed a unique minimum time before overhaul (MTBO) cost function as shown in:

$$\text{MTBO}(\text{hours}) = \sum_{i=0}^8 b_i \times \theta^i, \quad (2.5)$$

where, θ is the loading % of the diesel engine - generator set. The value of the coefficients is shown in table 2.9.

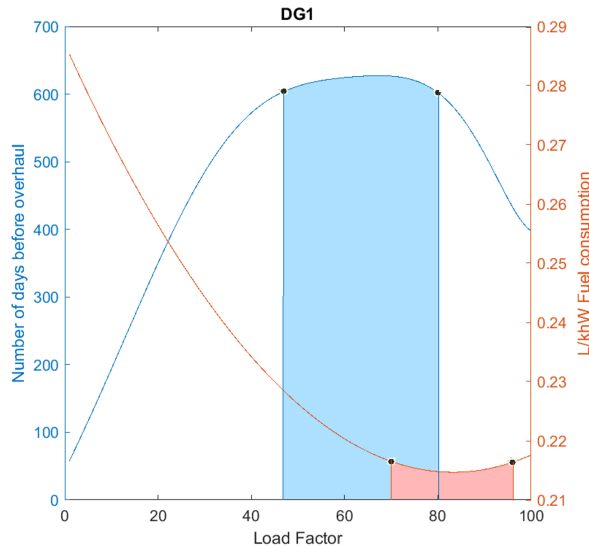
Table 2.9: Coefficient values

Coefficient	Value
b0	1040.898
b1	3.429×10^4
b2	1.66×10^4
b3	4.971×10^4
b4	-3.429×10^4
b5	-5.504×10^5
b6	2.803×10^6
b7	-3.174×10^6

Figures 2.18, 2.19 depict MTBO curves plotted with the SFOC curves of two DG's. It can be seen from figure 2.18 that the optimum region to operate the diesel engine in terms of fuel efficiency lies between 70 % load factor to 95 %. However, the overhaul costs are more or less constant in the regions between 45 % load factor to 80 % load factor. Hence a balance must be established between fuel costs and the over-haul time. This is, of course, dependent on the fuel price and the overhaul costs at that given time. A similar curve but different operating regions of overlap are shown in figure 2.19.

In this study, the maintenance operational limits are included in the optimization problem. The maintenance savings is calculated outside the optimization problem and is described by the equation (2.6). Here, Cdg_n denotes the cost of the DG, T represents the total number of time periods, Θ_{itn}^i indicates the current loading percentage of generator n at time t, and i refers to the exponential power. On the other hand, θ_{itn}^i represents the optimized loading percentage of generator n at time t, where i is the exponential power.

$$\sum_{n=1}^5 (0.5 \times Cdg_n \left(\frac{\sum_{t=1}^T (\sum_{i=1}^7 (\Theta_{itn}^i - \theta_{itn}^i) \times b_i)}{T} \right)) \quad (2.6)$$

**Figure 2.18:** SFOC curve with maintenance curve - DG 1

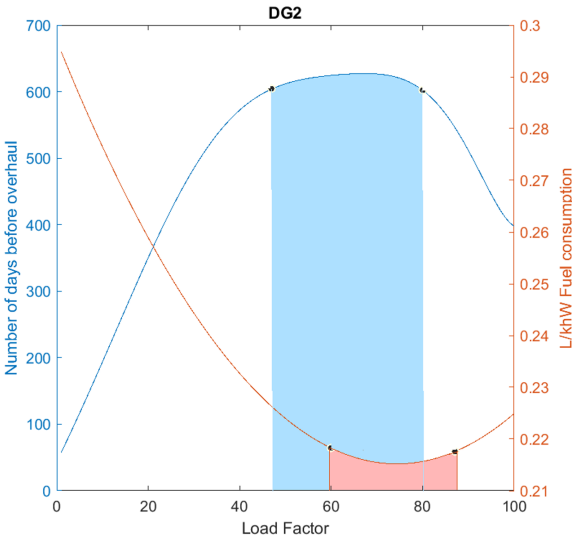


Figure 2.19: SFOC curve with maintenance curve - DG 2

3

Cable Laying Vessel System

3.1. Current system

This section describes the current electrical power plant of the vessel system in discussion. The vessel comprises (see figure 3.1) of five DG's, which are presented in table 3.1.

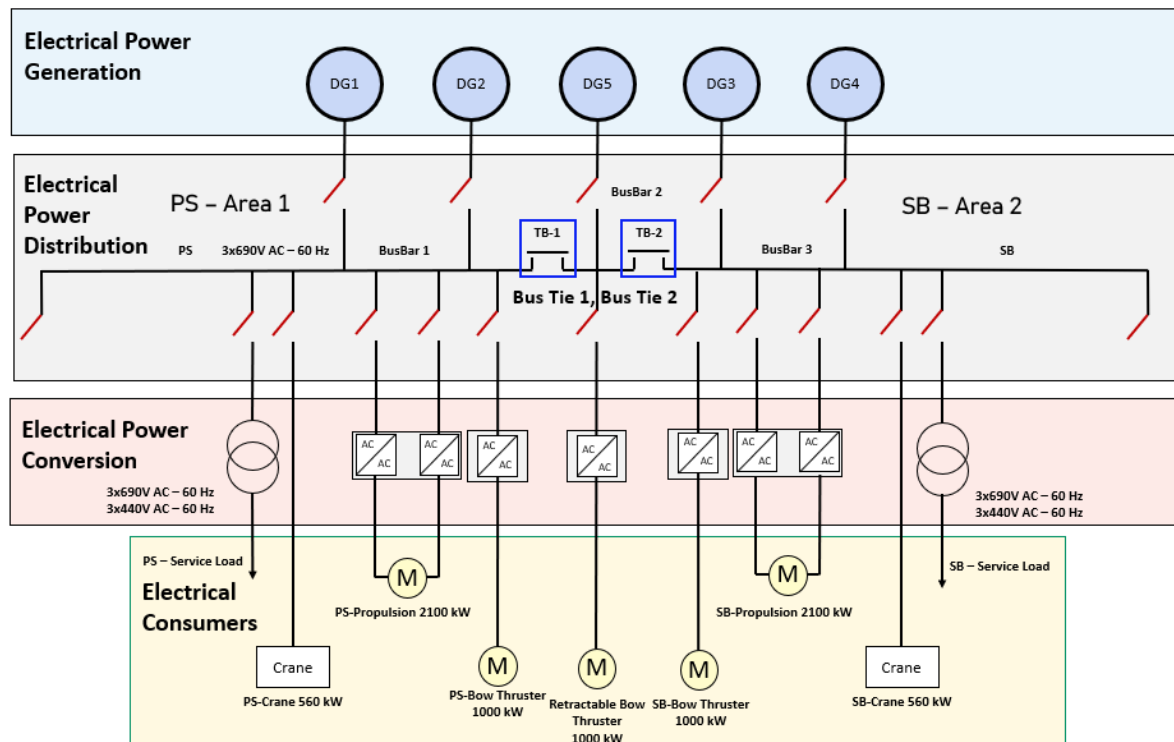


Figure 3.1: Cable Laying Vessel

Table 3.1: Diesel Generator Ratings

Diesel Generator	Rating kW
Diesel Generator 1 (DG1)	1912
Diesel Generator 2 (DG2)	2560
Diesel Generator 3 (DG3)	2560
Diesel Generator 4 (DG4)	1912
Diesel Generator 5 (DG5)	1360

The Cable laying vessel comprises of two bus tie breakers to provide electrical isolation from the port side (PS) and starboard side (SB) during critical operation. Based on the position of the tie-breakers the following notations are used throughout the document as shown in 3.2.

Table 3.2: Notations based on Bus Tie breakers

Notation	TB1	TB2	Mode
Case 00	Open	Open	Auto mode
Case 01	Open	Closed	Non-Critical DP
Case 10	Closed	Open	Non-Critical DP
Case 11	Closed	Closed	DP (Critical)

It can be observed that during cases 00, 01, and 10 the PS and SB sides are electrically separated. The difference is that DG5 is available as an extra generator on the SB and PS sides in cases 01 and 10, respectively. The chosen cable-laying vessel has five operation tasks: harbor, maneuvering, free sailing, loading/unloading, and DP mode. Table 3.3 provides the maximum available power and the maximum possible available power in each mode. The available power is based on the current PMS and adheres to the class requirements mandated by DNV GL. The possible power consumption is the summation of the maximum capacity of each load for every task.

Table 3.3: Modes of operation

Tasks	Possible power consumption	Available power	Mode
Harbour	851 kW	1360 kW	Case 11
Manoeuvring	5165 kW	8392 kW	Case 11
Free sailing	5740 kW	7032 kW	Case 11
Load/Unload	6529 kW	10304 kW	Case 00
DP	6971 kW	10304 kW	Case 00 10 01

The SFOC consumption for the DG's is shown in figures 3.2. The SFOC functions of the generators are listed in equations (3.1)-(3.3). The SFOC coefficients are shown in Table 3.4-3.5.

$$SFOC_{DG1,DG4} = 0.1043 \times PG^2 - 0.1737 \times PG + 0.287 \quad (3.1)$$

$$SFOC_{DG2,DG3} = 0.1479 \times PG^2 - 0.2200 \times PG + 0.2977 \quad (3.2)$$

$$SFOC_{DG5} = 0.2423 \times PG^2 - 0.3121 \times PG + 0.3552 \quad (3.3)$$

PG refers to the power output of the DG.

Table 3.4: SFOC coefficients

Diesel Generator	$\alpha \frac{\text{Liters}}{\text{MWh}^2}$	$\beta \frac{\text{Liters}}{\text{MWh}}$	$\gamma \text{ Liters}$
Diesel Generator 1,4	0.1043	-0.1737	0.2870
Diesel Generator 2,3	0.1479	-0.2200	0.2977
Diesel Generator 5	0.2423	-0.3121	0.3552

Table 3.5: MILP Coefficients for Generator 1-5

Diesel Generator	$\alpha \frac{L}{\text{kWh}}$	$\beta \frac{L}{h}$
Diesel Generator 1,4	0.1918	33.778
Diesel Generator 2,3	0.1869	54.9209
Diesel Generator 5	0.2351	20.024

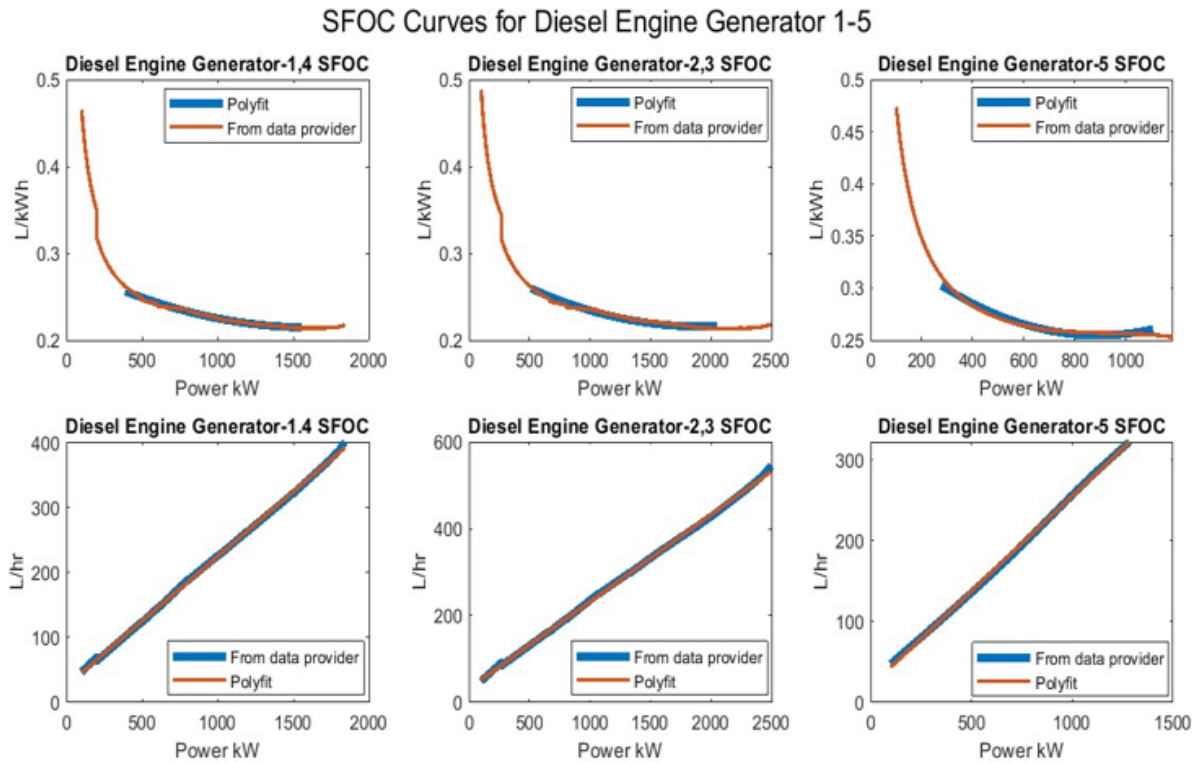


Figure 3.2: SFOC for DG 1-5

3.2. Hybrid system requested

The vessel owner has requested to introduce battery systems to optimize fuel consumption and reduce maintenance costs. The requested proposal has the following requirements,

1. Run batteries as spinning reserve (virtual generator) in DP mode
2. In case of DP mode, provide 15-20 mins of reserve in case of the required switchover of generators or unexpected shutdown
3. Start second Gen-Set at 80% load in DP mode
4. Start second Gen-Set at 80% load in auto mode or non-critical DP mode

Figure 3.3 shows the proposed electrical architecture of the vessel. It can be observed that two BESS are added to the system (one on each side). In addition to this, two bidirectional AC-DC converters are required for the storage systems. This implies that during the auto mode, a total capacity of BESS-1+BESS-2 is available. Whereas, during DP mode, PS has a capacity of BESS-1, and the SB side has a capacity of BESS-2.

The cable-laying vessel has recorded two separate operational profiles, Taiwan (256 days) and the North Sea (285 days). The first set of data is recorded in Taiwan where the sea is calmer. Whereas the second data set is recorded in the North Sea which has rougher environmental conditions.

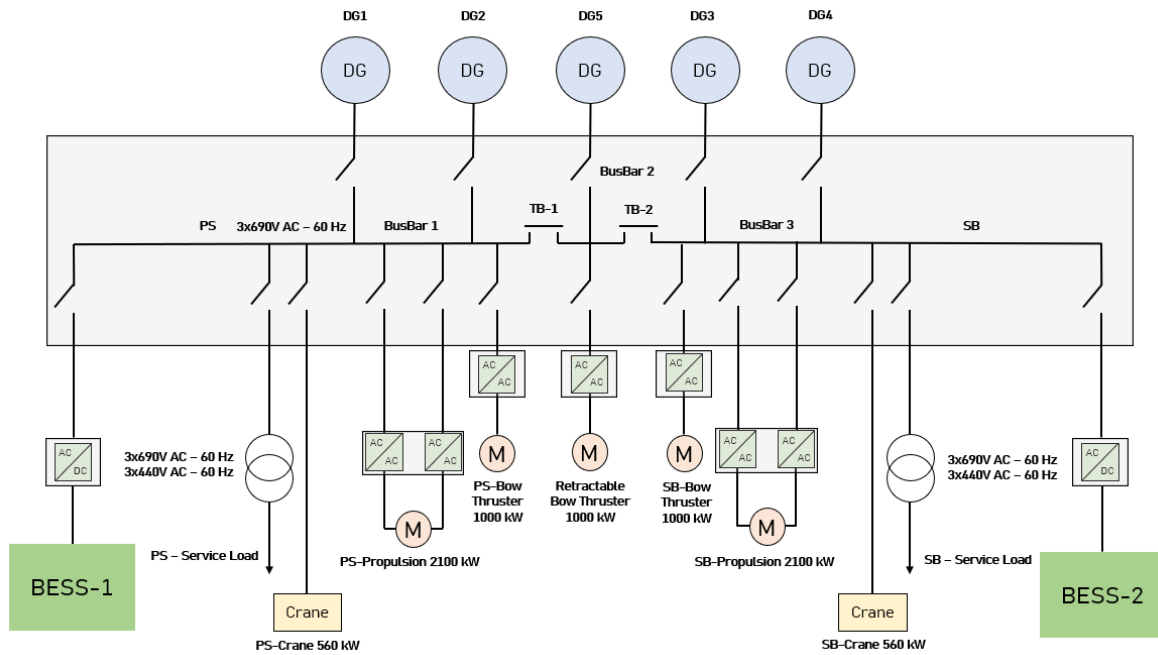


Figure 3.3: Cable laying vessel with BESS

3.3. Proposed BESS sizing and optimal scheduling solution

Based on the literature survey covered in Section 2.5, a BESS sizing methodology has been proposed as shown in figure 3.6.

The first step involves the functionality requirement analysis. In this stage of the process, the requirements are listed (see section 5.5). These include but are not limited to,

1. Functionality of battery: Spinning reserve, peak shaving, load leveling, etc.
2. Define battery C-rate constraints.
3. Lifetime requirement of the battery, budget, etc.

The next step involves analyzing class requirements. This involves finding the generator constraints related to their commitment, redundancy, and maximum powers allowed. This is followed by a load profile analysis, which is segregated based on different scenarios and analyzed. Event analysis is a parallel step to see how often a specific event in focus occurs. This step aims to clean data, segregate data based on scenarios and understand the data better. In this step it is also important to list out the constraints.

From the event analysis and energy analysis, the minimum power requirement and energy requirement can be found. This serves as the lower limit for the sample space of potential battery sizes. A realistic upper limit can be estimated based on the budget. The 5th step involves calculating the fuel savings of the battery system. This is a MILP problem. Finally, based on the different fuel savings results for different battery sizes, the best battery size is selected. In the final step, maintenance costs, and power electronic costs are also considered. The MILP considerations and the overall consideration of the battery sizing solution is depicted in figure 3.4.

The best solution obtained from the MILP optimization then goes through the BOOSTER, where the considerations are depicted in figure 3.5. The BOOSTER is similar to the MILP optimization formulated later. However, it also includes the fuel prices and the energy throughput costs of the battery (cost/kWh). As a result an operational matrix is provided that shows the usability of the BESS as a function of fuel price and power demand. In addition to this, an optimal DG scheduling (priority table) is provided.

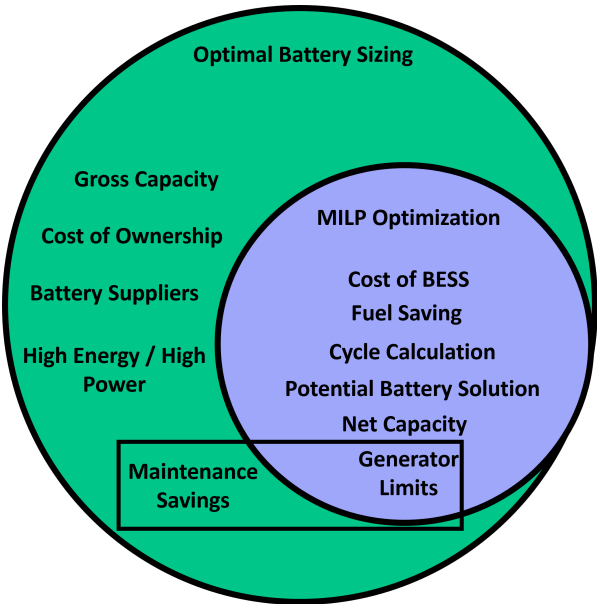


Figure 3.4: Battery Sizing Model

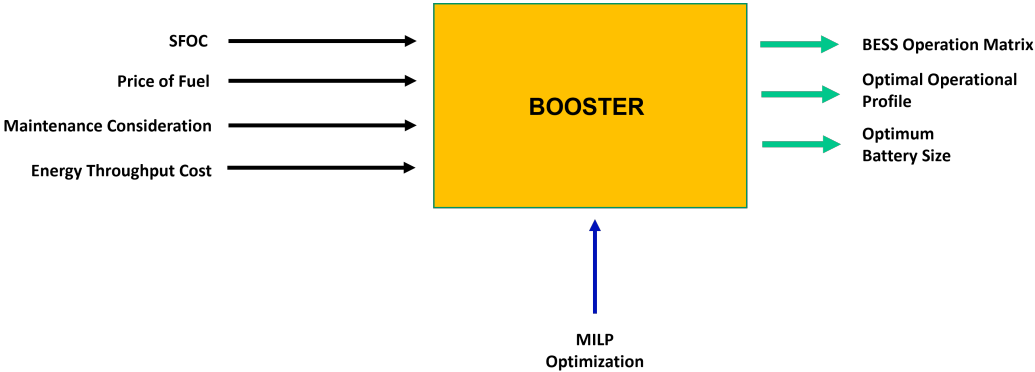


Figure 3.5: BOOSTER considerations and output

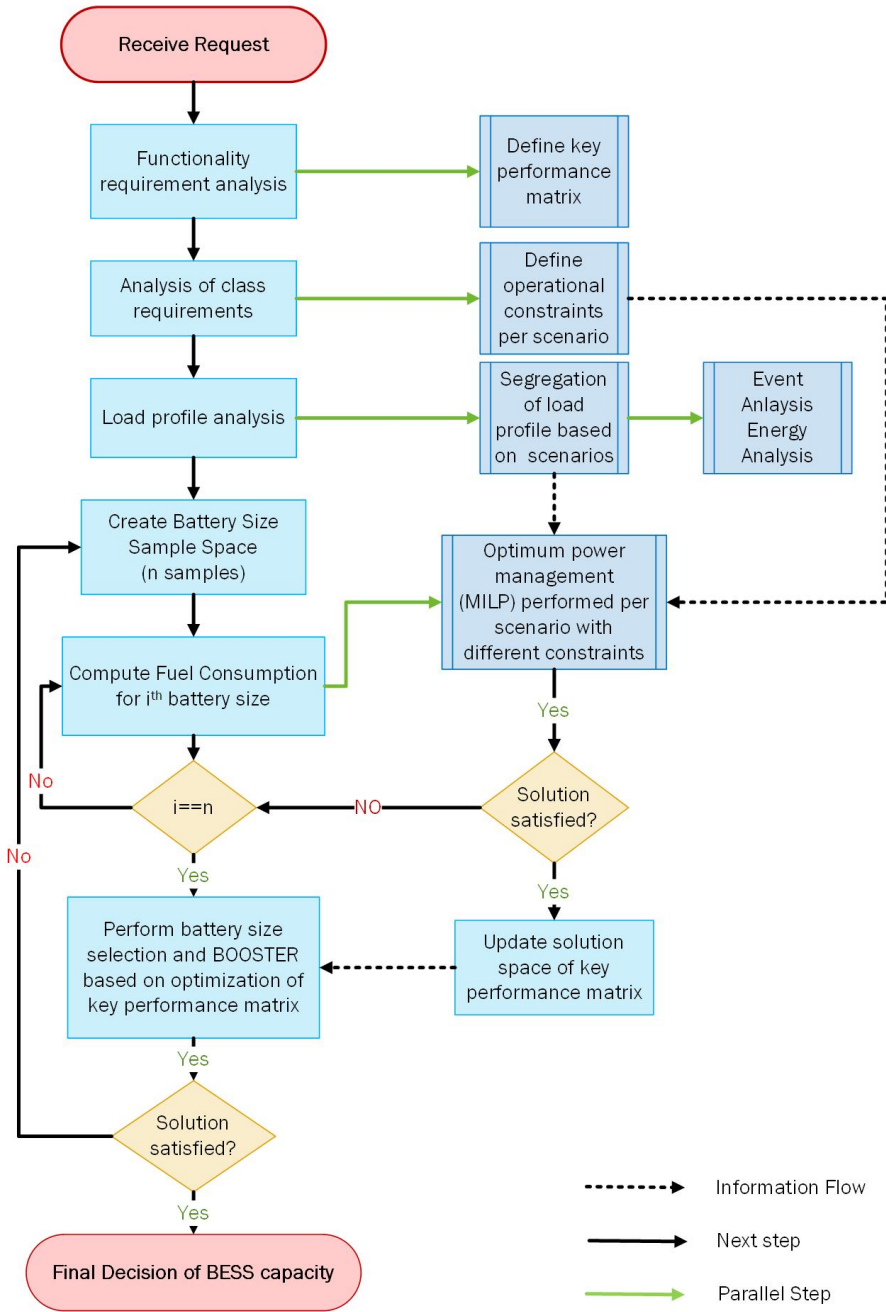


Figure 3.6: Proposed BESS sizing solution

3.3.1. Solution space and key performance matrix

Table 3.6 presents the solution/sample space that includes twelve potential solutions for battery configuration. These configurations are used in the optimization model. There are two types of batteries: HP and HE. Battery supplier 1 provides HE batteries, while battery supplier 2 provides HP batteries. HE batteries have a maximum C rate of 1C, while HP batteries have a maximum C rate of 3C. Solutions 1-3 only use HE batteries. Solution 4-6 Use HP batteries and solution 7-9 use HE and HP batteries. In solutions 7-9 HP batteries are only there for class requirement satisfaction of DP mode and is not used in auto mode. Solution 10-12 comprise of HE batteries only and is used only in auto mode, it does not meet DP class requirements. The battery energy throughput costs are also presented in Table 3.6. The solution space has been expanded to include three variations of DoD $\in \{-70\%, 75\%, 80\%$ of gross capacity.

Key Performance Matrix

Three key performance indicators are part of the key performance matrix. These are,

1. Payback time
2. Years of profitability
3. Return on investment

Payback time is defined as the total number of years it takes to break even on the initial capital investment. It is given by the formula:

$$\text{Pay Back Time} = \frac{\text{Total Investment}}{\text{Yearly Savings}}. \quad (3.4)$$

The years of profitability are defined as the difference between the battery lifetime and the payback period. The return on investment (ROI) is defined as the ratio of the net income to the initial investment. It is given by the equation:

$$\text{ROI} = \frac{\text{Yearly Savings} \times \text{Years of Profitability} - \text{Total Investment}}{\text{Total Investment}}. \quad (3.5)$$

$$\text{Battery Life Time} = \frac{\text{Total Number of Cycles}}{\text{Yearly Cycles} + \text{Calendar Aging}(\text{Cycle Equivalent})} \quad (3.6)$$

A 3% year on year calendar aging degradation is considered as per [42].

$$\text{Years of Profitability} = \text{Battery Life Time} - \text{Pay Back Time} \quad (3.7)$$

The values of the following performance indicators are set to

$$\begin{aligned} \text{Payback Time} &\leq 6 \text{ years,} \\ \text{Years of Profitability Time} &\geq 4 \text{ years,} \\ \text{ROI} &\geq 0.9 \end{aligned}$$

Table 3.6: Battery solution space

Solution type	Battery size (netto)	Quantity	DoD	Battery type	Gross	Cost (€)	Number of cycles	Company	Cost (€/kWh)
HE	1530	2	0.7	High Energy	4371	2185714	10000	Battery supplier 2	0.0500
HE	1530	2	0.75	High Energy	4080	2040000	7500	Battery supplier 2	0.0667
HE	1530	2	0.8	High Energy	3825	1912500	5000	Battery Supplier 1	0.1000
HP	510	2	0.7	High Power	1457	1165714	12133	Battery Supplier 2	0.0659
HP	510	2	0.75	High Power	1360	1088000	9166	Battery Supplier 2	0.0873
HP	510	2	0.8	High Power	1275	1020000	6200	Battery Supplier 2	0.1290
HE + HP	1000 + 175	2	0.7	High Energy	2857	1564571	10000	Battery Supplier 2	0.0595
HE + HP	1000 + 175	2	0.75	High Energy	2667	1605333	7500	Battery Supplier 2	0.0803
HE + HP	1000 + 175	2	0.8	High Energy	2500	1522000	5000	Battery Supplier 1	0.1218
HE (Auto only)	1000	1	0.7	High Energy	1428	714286	10000	Battery Supplier 2	0.0500
HE (Auto only)	1000	1	0.75	High Energy	1333	666667	7500	Battery Supplier 2	0.0667
HE (Auto only)	1000	1	0.8	High Energy	1250	625000	5000	Battery Supplier 1	0.1000

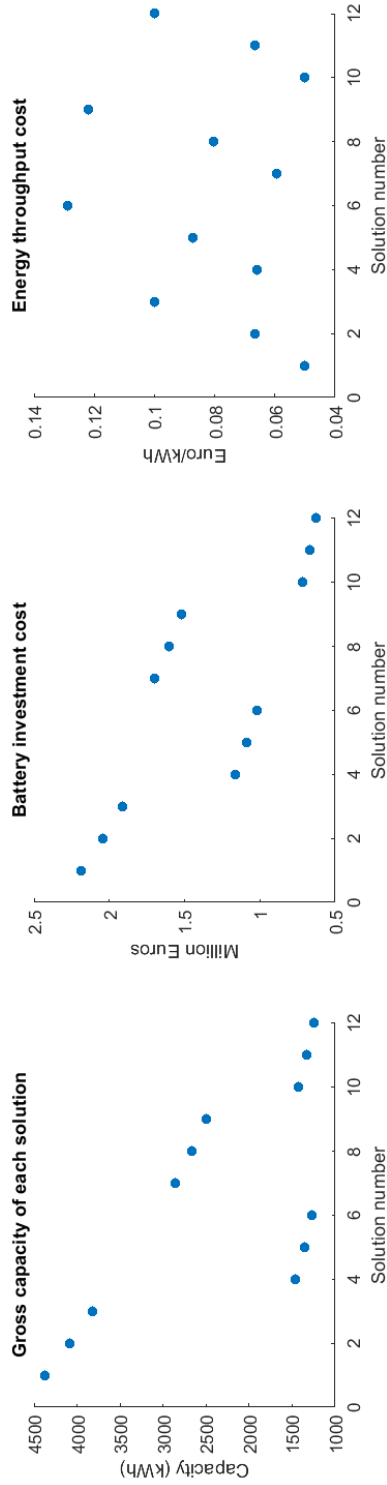


Figure 3.7: Visual description of various solutions

4

Data Analysis of Load Profile

Accurate knowledge of a ship's load power profile is crucial for the effective use of technologies such as energy management systems, power generation systems, and energy storage systems. The propulsion system is a major factor that affects the load power profile, and it can vary significantly depending on weather conditions and operational requirements. This makes it challenging to predict the load power profile for a specific ship. Therefore, it is important to regularly monitor and collect data on a ship's power usage to improve predictions and optimize energy management. This section focuses on performing an event analysis of the load profile to better understand the peak shaving requirements of the ship.

Section 4.1 shows the analysis of the load profile of the vessel recorded in the Taiwan Sea. The data was recorded over the period of 256 days and section 4.2 analysis the data recorded in the North Sea for 285 days.

4.1. Taiwan Sea load profile analysis

The data recorded in the sea in Taiwan comprises of data with a sample rate of 5 mins between each recorded data. Figure 4.1 shows the recorded load profile. The average power during this time period was recorded to be 1054 kW.

Figure 4.2 shows the load profile during the operation of DP mode. It is interesting to note that over the period of 256, the ship operates in a DP mode for 134.5 days. Since the given vessel is a DP-2 vessel, the vessel is expected to operate under extra redundancy during this period. The average power seen during this period was 519 kW and 445 kW on the PS and SB sides respectively. Figure 4.2 shows the operational profile during auto mode for 91.9 days. During this period the tiebreakers are closed (Case 11). The average power seen during this time period was 917 kW. Figure 4.4 represents case 10. This case is non-critical DP mode and spans a total of 9.4 days. During this period the average powers were 896 kW and 897 kW on the PS and SB sides respectively. Similarly, figure 4.5 represents noncritical DP-mode and has average powers of 667 kW and 698 kW respectively.

Table 4.1 shows the DG loading of the generators for the various time periods. It can be seen from the table that the generators are severely under-loaded. This gives the potential room for the hybridization of the power system.

Optimum fuel saving can be observed between 60% to 80% of rated power of DG1 or DG4. This implies minimum a power of 1100kW. In order to analyze the power and energy required for the peak shaving function, an event analysis is done. An event is defined as a situation where the power demand is greater than 1100 kW. The periods for which the power is greater than 1100kW are recorded, and the energy requirements for such periods are also noted in table 4.2. 3 different cases are analyzed, Case 00, Case 00 followed or preceded by 01 or 01. This is because in these situations, the port side and starboard side are always isolated from one another.

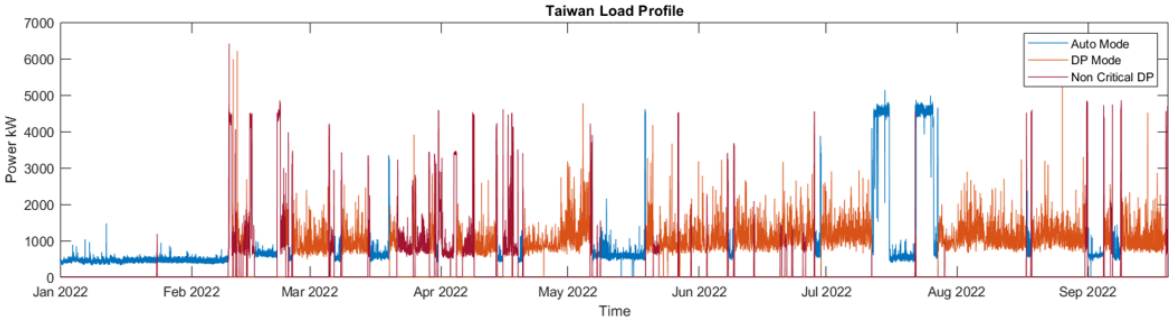


Figure 4.1: 8.5 Months Taiwan load profile

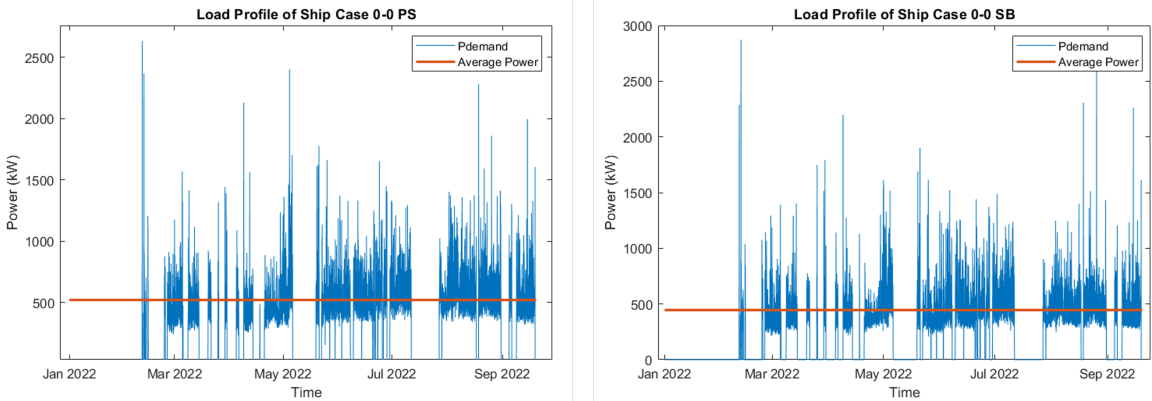


Figure 4.2: DP mode operation (left- port side, right starboard side)

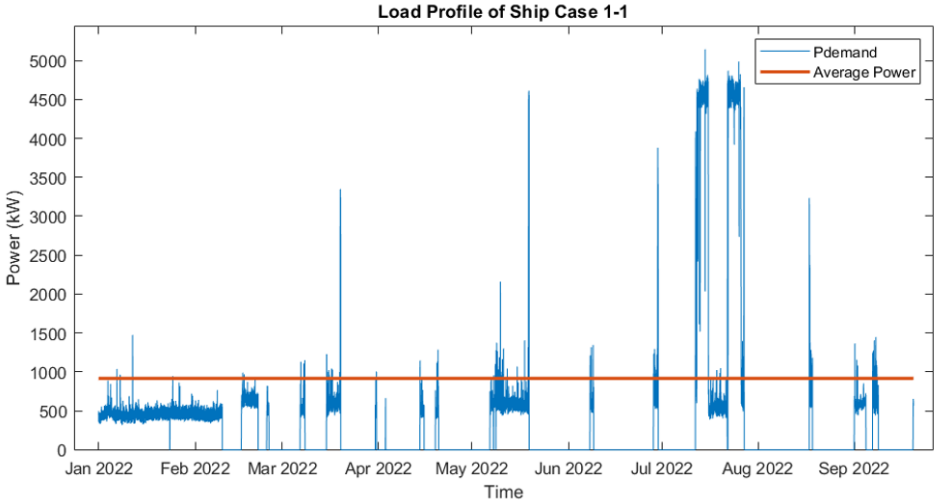


Figure 4.3: Auto mode (11) (Operation (left- port side, right starboard side)

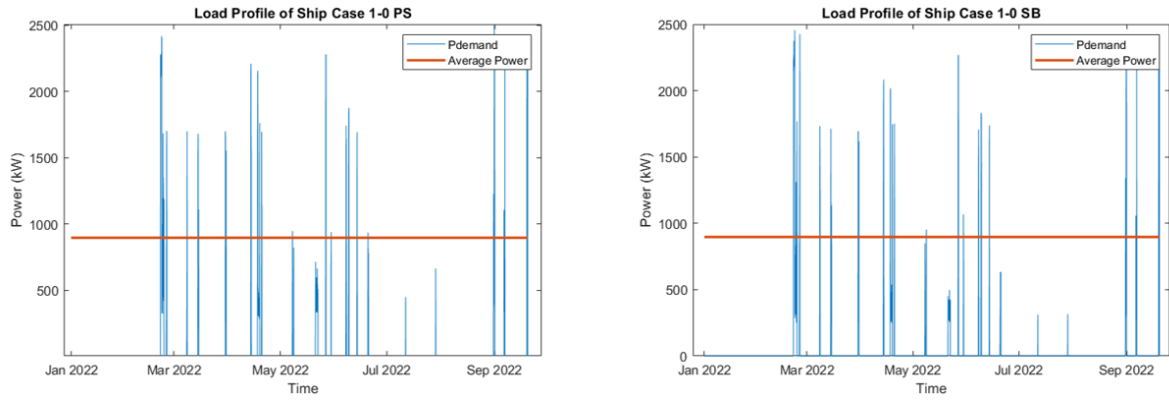


Figure 4.4: NC DP 10 (operation (left- port side, right starboard side))

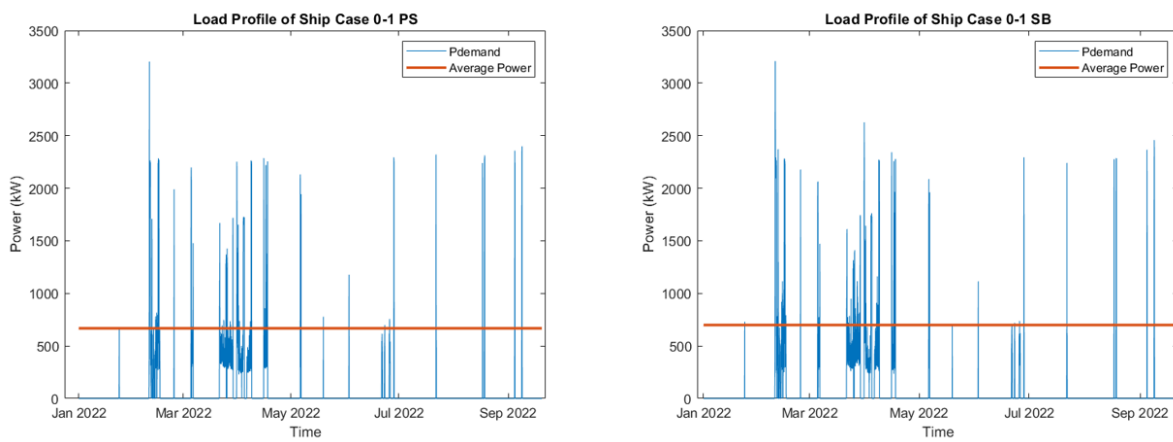


Figure 4.5: NC DP 01 (operation (left- port side, right starboard side))

Table 4.1: Taiwan DG loading

Case	Generator	Loading (%)	Time (days)
11	Only DG1	10-40	35.2
	Only DG4	10-40	42.1
00	DG1	0-30	118.3
	DG2		102.2
	DG3		103
	DG4		118.1
10 + 01	DG1	0-30	20.4
	DG2		8.3
	DG3		9.8
	DG4		18.4

Table 4.2: Event analysis: power

Case	Number of Events	t<30	<30 & 0-300 kW	t<30 & 300-600 kW
00	227	221	168	36
00+01 (PS)	187	156	122	22
00+10 (SB)	132	110	78	15

It can be seen in table 4.2 that a total of 227, 187, and 132 events occurred in the 3 different situations. This is less than one case per day for each situation. In case 00 a total of 221 events out of the total 227 events last for lesser than 30 mins. Of this, 168 such events had a power requirement between 0-300 kW above the 1100 kW threshold. A similar analysis is done for the other 2 situations. Table 4.3 shows the event analysis in terms of energy required when the event period is lesser than 30 mins. The maximum observed requirement lies between 400-500 kWh. This can be achieved with an average power of 200-250 kW at 0.5C.

Table 4.3: Event analysis: energy

Case	<100 kWh	100-200 kWh	200-300 kWh	300-400 kWh	400-500 kWh
00	213	8	0	0	0
00+01 (PS)	146	7	1	1	1
00+10 (SB)	100	6	4	0	0

4.2. North Sea load profile analysis

The data recorded in the North Sea comprises data for 9 months with a sample rate of 1 min between each recorded data. Figure 4.6 shows the recorded load profile. The average power during this time period was recorded to be 1204 kW.

Figure 4.7 shows the load profile during the operation of DP mode. It is interesting to note that over the period of 286 days, the ship operates in DP mode for 115.7 days. The average power seen during this period was 576 kW and 487 kW on the PS and SB sides, respectively. Figure 4.8 shows the operational profile during auto mode for 140 days. During this period, the tiebreakers are closed (Case 11). The average power seen during this time period was 1142 kW. Figure 4.10 represents case 10. This case is non-critical DP mode and spans a total of 10.12 days. During this period the average powers were 1109 kW and 1046 kW on the PS and SB side respectively. Similarly, figure 4.9 represents noncritical DP-mode and has average powers of 1147 kW and 1144 kW respectively.

Table 4.4 shows the DG loading of the generators for the various time periods. It can be seen from the table that the DG's are severely under-loaded. This gives the potential room for the hybridization of the power system.

An event analysis is done where the periods for which the power is greater than 1100kW are recorded, and the energy requirements for such periods are also noted in table 4.5. 3 different cases are analyzed, Case 00, Case 00 followed or preceded by 01 or 01. This is because in this situation the port side and starboard side are always isolated from one another.

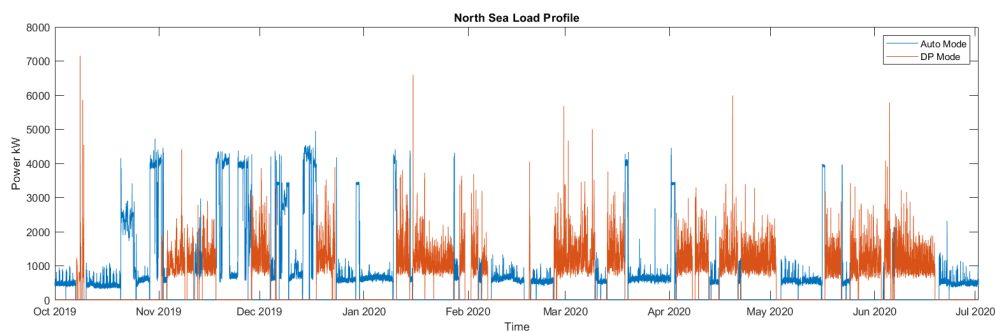


Figure 4.6: 9 Months North Sea load profile

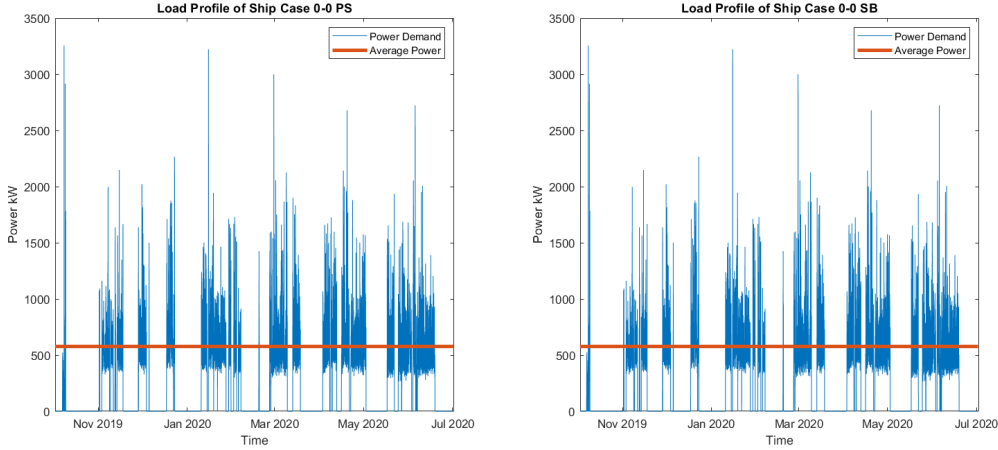


Figure 4.7: DP mode operation (left - port side, right starboard side)

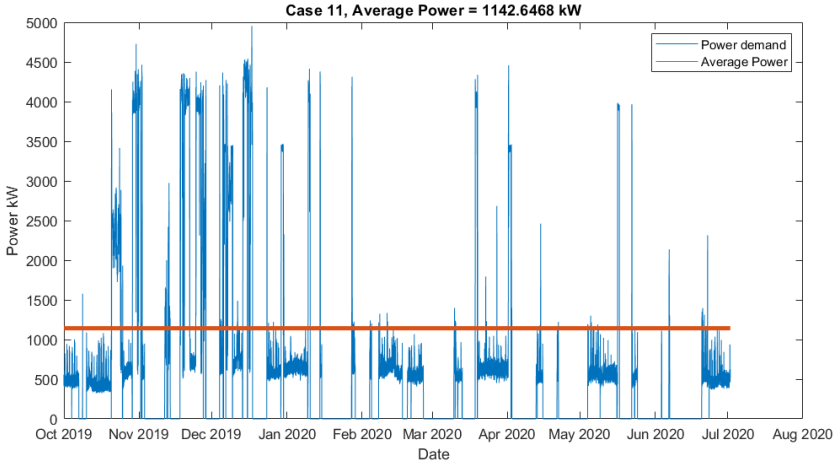


Figure 4.8: Auto mode operation

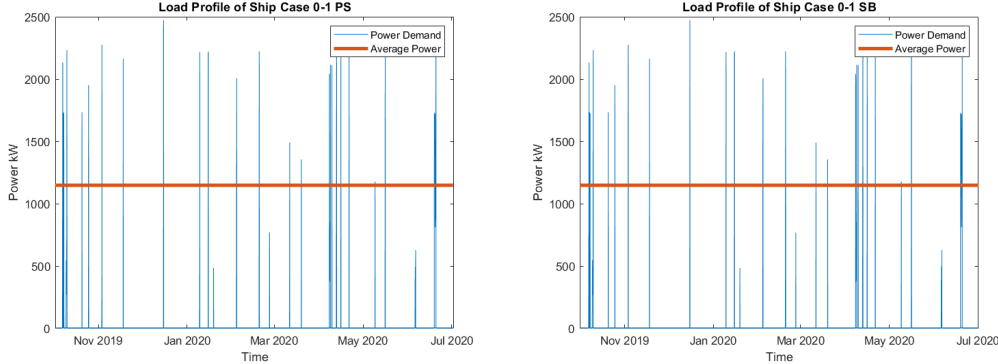


Figure 4.9: Non-critical mode (01) operation

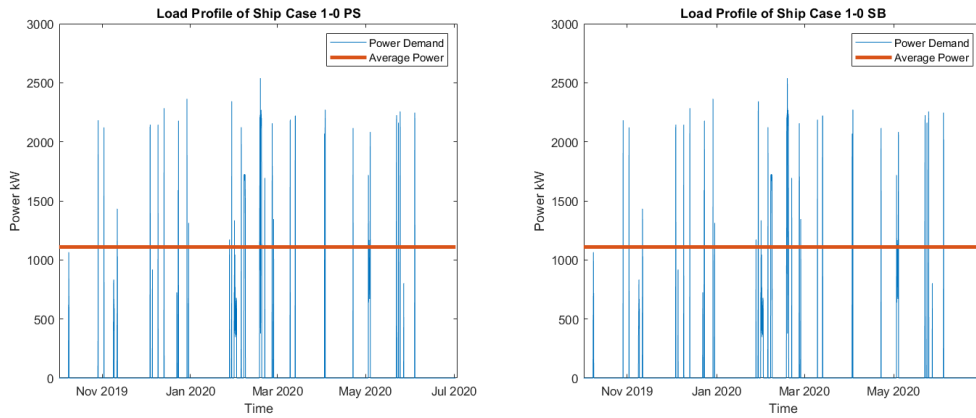


Figure 4.10: Non-critical mode (10) operation

Table 4.4: North Sea DG loading

Case	Generator	Loading (%)	Time (days)
11	DG1	1-30	27.2
	DG4		16.3
	DG3		10.8
	DG2		3.1
00	DG4		65.9
	DG1		63.09
	DG2		61.62
	DG3		53.04
01	All DG's		6.8
10	All DG's		11.9

Table 4.5: Event analysis : power

Case	Number of Events	<5 mins	5-10 mins	10-30 mins
00	1661	1455	112	76
01	125	52	5	21
10	183	92	11	27
11	600	472	23	35

It can be seen in table 4.5 that a total of 1661, 125 and 183, and 600 events occurred in the 4 different situations. In case 00 a total of 1661 events out of the total 1445 (87%) events last for lesser than 5 mins. Table 4.6 shows the event analysis in terms of energy required when for various time periods. It can be observed that the most frequent of the energy requirements above 1100 kW lies less than 100 kWh.

Table 4.6: Event analysis : energy

Case	<100 kWh	100-200 kWh	200-300 kWh	300-400 kWh
00	1461	119	25	21
01	56	3	2	6
10	96	6	10	5

5

MILP Optimization

Intlinprog on MATLAB is used to solve the global optimization problem [91]. The solver is capable of minimizing an objective function while considering, equality, inequality, upper bound, lower bound, and integer constraints. Section 5.1 describes the various aspects of considerations of the MILP model. Section 5.2 describes the different variables and constants in the MILP model. Section 5.3 illustrates the various constraints in the optimization model. Section 5.5 presents the variable conditions for different optimization scenarios.

5.1. Model considerations

The mathematical model developed considers the following,

1. Fuel price
2. Fuel savings
3. Cycle calculation
4. Maintenance savings through generator limits
5. Energy throughput costs

The model is simulated for all four cases of the tie-breaker position. In auto mode, the battery is allowed to charge / discharge. Whereas in other cases, the battery assumes the role of a virtual generator, and only necessary generators are turned on. The NC DP and DP modes are optimized by running the MILP model separately for the PS and SB side. The auto-mode is optimized without and with BOOSTER considering the energy throughput costs. The results obtained are shared in Chapter 6.

5.2. Decision variables and constants

Decision variables can take a specific value to minimize or maximize an objective function. There are two types of variables in MILP programming. Integer variables and continuous variables. The integer variables can take the values of 0 or 1. The continuous variables can take in any value between a specified range. The variables chosen are listed in table 5.1. The subscript i denotes the DG number, while the subscript t denotes the time step.

Table 5.1: Mathematical modelling notations

Notation	Units	Variable type	Comment
u_{it}	–	Boolean variable	DG ON/OFF state
PG_{it}	kW	Variable	DG power output
$Ebat_t$	kWh	Variable	Battery charge
Ton_i	–	Boolean variable	Generator ON segment
$Ebatcharging_t$	kWh	Variable	Battery charging
Uon_{it}	–	Boolean variable	DG turn on
$\delta_{i,i't}$	–	Boolean variable	$DG_i, DG_{i'}$ parallel loading
M_t	–	Boolean variable	Battery charging state
α_i	$\frac{tons}{kW}$	Constant	SFOC curve
β_i	$Tons$	Constant	SFOC curve
C_i	$Tons$	Constant	Generator startup cost
PG_{rated_i}	kW	Constant	DG rated power
ETC	$\frac{\epsilon}{kWh}$	Constant	Energy throughput cost
<i>Lower limit</i>	–	Constant	Lower bound of DG power
<i>Upper limit</i>	–	Constant	Upper bound of DG power
E_{max}	kWh	Constant	Maximum possible battery power
C_{rate}	C	Constant	Charging / discharging rate
P_{demand_t}	kW	Constant	Power demand
N_{cycles}	<i>Cycles</i>	Constant	Maximum battery cycles
Δt	<i>Hours</i>	Constant	Sample time
M, X	–	Constant	Big M integer
$MinTime$	<i>Hours</i>	Constant	Minimum generator ON time
Ri_{rate}	–	Constant	% of DG ramp up-down allowed
η	–	Constant	One way charging / discharging efficiency

5.3. Objective function

An objective function is a mathematical expression that describes the quantity to be minimized or maximized in an optimization problem. The objective function to be minimized is,

$$Obj(\epsilon) = FOC + Startup\ Costs + Energy\ Throughput\ Cost. \quad (5.1)$$

Here, FOC is the fuel oil consumption cost of the DG that is cost due to the production of electrical power. Startup costs are costs associated with starting up the DG. The ETC is the energy throughput costs of the battery system.

5.3.1. FOC cost function

The fuel oil consumption of the DG was previously described in section 3.1. The SFOC graphs of Generators DG1-5 have been described in equations (3.1), (3.2), (3.3).

$$FOC = Price\ of\ Fuel \times \sum_{t=1}^T \left(\sum_{i=1}^{DG_n} (\alpha_i \times PG_{it} + \beta_i) \right) \times \Delta t \quad (5.2)$$

Here, T refers to the final time step that the cost function must minimize, and DG_n refers to the generators that are to be included in the cost function. DG_n represents the DG's where n is a subset of values belonging to $\{1, 2, 3, 4, 5\}$. The objective is to minimize this function.

5.3.2. Start up cost function

The startup costs of the DG refer to the amount of fuel consumed by the DG to start up. This model considers the shut-down costs to be included in the start-up cost since if a DG starts up, it must also

shut down at some point.

$$\sum_i^T \left(\sum_{i=1}^{DG_n} (0.5 \times C_i ((u_{it} - u_{i(t-1)}) + (u_{it} - u_{i(t-1)})^2)) \right) \quad (5.3)$$

Here, T refers to the final time step that the cost function must minimize. C_i refers to the fuel costs that the generator i takes to start and stop. The objective is to minimize this function.

The equation (5.3) is formulated for MINLP. For MILP the equations are as follows,

$$u_{it} - u_{i(t-1)} \geq 1 + 0.001 - M(1 - Uon_{it}) \quad (5.4)$$

$$u_{it} - u_{i(t-1)} \leq 1 + M(Uon_{it}) \quad (5.5)$$

$$C_i \times \sum_i^T \left(\sum_{i=1}^{DG_n} (Uon_{it}) \right) \quad (5.6)$$

Here, u_{it} represents the state of the DG (ON/OFF). Uon_{it} is a boolean variable that is 1 only at the time step that DG_{it} turns ON. M is a big integer value. The objective function aims to minimize equation (5.6).

5.3.3. Battery throughput cost

The battery throughput costs are considered by adding the battery capacity used and multiplying it with the energy throughput costs (€ per kWh).

$$ETC \times \sum_i^T Ebatcharging_t \quad (5.7)$$

Here, $Ebatcharging_t$ is the total amount of charging a battery undergoes at time t . The value is 0 if it is not charging.

5.4. Constraints

As stated earlier, constraints are linear, inequality, upper bound, and lower bound constraints. This section will discuss the constraints of the model.

5.4.1. Lower bound and upper bound constraints

Unit Commitment Constraints

The unit commitment variable u_{it} can take only the values of 1 or 0. Hence the variable must be greater than or equal to zero and lesser than or equal to 1.

DG constraints

These constraints are for the decision variable PG_{it} . Lower bound constraints refer to the minimum amount of power a generator can operate at. This constraint can be represented by,

$$PG_{it} \leq Lower.limit \times PG_{ratedi} \quad (5.8)$$

Upper bound constraints refer to the maximum amount of power a generator is allowed to operate at. This constraint is represented by:

$$PG_{it} \geq Upper.limit \times PG_{ratedi} \quad (5.9)$$

The lower limit value is set for 40% of the DG-rated power (from maintenance curves) and the upper limit value requested is 80% of the generator-rated power.

Energy storage constraint

These constraints are for the decision variable $Ebat_t$. At any given point in time, the decision variable cannot go below 0 and above the maximum possible storage capacity (E_{max}).

$$Ebat_t \geq 0 \quad (5.10)$$

$$Ebat_t \leq E_{max} \quad (5.11)$$

Minimum ON-time variable

The minimum ON-time variable is an integer variable. Hence, the variable should be equal to 0 or 1.

Battery charging variable

These constraints are for the decision variable $Ebatcharging_t$. At any given point in time, the decision variable cannot go below 0 and the C-rate of the battery limits the maximum possible value it can take. The constraints are represented as,

$$Ebatcharging_t \leq C_{rate} \times E_{max} \Delta t, \quad (5.12)$$

$$Ebatcharging_t \geq 0. \quad (5.13)$$

$Ebatcharging_t$ holds the values of the battery capacity when it is charging.

5.4.2. Inequality constraint

Inequality constraints are represented as lesser than or equal to constraints in MATLAB.

Unit commitment and DG Relationship

The unit commitment u_{it} and power generation PG_{it} variables are related by the equations below,

$$PG_{it} \geq u_{it} \times PG_{ratedi} \times Lower.limit \quad (5.14)$$

$$PG_{it} \leq u_{it} \times PG_{ratedi} \times Upper.limit \quad (5.15)$$

Here, if the generator is off, $u_{it} = 0$ and PG_{it} takes the value of 0. If the generator is on, $u_{it} = 1$, and PG_{it} takes the value that the lower bound constraints allow.

Maximum and minimum DG ramp rate

DG's have a maximum amount of rate at which they can increase or decrease their production. This is represented as Ri_{rate} and is a constant value for generator i .

While ramping up:

$$PG_{it} - PG_{i(t-1)} \leq ((0.3 \times (1 - u_{i(t-1)})) + Ri_{rate}) \times PG_{ratedi}, \quad (5.16)$$

and while ramping down,

$$PG_{i(t-1)} - PG_{it} \leq ((0.3 \times (1 - u_{i(t)})) + Ri_{rate}) \times PG_{ratedi}, \quad (5.17)$$

Maximum and minimum C-rate constraint

The minimum C-rate constraint ensures that the battery system does not charge/discharge more than it is technically capable of. A single charging and discharging C-rate is considered. If a battery is capable of charging at a specified C-rate then the following conditions apply.

When charging,

$$Ebat_t - Ebat_{t-1} \leq C_{rate} \times E_{max} \times \Delta t, \quad (5.18)$$

and when discharging,

$$Ebat_{t-1} - Ebat_t \leq C_{rate} \times E_{max} \times \Delta t. \quad (5.19)$$

Big M method for charging Calculation

In linear formulation, using $\max(A, B)$ directly in the model is not possible. To create a linear formulation, an auxiliary continuous variable must be defined. This continuous variable is defined as $Ebatcharging_t$. In addition, another decision variable is called "The big M" variable M_t . must be introduced to force the value of $Ebatcharging_t$ to take the maximum between two numbers. The following equations apply:

$$Ebatcharging_t \geq 0, \quad (5.20)$$

$$Ebatcharging_t \geq Ebat_t - Ebat_{t-1}, \quad (5.21)$$

$$Ebatcharging_t \leq 0 + M \times M_t, \quad (5.22)$$

$$Ebatcharging_t \leq Ebat_t - Ebat_{t-1} + M \times (1 - M_t). \quad (5.23)$$

If $Ebat_t - Ebat_{t-1} > 0$, the value of M_{T-1} is 0 and $Ebatcharging_t$ is forced to take the positive difference. If $Ebat_t - Ebat_{t-1} < 0$, then M_{T-1} is 1 and $Ebat_t - Ebat_{t-1}$ is forced to 0.

Limiting battery degradation

The number of cycles per time segment T_s is represented by N_{cycles} . The number of charging cycles can be limited with the following relations:

$$\sum_{t=1}^{T_s} E_{bat_{charging}t} \leq E_{max} \times N_{cycles}. \quad (5.24)$$

Parallel loading of DG

When 2 or more generators are online at the same time, the generators are parallely loaded. The loading of generators in parallel is done similarly to the work done by the authors in [27]. The equations below show the linear formulation for parallel loading of generators.

Table 5.2: Parallel loading

DG 1	DG 2	DG 3	Variable
0	1	1	$\delta_{2,3}$
1	0	1	$\delta_{1,3}$
1	1	0	$\delta_{1,2}$
1	1	1	$\delta_{1,2,3}$

The relationship for parallel loaded generators shown below for Generator 1 and Generator 3 are on:

$$u_{2t} + u_{3t} \geq 1 + 0.001 - M \times (1 - \delta_{2,3}), \quad (5.25)$$

$$u_{2t} + u_{3t} \leq 1 + M \times \delta_{2,3}, \quad (5.26)$$

$$\frac{PG_{3t}}{PG_{3rated}} - M \times (1 - \delta_{2,3}) \leq \frac{PG_{2t}}{PG_{2rated}} \leq \frac{PG_{3t}}{PG_{3rated}} + M \times (1 - \delta_{2,3}) \quad (5.27)$$

5.4.3. Equality constraint

Load balance

The equality constraint for load balance guarantees that the electrical system receives adequate power. The load balance can be in one of two modes, depending on whether the battery is charging or discharging. While Charging,

$$E_{bat_t} = E_{bat_{t-1}} + \eta \times \Delta t \left(\sum_{i=1}^T PG_{it} - P_{demand_t} \right) \quad (5.28)$$

This can be mathematically modelled as,

$$E_{bat_t} \geq E_{bat_{t-1}} + \eta \times \Delta t \left(\sum_{i=1}^T PG_{it} - P_{demand_t} \right) - X \times (1 - M_t) \quad (5.29)$$

$$E_{bat_t} \leq E_{bat_{t-1}} + \eta \times \Delta t \left(\sum_{i=1}^T PG_{it} - P_{demand_t} \right) + X \times (1 - M_t) \quad (5.30)$$

While discharging,

$$E_{bat_t} = E_{bat_{t-1}} - \frac{\Delta t \left(P_{demand_t} - \sum_{i=1}^T PG_{it} \right)}{\eta} \quad (5.31)$$

This can be linearly modelled as,

$$E_{bat_t} \geq E_{bat_{t-1}} - \frac{\Delta t \left(P_{demand_t} - \sum_{i=1}^T PG_{it} \right)}{\eta} - X \times M_t \quad (5.32)$$

$$Ebat_t \leq Ebat_{t-1} - \frac{\Delta t \left(P_{demand_t} - \sum_{i=1}^T PG_{it} \right)}{\eta} + X \times M_t \quad (5.33)$$

Here, η is the charging-discharging efficiency and X is a big integer equal to 8×10^3 . A round trip efficiency of 96% is considered. P_{demand} is the demand power at time t .

Minimum time ON constraint

The minimum ON-time ensures that the generators are on for a minimum specific duration. This is described by the equation:

$$\sum_{t=1}^{Min\ Time} (u_{it}) = Min\ Time \times Ton_i \quad \forall T. \quad (5.34)$$

Here Ton_i is a boolean decision variable that ensures that the sum of the unit commitment variable U_{it} is either ON for the minimum specified duration or OFF. The value of minimum ON-time is set to 20 minutes.

5.5. Optimization method

As mentioned earlier, the MILP optimization is performed on each "section" of the data for different cases. This "section" comprises of a continuous time period where the mode is auto mode or NC DP or DP mode. The individual results of these sections are then grouped together and presented as a result for the whole load profile.

The optimization is performed first with no energy throughput costs. The best solution is then performed considering energy throughput costs. The results for the two are shown in Section 6.1 and 6.2. When no energy throughput costs are considered, the price of fuel in equation (5.2) is considered as 1 to find the total fuel saved. The daily fuel prices are considered to find the cost of fuel saved in the objective function, and the energy throughput costs are considered as 0 (equation (5.7)).

Table 5.3 show the limits of variables and specific constant values for the different modes of operation. The battery capacity at the end of auto mode is set to the maximum net capacity to behave as a virtual generator in DP or NC DP modes. The maximum possible C-rate allowed is set to 0 as the battery operates as a virtual generator in DP or NC DP modes. In addition to this, $Ebatcharging_t$ is set to 0 for DC and NC DP modes. It is important to mention that the RAMP limit and minimum time on constraint had little to no effect on the results and was eventually deactivated. This was because of the large time step size.

Table 5.3: Variable limits and constant values

Notation	Auto mode	NC DP and DP mode
α_i	As per table 3.5	As per table 3.5
β_i	As per table 3.5	As per table 3.5
C_i	As per table 3.5	As per table 3.5
PG_{ratedi}	As per table 3.1	As per table 3.1
ETC	As per table 3.6	As per table 3.6
<i>Lower limit</i>	0.4	0.2
<i>Upper limit</i>	0.8	0.8
E_{max}	As per table 3.6	As per table 3.6
C_{rate}	1C for HE bat, 3C for HP	1C for HE bat, 3C for HP
P_{demand_t}	North Sea and Taiwan	North Sea and Taiwan
N_{cycles}	As per table 3.6	As per table 3.6
Δt	1/60 NS, 1/12 Taiwan	1/60 NS, 1/12 Taiwan
M, X	8000, 8000×10^6	8000, 8000×10^6
$MinTime$	1/3 hours	1/3 hours
Ri_{rate}	0.5	0.5
η	0.98	0.98

Since fuel prices vary over the period of the year, 3 different scenarios are considered. These scenarios are shown in table 5.4. Each solution is optimized for each of three scenarios.

Table 5.4: Fuel price per scenario

Scenario number	Percentage of time		
	450 €/ton	650 €/ton	850 €/ton
1	33	50	17
2	50	33	17
3	50	50	0

For the outer loop maintenance savings calculation, the value of Cdg_n is considered as 250,000 euros for all the five generators.

6

Results and Discussion

In section 6.1, the text delves into the fuel savings measured in tons without factoring in energy throughput costs. Moreover, the section also highlights the fuel savings achieved when energy costs are not considered, along with the maintenance savings attributed to overhaul costs. Section 6.2 discusses the usage of batteries considering the energy throughput costs and the recommendation for the PMS-EMS. Section 6.3 presents the payback period and years of profitability for 3 different fuel price scenarios. Finally, section 6.4 answers the research questions.

6.1. Result : No energy throughput costs

Figure 6.1 shows the optimized results for Taiwan. The figure comprises of three plots, i.e., daily fuel consumption, cumulative fuel consumed, and the number of cycles. Since no energy throughput costs are incorporated into the model, the fuel savings and the number of cycles can be grouped based on similar battery net capacities and power capabilities. Table 6.1 summarises the simulated model's findings for Taiwan over 256 days. Solutions 4-6 and solutions 7-9 are not visible in subplot 2 due to results being very close to solutions 1-3.

Table 6.1: Taiwan result - no energy throughput cost

Solution Number	Fuel Savings (tons)	Number of Cycles	Time Period (days)
1-3	425.08	289.7	256
4-6	424.9	644.7	
7-9	416.3	400	
10-12	98.3	652.2	

The maximum fuel savings observed is in the case of HE solutions (1-3) where 425.08 tons of fuel is saved. Solutions 10-12 provide the least amounts of fuel saved. The most fuel saved is in the DP and Non-Critical DP modes. This is due to the absence of redundant generators operating at low operational points.

Least number of cycles are observed in solutions 1-3. This is due to the low charging rates and larger battery capacity. The percentage of fuel savings is depicted in figure 6.2 for solutions 1-9. The fuel savings for solutions 10-12 all come in auto mode.

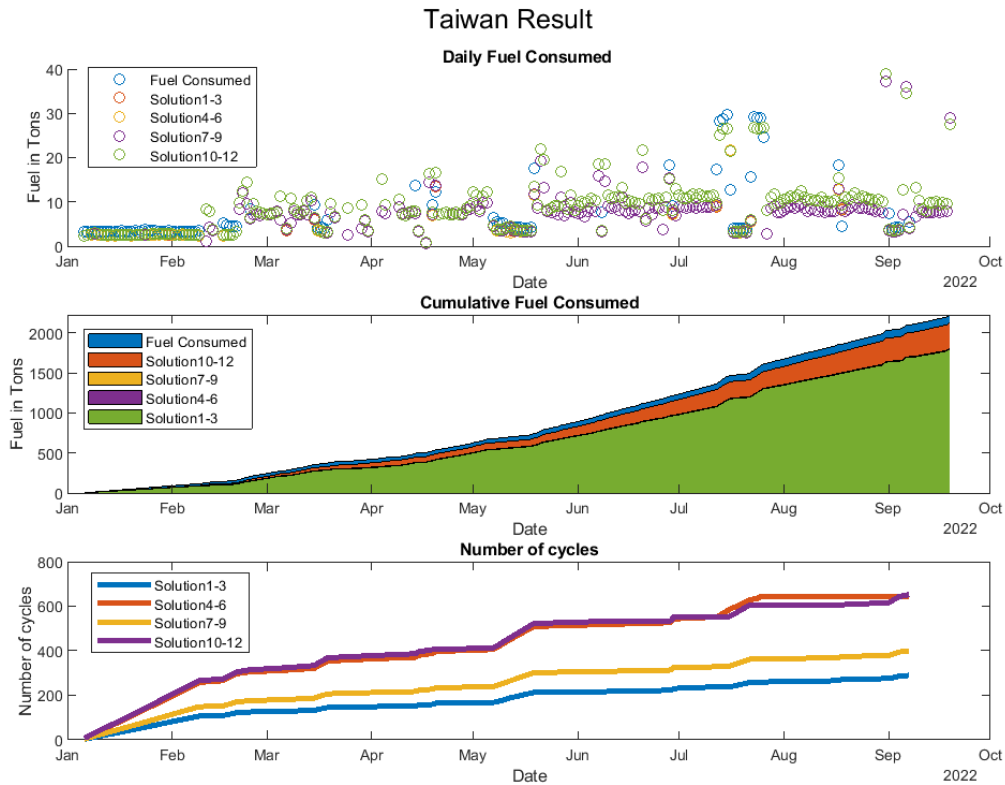


Figure 6.1: Optimized Taiwan results

Solution 1-9 Fuel savings as a percentage

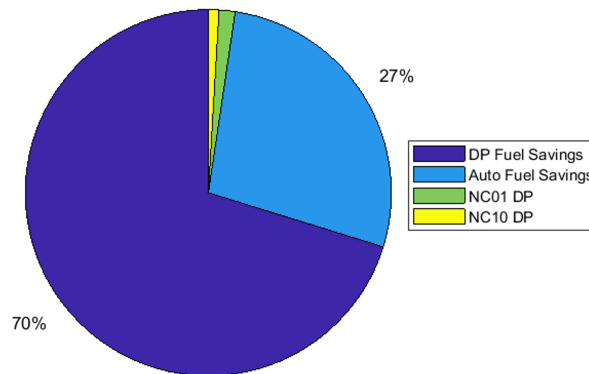


Figure 6.2: Percentage of fuel savings per scenario - Taiwan

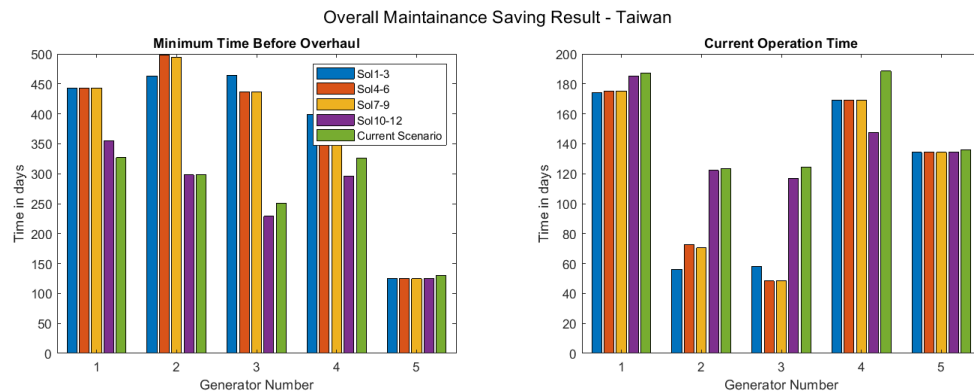
Table 6.2, 6.3 represent the running time of generators prior to the time before overhaul and the current running time. The solutions are represented for five DG's and for 12 solutions. It can be observed that the minimum time for an overhaul in the optimized solutions is higher as a result of the higher loading of the generators. This directly leads to maintenance savings. Table 6.3 shows that certain generators have a higher operational time in the optimized solution. This is a result of turning OFF generators and minimizing the use of alternate generators. The results of table 6.3 and 6.2 are graphically depicted in figure 6.3.

Table 6.2: Taiwan DG - maintenance

	Running Time of Generators Before Overhaul (Days)				
	Solution 1-3	Solution 4-6	Solution 7-9	Solution 10-12	Current Scenario
DG-1	442.6	443.5	443.5	354.7	326.9
DG-2	463.4	498.4	494.8	297.9	298.8
DG-3	464.7	436.9	436.9	228.8	250.4
DG-4	398.3	398.3	398.3	296.2	326.2
DG-5	124.8	124.8	124.8	125.1	130.4

Table 6.3: Taiwan DG - running time

	Running Time of Generators (Days)				
	Solution 1-3	Solution 4-6	Solution 7-9	Solution 10-12	Current Scenario
DG-1	174.3	175.3	175.3	185.0	187.4
DG-2	56.3	72.5	70.4	122.2	123.5
DG-3	58.2	48.4	48.4	116.9	124.4
DG-4	169.3	169.3	169.3	147.3	188.5
DG-5	134.2	134.2	134.2	134.4	136.1

**Figure 6.3:** Optimized Taiwan results

The figure 6.4 shows the optimized results for North Sea. The figure comprises of three plots, i.e daily fuel consumption, cumulative fuel consumed and number of cycles. Since no energy throughput costs are incorporated into model, the fuel savings and number of cycles can be grouped based on similar battery net capacities and power capabilities. Table 6.4 summarises the findings of the simulated model for Taiwan over a period of 285 days.

Table 6.4: North Sea Result - no energy throughput cost

Solution Number	Fuel Savings (tons)	Number of Cycles	Time Period (days)
1-3	470.9	357.1	285
4-6	467.3	900.9	
7-9	459.6	554.1	
10-12	152.6	925.6	

The maximum fuel savings observed as in the North Sea is in the case of High Energy solutions 470.9 tons of fuel saved. Solutions 10-12 provide the least amounts of fuel saved. The largest portion of fuel saved is in the DP and Non-Critical DP modes. This is due to the absence of redundant generators operating at low operational points. The least number of cycles are observed in solutions 1-3. This is due to the low charging rates and larger battery capacity. The percentage of fuel savings is depicted

in figure 6.5 for solutions 1-9. The fuel savings for solutions 10-12 all come in auto mode. 61 % of the fuel saved comes in DP mode, whereas 38 % is in auto mode. However, all the battery cycles are exhausted in auto mode. Solutions 4-6 and solutions 7-9 are not visible in subplot 2 due to results being very close to solutions 1-3.

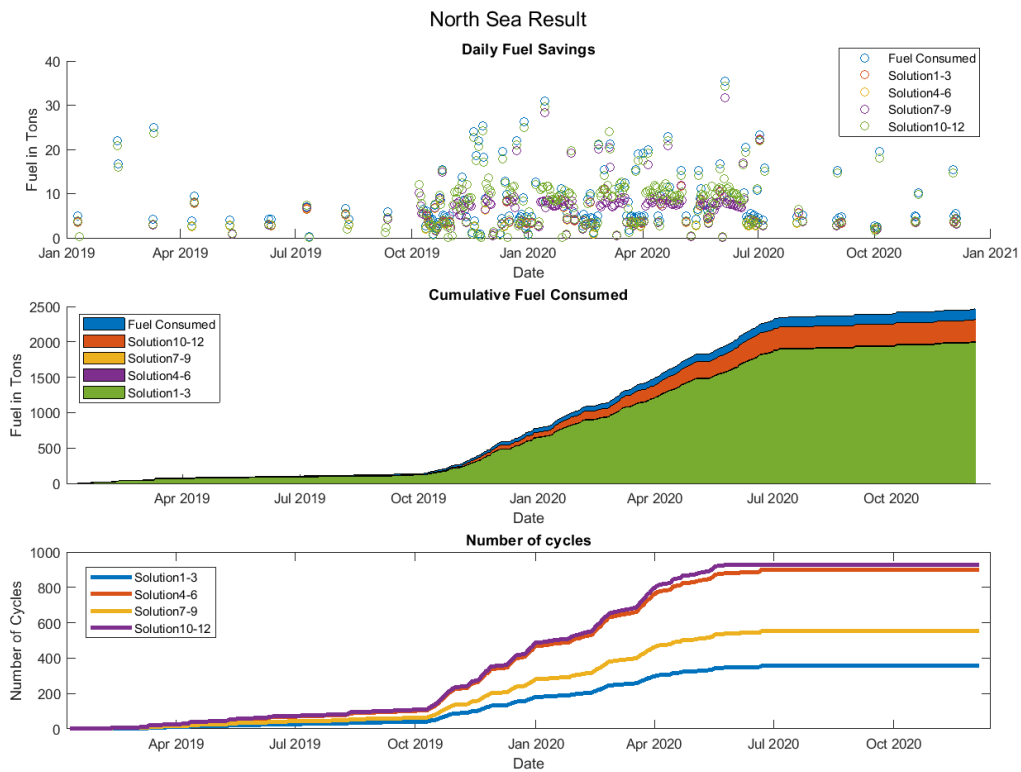


Figure 6.4: Optimized North Sea results

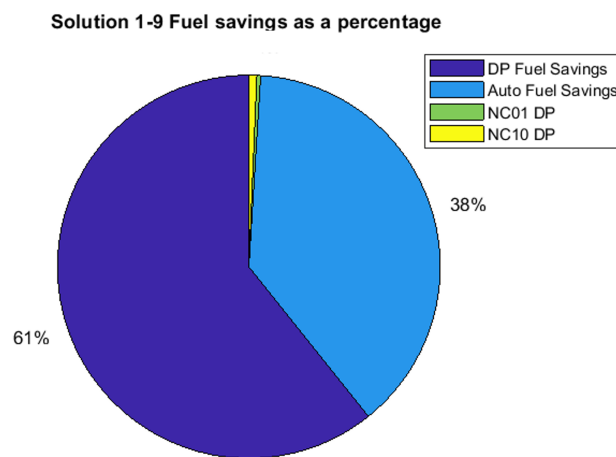


Figure 6.5: Percentage of fuel savings per scenario - North Sea

Table 6.5, 6.6 represent the running time of generators prior to the time before overhaul and the current

running time. The solutions are represented for five generators and for twelve solutions.

It can be observed that the minimum time for an overhaul in the optimized solutions is higher as a result of the higher loading of the generators. This directly leads to maintenance savings. In table 6.6 we can observe that certain generators have a higher operational time in the optimized solution. This is a result of turning off generators and minimizing the use of alternate generators. The results of table 6.6 and 6.5 are graphically depicted in figure 6.6.

Table 6.5: North Sea DG - maintenance

	Running Time of Generators Before Overhaul (Days)				
	Solution 1-3	Solution 4-6	Solution 7-9	Solution 10-12	Current Scenario
DG-1	486.7	505.0	495.2	452.1	378.9
DG-2	603.3	603.1	603.0	440.1	393.6
DG-3	619.6	619.2	619.2	369.7	339.7
DG-4	414.7	414.7	414.7	378.4	406.3
DG-5	151.3	151.3	151.3	151.1	303.8

Table 6.6: North Sea DG - running time

	Running Time of Generators (Days)				
	Solution 1-3	Solution 4-6	Solution 7-9	Solution 10-12	Current Scenario
DG-1	145.4	168.5	155.4	140.9	145.3
DG-2	57.5	67.3	77.7	111.3	91.6
DG-3	34.4	21.1	21.1	87.6	100.2
DG-4	127.5	127.5	127.5	79.9	107.2
DG-5	115.6	115.6	115.6	115.7	183.4

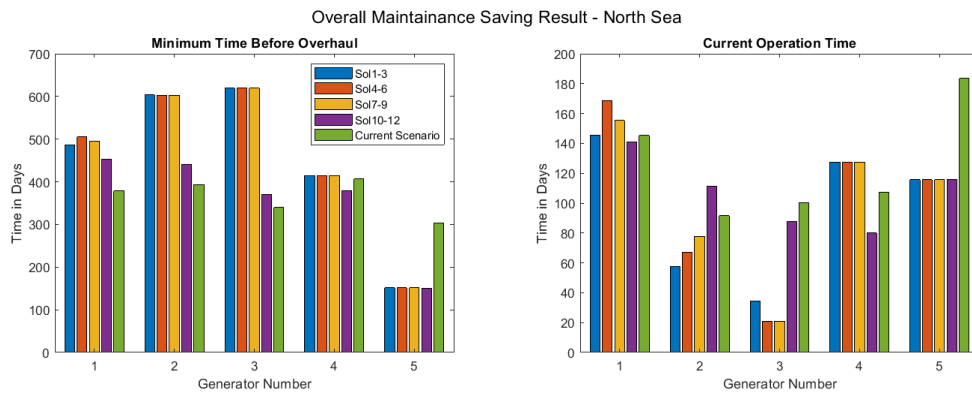


Figure 6.6: Optimized North Sea results

The annual savings and maintenance are calculated based on the average of the results obtained in Taiwan and the North Sea in table 6.7. The fuel savings in solutions 1-9 don't differ greatly due to the deep cycling of the batteries. However, they have a significant impact on the lifetime of the batteries since the high-power solutions have a lower energy capacity and a higher charging rate. Significant DG maintenance savings are also observed in solutions 1-9.

Solution 1 has the highest lifetime, this solution can be considered highly attractive for new-build vessels with a lifetime of 13+ years. Moderate solutions such as 2,7 are interesting for re-fit projects that are expected to last around 10-11 years. Solutions 3,4,8 could be of interest based on the ROI.

Table 6.7: Solutions summarized (Taiwan + North Sea)

Annualised result for Taiwan + North Sea			
Solution Number	Annual Fuel Savings (tonnes)	DG Maintenance Savings (€)	Life Time (years)
1	604.5	101863	13.6
2	604.5	101863	11.36
3	604.5	101863	8.54
4	601.5	100472	8.67
5	601.5	100472	6.99
6	601.5	100472	5.07
7	590	100706	10.64
8	590	100706	8.67
9	590	100706	6.33
10	167.5	16000	7.37
11	167.5	16000	5.85
12	167.5	16000	4.14

6.2. Result: Throughput energy costs - Alewijnse BOOSTER - Battery optimization for optimal sizing and throughput energy regulation

The energy throughput costs are considered as per table 3.6. The results of the inclusion of energy throughput costs can be seen in figure 6.7. The x-axis represents the fuel price in Euros and the y-axis represents the Power demand. The MILP model developed recommends the usage of batteries in the regions that are colored in blue only. In regions that are colored white, it is not recommended to use the battery. This means that the incremental fuel savings obtained by increasing the loading percentage of the DG set outweigh the energy throughput costs of the battery energy storage system in regions colored in blue. However, for regions colored in white, the energy throughput costs outweigh the additional fuel savings realized.

Solutions 1,7,10 have the highest regions of operation due to their lower throughput costs. This is an important observation for the vessel owner to ensure its usage only in these conditions to maximize the lifetime of the battery system and also the ensure profitability per cycle of operation in auto mode. The MGO Fuel price as seen in the port of Rotterdam in [92] shows a great degree of variability (650 € - 1377 € per ton) over the last 1.5 years. This could make the ETC of solutions 1,7,10 highly lucrative as their operation in auto mode would also result in profitability.

Solutions 2,4,11 have a limited region of operation due to their slightly higher throughput costs. It is advised to use these solutions and go ahead with the investment if the predicted future fuel prices are consistent with what has been observed over the last 1.5 years. Investment in these solutions doesn't yield complete profitability in case of lower fuel prices, however, fuel savings in DP mode (case 00) could potentially make these solutions worthwhile if there are initial capital investment constraints.

Solutions 3,5-9,12 have no region of operation due to their higher throughput costs. It is not advised to use these solutions if the predicted future fuel prices are consistent with what has been observed over the last 1.5 years. The break-even fuel price is 1650 € per ton of fuel for a power demand of 450 kW. Investment in solutions 3, 5-9 could yield profitability on the investment due to their savings in DP mode. Solution 12 does not have any such savings in DP mode.

Alewijnse **BOOSTER** - Battery Optimization for Optimal Sizing and Throughput Energy Regulation considers : energy throughput costs during the optimal sizing and operation of the battery system, providing optimal return on every kwh invested. The BOOSTER algorithm is implemented for solution 7 and the improved key performance indicators are shown in figure 6.9.

6.3. Result: Payback time and years of profitability

The payback time and years of profitability are considered for 3 different scenarios. The payback time is calculated by dividing the capital investment of each solution by annual savings per year. The years of profitability are calculated by subtracting the expected lifetime from the payback period.

The payback period is depicted in table 6.9 and the years of profitability are provided in table 6.10. Solution 6 provides the fastest payback period between 3.6-3.9 years. The highest payback periods for two battery solutions are seen in solution 1 which spans from 6.3-6.8 years. Solutions 10-12 have the least lucrative payback periods and the least number of years of profitability, thus making them infeasible solutions.

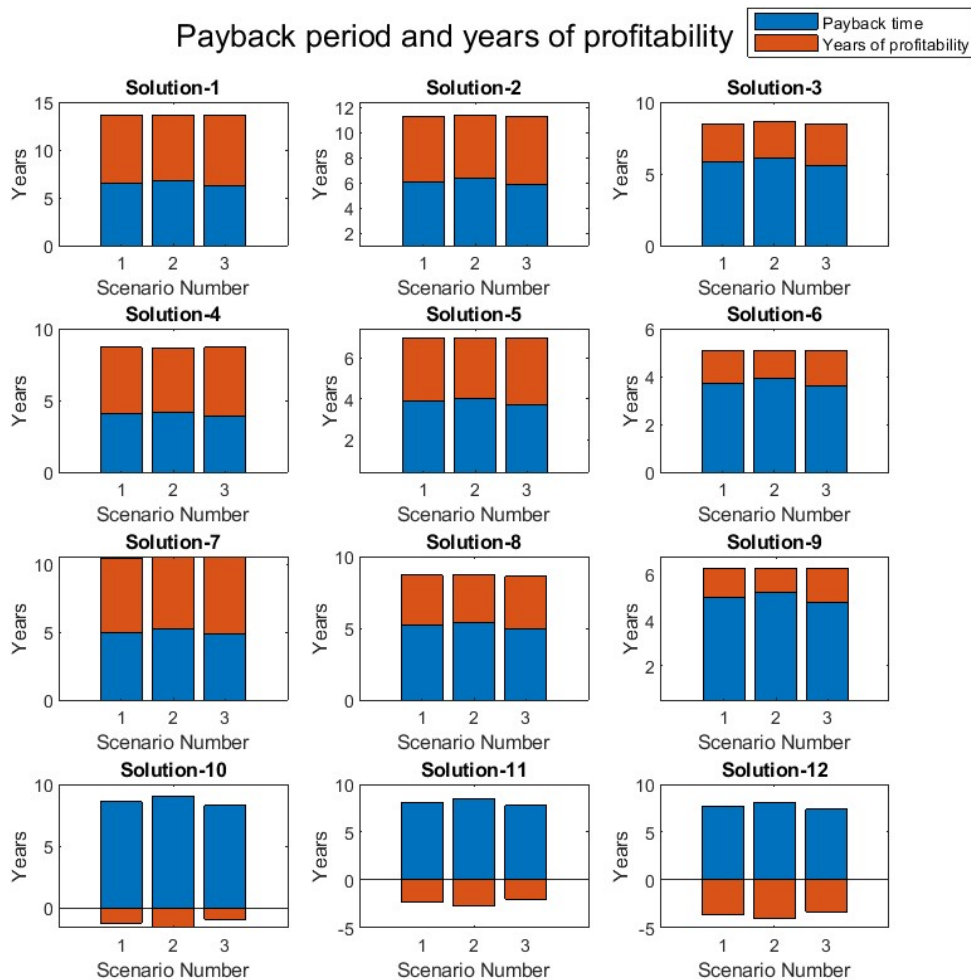


Figure 6.8: Payback period and years of profitability solutions 1-12

Figure 6.9 shows the optimized result for the operation of the battery system with the inclusion of the energy throughput costs and the increase in ROI for the three scenarios (1-3) are 21.88%, 81.63%, and 32.67% respectively. However, the payback periods see an increase of 4%, 3.7%, 16.33% in the three scenarios.

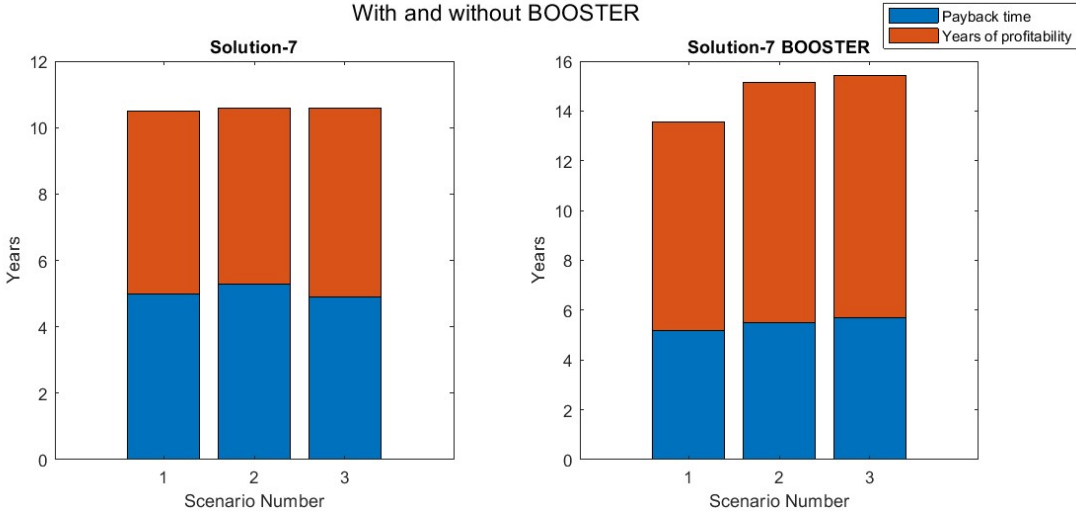


Figure 6.9: Payback period and years of profitability with and without BOOSTER

Table 6.9: Payback period

Solution Number	Investment in €			Payback Period in Years		
	Battery Investment	Converter Cost	Capital Investment	Scenario 1	Scenario 2	Scenario 3
1	2185714	500000	2685714	6.5	6.8	6.3
2	2040000	500000	2540000	6.1	6.4	5.9
3	1912500	500000	2412500	5.8	6.1	5.6
4	1165714	500000	1665714	4.1	4.2	3.9
5	1088000	500000	1588000	3.9	4.0	3.7
6	1020000	500000	1520000	3.7	3.9	3.6
7	1564571	500000	2064571	5.1	5.3	4.9
8	1605333	500000	2105333	5.2	5.4	5.0
9	1522000	500000	2022000	5.0	5.2	4.8
10	714286	166667	880952	8.6	9.0	8.3
11	666667	166667	833333	8.1	8.5	7.8
12	625000	166667	791667	7.7	8.1	7.4
7 - BOOSTER	1564571	500000	2064571	5.2	5.5	5.7

Table 6.10: Years of profitability

Solution Number	Years of Profitability			ROI		
	Scenario 1	Scenario 2	Scenario 3	Scenario 1	Scenario 2	Scenario 3
1	7.1	6.8	7.3	1.26	0.99	1.19
2	5.2	5.0	5.4	0.98	0.76	0.93
3	2.7	2.5	2.9	0.54	0.40	0.52
4	4.6	4.4	4.8	1.31	1.03	0.85
5	3.1	3.0	3.3	0.93	0.72	0.58
6	1.4	1.2	1.5	0.43	0.31	0.27
7	5.5	5.3	5.7	1.25	0.98	1.01
8	3.5	3.3	3.6	0.77	0.59	0.64
9	1.3	1.1	1.5	0.31	0.21	0.27
10	-1.2	-1.6	-0.9	-0.17	-0.18	-0.04
11	-2.3	-2.7	-2.0	-0.33	-0.31	-0.09
12	-3.6	-4.0	-3.3	-0.54	-0.48	-0.15
7 - BOOSTER	8.3	9.6	9.7	1.6	1.78	1.5

6.4. Discussion : Research question, best battery solution

The goal of this master thesis was to find out what the most effective methodology for determining the ideal battery size, technology, and accurate return on investment time frame while considering battery degradation, to create an optimal power generation schedule for the cable laying vessel's power system is. To answer this, the primary research question with 4 sub-questions was defined in section 1.2. Sections 6.4.2-6.4.5. Section 6.4.1 presents the best battery solution and the reasons behind this selection. Finally 6.4.6 provides the limitations and scope for further work based on this master thesis.

6.4.1. Best battery solution

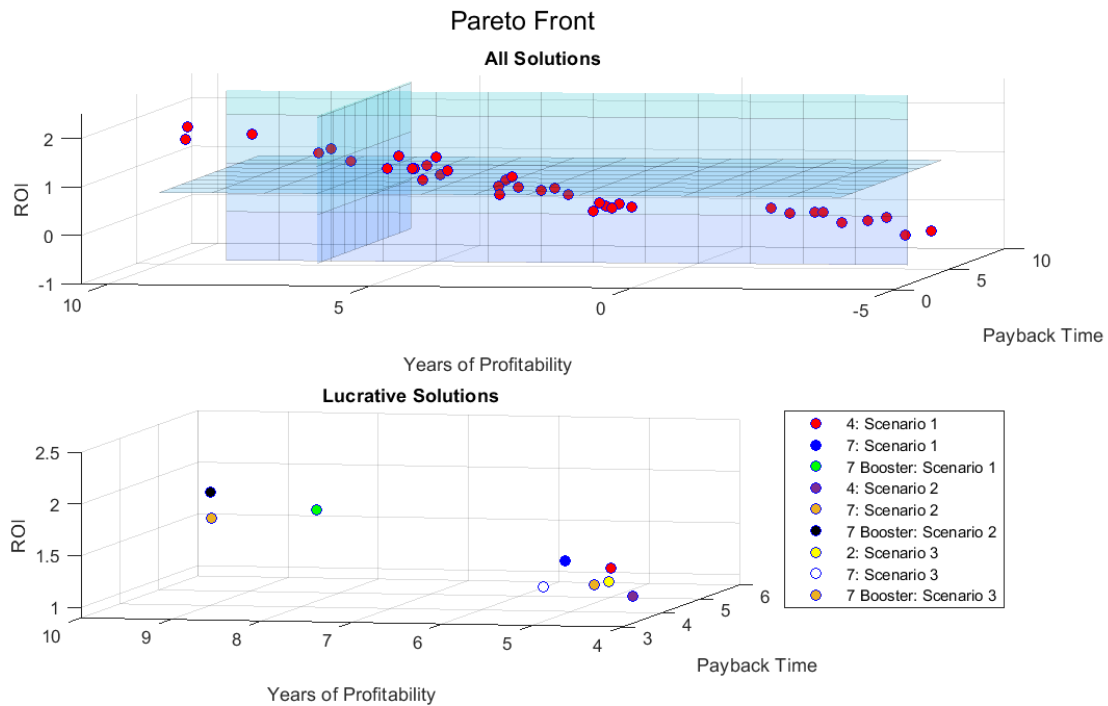


Figure 6.10: Pareto front of all possible solutions

Figure 6.10 (top) shows the "Pareto Front" of the list of solutions. Based on the key performance indicators, figure 6.10 (bottom) presents the lucrative solutions. The best solutions presented, according to the Author, belong to solutions 4 and 7 since they meet the criteria for at least two scenarios. BOOSTER optimization was performed on solution 7 since it meets the criteria in all three scenarios and the results show an increase in the years of profitability and ROI as depicted in table 6.9,

6.4.2. Sub question 1:

What is the best mathematical model for optimizing the integration of the BESS into the power system of DP-2 vessels?

Based on the author's experience and results obtained the following mixed integer mathematical models serves the purpose of optimizing the operation and sizing of systems. This could either be linear or non-linear based on the solver available, computational capabilities, and other requirements. Mixed integer programming allows having if - else conditions in the mathematical model that help in battery system selections, generator on-off, parallel loading of generators, etc.

In addition to this, an "inner" single objective function to be minimized is optimal as it is easier to handle. From the perspective of a systems integrator, adding weights to the different objectives with different dimensions such as ROI, years of profitability, and payback time could prove to be challenging and

hence should be left to the customer. It is beneficial to have a possible list of solutions in a Pareto front than assigning a weight to a multi-objective function and finding the "Highest" or "Lowest" weighted solution.

In addition to the above, it is important to consider the costs and the technical capabilities of battery systems based on battery systems that exist in the market rather than allowing the technical decision variables as a free-floating continuous variable as seen in most of the current literature. Furthermore, the variability in fuel prices is important in deciding not only the go-no go of an investment but also the extent of usage of battery during its operation as shown in section 6.2. Finally, this thesis shows that the maintenance cost savings are additional benefits of employing a battery system that is often overlooked in other works.

6.4.3. Sub question 2:

How do different operational profiles impact the sizing requirements of the battery energy storage system (BESS)?

It can be observed from the results that the cycles per ton of fuel saved are far more in the case of the North Sea as compared to Taiwan. This is due to the high power requirements of the North Sea which results in higher DG loading currently and faster battery discharge as compared to Taiwan.

A higher energy throughput usage is shown for the North Sea results as a result of the sample time of the North Sea being 1 sample per min compared to Taiwan (1 sample per 5 mins). Due to this, the North Sea data recorded more spikes in power as compared to the Taiwan data which might have missed these spikes. For future work, implementation of a penalty fuel costs can also be considered for increasing/decreasing generator power.

If the customer had to make a decision only based on the result of the North Sea, the customer would realize that the current investments would result in a longer payback period and a shorter lifetime of the battery system as compared to the averaged result presented in this report. The converse is true for Taiwan.

Finally, if DP-2 vessels operate in DP mode for extended periods of time, investments become highly profitable. The great bulk of fuel savings, as shown in figures 6.2 and 6.5, occur in DP mode. The majority of the maintenance savings are also visible in DP mode in addition to the fuel savings. Although DP mode shows the greatest fuel savings, no cycles are occurring in this mode. This is a result of the battery system's virtual generator-like behavior. Because the high energy system is employed and the high power battery system is only there for class rules, the combination of High Energy + High Power Battery System is profitable.

6.4.4. Sub question 3:

How does including energy throughput costs in the cost function affect the sizing of the BESS, lifetime, and return on investment?

The inclusion of the cost of ownership is imperative for optimization models and energy management models. If the cost of ownership and the energy throughput costs are not included in the battery sizing model, then the battery will be undersized for the given application. However, if it is not included in the EMS then the battery system will undergo more cycles even during situations when the marginal fuel savings outweigh the energy throughput cost. This is why the BOOSTER for hybrid vessels is presented.

An increase of 21.88%, 81.63%, and 32.67% in ROI, for Solution 7 can be observed in the BOOSTER optimization due to mindful operation of the EMS-PMS through the inclusion of the energy throughput cost and the purchasing fuel price.

While, the overall fuel savings per year is reduced in the BOOSTER method, the number of years of

profitability is increased, thus the lifetime savings of fuel in increased. This is due to the disproportional fuel savings seen in DP mode. There is an increase of 9% in the fuel savings that corresponds to 594.2 tons of fuel for Scenario 1, 17% increase in the fuel savings corresponding to 1039.02 tons for Scenario 2 and 21 % fuel savings in Scenario 3 that corresponds to 1316 tons of fuel saved. Extending the battery lifetime results in annual savings on maintenance costs for a greater number of years, which is an additional advantage.

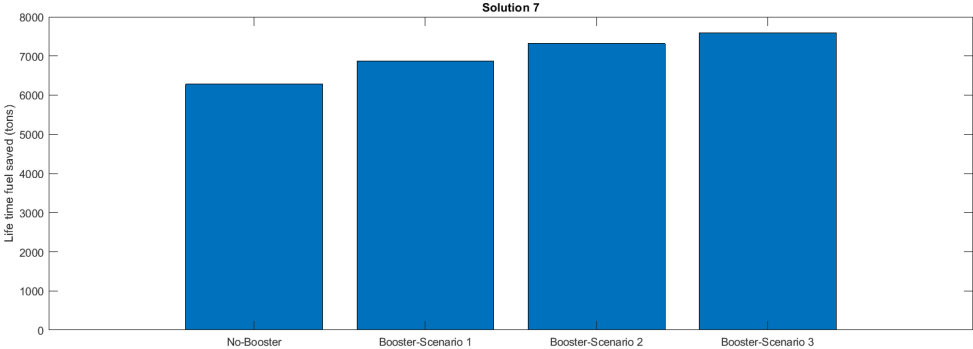


Figure 6.11: Payback period and years of profitability with and without BOOSTER

6.4.5. Sub question 4:

Can the existing Power Management System (PMS) and Energy Management System (EMS) be extended to incorporate optimal scheduling of the diesel engine generators and integration of the BESS?

The figure 6.7 is a BESS operation matrix that advises the best usage of the battery system based on the fuel price and the power during a specific period of operation. It is feasible to establish a matrix of this nature since the load profiles in Taiwan and the North Sea exhibit extended periods of power demands with minimal fluctuations. The operation matrix is an important guide for the management systems to economically dispatch power to the loads. The crew on the board must also be informed and equipped with sufficient knowledge towards using the BESS in this manner.

In addition to the operation matrix, table 6.8 shows the most economic operation strategy of the generators in case of charging and discharging of the battery system. The strategy optimised in the table is based in the combined SFOC curves observed when parallel operation takes place while 2 or more generators are on. This is shown in figure 6.12.

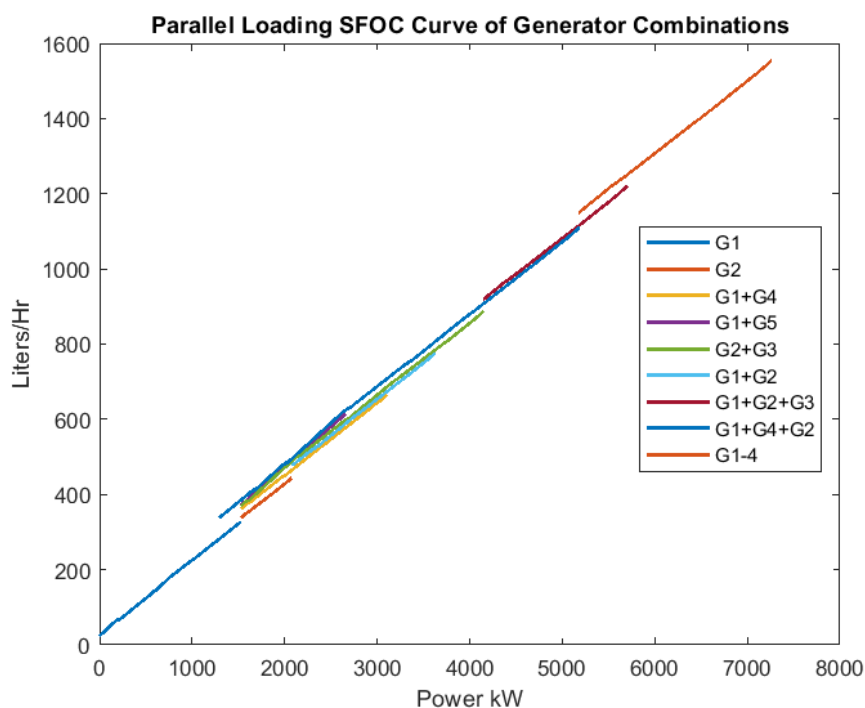


Figure 6.12: SFOC of DG-set in case of parallel loading

To integrate the BOOSTER operation into the PMS and EMS system, the existing vessel management system must be upgraded to input the purchased fuel price and the vessel's mode of operation (refer to table 3.3). A thorough analysis of data (see section 4) indicates that power demand remains generally stable between periods, except during mode changes (auto, DP, NCDP). Therefore, to implement this idea on the vessel, vessel management system development and educating the vessel operators are essential. The upgrades, which are necessary but not limited to are

Power management system upgrades

1. Integrate the recently upgraded EMS into the PMS operations
2. The battery system can be activated in two states: Charge and discharge, which are managed through commands from EMS
3. In auto Mode, utilize the battery's discharge mode to incorporate peak shaving and load leveling functionalities

4. Use the most cost-effective DG or a combination of DG's during charging, considering the charging rates and battery size
5. Optimize fuel consumption by choosing the right DG during battery charging. (EMS partially performs this task)
6. Prevent battery discharge during peak shaving in charge mode

Energy management system upgrades

1. Develop a new interface to integrate the PMS, BMS, and EMS
2. Allocate power from the DG's and BESS based on the operational task In the example sailing mode, if "x" MW power is currently available from DG's, then when a new BESS is included, the DG's must be deactivated, and the BESS should be included during discharge mode. In charge mode, additional DG's must be included to charge the BESS if necessary
3. Implement two modes in auto mode: charging and discharging
4. Allocate additional BESS power for discharging and adjust the number of operating DG's accordingly
5. Add additional DG's to the available DG's list per task when necessary for charging the BESS
6. Consider purchasing fuel cost and the cost of the BESS in the EMS decision-making process
7. Provide vessel operators the ability to input fuel prices for cost calculations
8. Incorporate maintenance cost prediction based on the proposed maintenance curve
9. Enhance DG usage information to optimize maintenance costs
10. EMS Upgrades for Dynamic Positioning (DP) or Non-Critical DP Modes
 - (a) Disable peak shaving and load levelling functionalities in DP or Non-Critical DP modes
 - (b) Restrict the BESS to function as a virtual generator after fault clearance only, coordinated with the tripping of circuit breakers. The battery has only charge mode.
 - (c) Ensure batteries fully charged before DP mode

Battery management system upgrades

1. Disable the BESS if an issue is raised from the BMS, and allocate new DG's to provide power that is no longer available from the BESS
2. Integrate the BMS into the overall Vessel Management System
3. Ensure seamless communication and data exchange between the BMS and other subsystems
4. Enable real-time monitoring and control of battery parameters such as state of charge, voltage, temperature, and health status
5. Implement appropriate safety mechanisms and protections for the battery system
6. Integrate battery performance data for analysis and decision-making within the EMS

To realize such a system, it is necessary and mandated by class providers to perform certain studies these are (but are not limited to),

1. Protection and coordination study: This study encompasses not only the protection and coordination requirements for the implementation of the virtual generator functionality in DP mode but also considers the impact of converter sizing and converter type on the short-circuit (S.C) analysis
2. Transient stability analysis: The purpose of this analysis is to evaluate how the BESS can contribute to improving transient modes and ensuring system stability during dynamic events. It will assess the capability of the BESS to provide support during transient conditions
3. Short-circuit calculation (SC-calculation): This study will focus on analyzing the short-circuit faults in the system and determining appropriate protective measures to ensure the safety and protection of the BESS. It will assess the impact of short-circuit faults on the BESS system and propose suitable protective devices and settings
4. Harmonic study: This study will assess the impact of the BESS on harmonics within the power system. It will evaluate potential harmonic distortions caused by the BESS and propose mitigation strategies if necessary. The study aims to maintain the power quality and minimize any adverse effects on the overall system due to harmonics. This study can further aid in filter design.

Prior to implementation, it is essential to ensure that the protection system is well-coordinated with PMS, BMS, and EMS, including their respective algorithms. The best way to achieve this is through hardware in loop (HIL) testing, which can be availed from providers such as Typhoon HIL, Siemens, and MATHWORKS. Here is a global framework for their individual testing,

1. A PMS upgrade can benefit from HIL, as it enables the simulation of DG's behavior and interaction with the PMS. To validate the functionality and performance of the upgraded PMS, the PMS software can be connected to physical or virtual DG hardware in real-time for thorough testing
2. The EMS system can be validated by using HIL to simulate how it interacts with power generation and storage components like DG's and BESS. This is done by connecting the EMS software to either virtual or physical hardware that represents these components. With this upgrade, the EMS can be tested in different scenarios such as sailing modes, charging modes, and coordination with the PMS. This comprehensive testing allows for an assessment of the EMS functionality and its integration with other systems
3. HIL technology allows for the verification of BMS integration with the vessel management system. Through connecting the BMS software to the virtual or physical hardware that represents the battery system, HIL enables testing of BMS functionality, communication interfaces, and coordination with the PMS and EMS. This ensures the seamless operation of the BMS within the vessel management system.

6.4.6. Limitations and further work

The author, to the best of his ability, has tried to incorporate as many realistic methodologies and considerations as possible. However, there are some limitations.

The costs associated with maintenance consider only the overhauling costs of the DG amount to roughly over 100,000 euros per year for the 5 DG's. According to experienced vessel operators, maintenance savings of up to 250,000 euros can be achieved, averaging at 50,000 euros per year. In scenario 1, solution 7 currently sees 24.83% of yearly savings from maintenance, with the rest coming from fuel savings. However, if the recommended maintenance savings by the vessel operators are implemented, the percentage of annual maintenance savings could increase by nearly 150%, resulting in yearly savings of 36.8%. Therefore, future efforts should prioritize developing more comprehensive models that consider fuel-savings and maintenance in the optimization process.

The battery system currently accounts for a three percent calendar aging. However, there is limited research on how calendar aging is affected by SOC, temperature, and cycling. Properly cycling the battery can reduce calendar aging, which is crucial for the longevity of the BOOSTER solution, especially if it will be in use for more than 10 years. The BOOSTER solution avoids using the battery during periods of high fuel prices and power demand. Therefore, future developments of this model need to consider calendar aging in relation to cycles, idle time, and SOC state. The impact of calendar aging on solution 7 is illustrated in 6.13.

The author acknowledges their lack of knowledge regarding future interest rates, inflation rates, and fuel prices as of Monday 3rd July, 2023, due to ongoing geopolitical and financial changes. As a result, these factors were excluded in calculating the payback period and ROI to maintain simplicity.

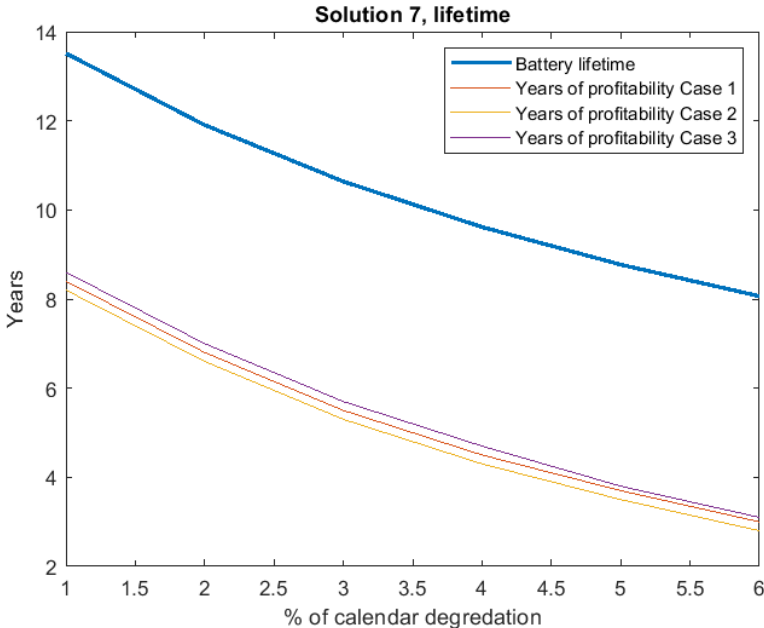


Figure 6.13: Solution 7 lifetime and years of profitability as a function of calendar degradation

References

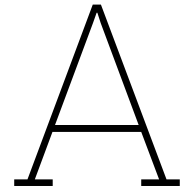
- [1] Jasper Faber et al. *Fourth Greenhouse Gas Study 2020*. 2021. URL: <https://www.imo.org/en/OurWork/Environment/Pages/Fourth-IMO-Greenhouse-Gas-Study-2020.aspx>.
- [2] Central Dredging Association. *Energy Efficiency Considerations for Dredging Projects and Equipment*. 2022. URL: <https://dredging.org/resources/ceda-publications-online/position-and-information-papers>.
- [3] Erik Fridell, Hulda Winnes, and Linda Styhre. “Measures to improve energy efficiency in shipping”. In: *Natural Resources and Infrastructure Division, UNECLAC*. 8th ser. 324 (2013).
- [4] Espen Skjong et al. “The Marine Vessel’s Electrical Power System: From its Birth to Present Day”. In: *Proceedings of the IEEE* 103.12 (2015), pp. 2410–2424. DOI: 10.1109/JPROC.2015.2496722.
- [5] Timothy J. McCoy. “Electric ships past, present, and future [technology leaders]”. In: *IEEE Electrification Magazine* 3.2 (2015), pp. 4–11. DOI: 10.1109/mele.2015.2414291.
- [6] A. Sinan KARAKURT and Yasin Ust. “Marine Steam Turbines”. In: Aug. 2011.
- [7] Ma Weiming. “Development of Vessel Integrated Power System”. In: *2011 International Conference on Electrical Machines and Systems* (2011). DOI: 10.1109/icems.2011.6073291.
- [8] NORBERT H. DOERRY and JAMES C. DAVIS. “Integrated Power System for Marine Applications”. In: *Naval Engineers Journal* 106.3 (1994), pp. 77–90. DOI: 10.1111/j.1559-3584.1994.tb02843.x.
- [9] David D. Walden et al. *Systems engineering handbook: A guide for system life cycle processes and activities*. Wiley, 2015.
- [10] Dinesh Kumar and Firuz Zare. “A comprehensive review of maritime microgrids: System Architectures, energy efficiency, power quality, and regulations”. In: *IEEE Access* 7 (2019), pp. 67249–67277. DOI: 10.1109/access.2019.2917082.
- [11] MariEMS. *Chapter 5 - Engines and Machinery Load and Utilisation Management*. URL: <https://erasmus-plus.ec.europa.eu/projects>.
- [12] Michael Lundh et al. “Estimation and optimization of vessel fuel consumption”. In: *IFAC-PapersOnLine* 49.23 (2016), pp. 394–399. DOI: 10.1016/j.ifacol.2016.10.436.
- [13] MathWorks. *Polynomial Curve Fitting*. URL: <https://nl.mathworks.com/help/matlab/ref/polyfit.html>.
- [14] Srinivasa K. Rao et al. “An exercise to qualify LVAC and LVDC power system architectures for a platform supply vessel”. In: *2016 IEEE Transportation Electrification Conference and Expo, Asia-Pacific (ITEC Asia-Pacific)* (2016). DOI: 10.1109/itec-ap.2016.7512973.
- [15] Hussein Mahdi, Bjarte Hoff, and Trond Ostrem. “A review of power converters for ships electrification”. In: *IEEE Transactions on Power Electronics* (2022), pp. 1–18. DOI: 10.1109/tpe1.2022.3227398.
- [16] Zhibin Zhou et al. “A review of Energy Storage Technologies for Marine Current Energy Systems”. In: *Renewable and Sustainable Energy Reviews* 18 (2013), pp. 390–400. DOI: 10.1016/j.rser.2012.10.006.
- [17] Muhammad Mutarraf et al. “Energy storage systems for shipboard microgrids—a review”. In: *Energies* 11.12 (2018), p. 3492. DOI: 10.3390/en11123492.
- [18] Denizhan Guven and M. Ozgur Kayalica. “Life-cycle assessment and life-cycle cost assessment of lithium-ion batteries for passenger ferry”. In: *Transportation Research Part D: Transport and Environment* 115 (2023), p. 103586. DOI: 10.1016/j.trd.2022.103586.
- [19] Henrik Helgesen. Vol. 2019-0217. Rev. 04. 2020.

- [20] Kyunghwa Kim et al. "Analysis of battery/generator hybrid container ship for CO₂ Reduction". In: *IEEE Access* 6 (2018), pp. 14537–14543. DOI: 10.1109/access.2018.2814635.
- [21] So-Yeon Kim et al. "A naval integrated power system with a battery energy storage system: Fuel efficiency, reliability, and quality of power". In: *IEEE Electrification Magazine* 3.2 (2015), pp. 22–33. DOI: 10.1109/mele.2015.2413435.
- [22] Peilin Xie et al. "Optimization-based power and Energy Management System in shipboard Microgrid: A Review". In: *IEEE Systems Journal* 16.1 (2022), pp. 578–590. DOI: 10.1109/jsyst.2020.3047673.
- [23] Damir Radan et al. "Optimization of load dependent start tables in marine power management systems with blackout prevention". In: 4 (Dec. 2005).
- [24] Sidun Fang et al. "Optimal sizing of shipboard carbon capture system for maritime greenhouse emission control". In: *IEEE Transactions on Industry Applications* 55.6 (2019), pp. 5543–5553. DOI: 10.1109/tia.2019.2934088.
- [25] Flavio Balsamo et al. "Power flow approach for modeling shipboard power system in presence of energy storage and Energy Management Systems". In: *IEEE Transactions on Energy Conversion* 35.4 (2020), pp. 1944–1953. DOI: 10.1109/tec.2020.2997307.
- [26] Siri Solem et al. "Optimization of diesel electric machinery system configuration in conceptual ship design". In: *Journal of Marine Science and Technology* 20.3 (2015), pp. 406–416. DOI: 10.1007/s00773-015-0307-4.
- [27] Chiara Bordin and Olve Mo. "Including power management strategies and load profiles in the mathematical optimization of energy storage sizing for fuel consumption reduction in maritime vessels". In: *Journal of Energy Storage* 23 (2019), pp. 425–441. DOI: 10.1016/j.est.2019.03.021.
- [28] Amjad Anvari-Moghaddam et al. "Optimal Planning and Operation Management of a ship electrical power system with Energy Storage System". In: *IECON 2016 - 42nd Annual Conference of the IEEE Industrial Electronics Society* (2016). DOI: 10.1109/iecon.2016.7793272.
- [29] Sidun Fang et al. "Two-Step Multi-Objective Management of Hybrid Energy Storage System in All-Electric Ship Microgrids". In: *IEEE Transactions on Vehicular Technology* 68.4 (2019), pp. 3361–3373. DOI: 10.1109/TVT.2019.2898461.
- [30] Fotis D. Kanellos, George J. Tsekouras, and Nikos D. Hatzargyriou. "Optimal demand-side management and power generation scheduling in an all-electric ship". In: *IEEE Transactions on Sustainable Energy* 5.4 (2014), pp. 1166–1175. DOI: 10.1109/tste.2014.2336973.
- [31] Yamin Yan et al. "Multi-objective design optimization of combined cooling, heating and power system for cruise ship application". In: *Journal of Cleaner Production* 233 (2019), pp. 264–279. DOI: 10.1016/j.jclepro.2019.06.047.
- [32] Fotis D. Kanellos, Amjad Anvari-Moghaddam, and Josep M. Guerrero. "A cost-effective and emission-aware power management system for ships with integrated full electric propulsion". In: *Electric Power Systems Research* 150 (2017), pp. 63–75. DOI: 10.1016/j.epsr.2017.05.003.
- [33] Priyesh J. Chauhan et al. "Fuel efficiency improvement by optimal scheduling of diesel generators using PSO in offshore support vessel with DC Power System Architecture". In: *2015 IEEE PES Asia-Pacific Power and Energy Engineering Conference (APPEEC)* (2015). DOI: 10.1109/appec.2015.7380963.
- [34] Eberhart and Yuhui Shi. "Particle swarm optimization: Developments, applications and resources". In: *Proceedings of the 2001 Congress on Evolutionary Computation (IEEE Cat. No.01TH8546)* (). DOI: 10.1109/cec.2001.934374.
- [35] Hai-Ming Chin, Chun-Lien Su, and Chi-Hsiang Liao. "Estimating power pump loads and sizing generators for ship electrical load analysis". In: *IEEE Transactions on Industry Applications* 52.6 (2016), pp. 4619–4627. DOI: 10.1109/tia.2016.2600653.
- [36] Armin Letafat et al. "Simultaneous energy management and optimal components sizing of a zero-emission ferry boat". In: *Journal of Energy Storage* 28 (2020), p. 101215. DOI: 10.1016/j.est.2020.101215.

- [37] Shuli Wen et al. "Allocation of ESS by interval optimization method considering impact of ship swinging on hybrid PV/diesel ship power system". In: *Applied Energy* 175 (2016), pp. 158–167. DOI: 10.1016/j.apenergy.2016.05.003.
- [38] Ahmet Aktaş and Yağmur Kirçiçek. "Solar Hybrid Systems and Energy Storage Systems". In: *Solar Hybrid Systems* (2021), pp. 87–125. DOI: 10.1016/b978-0-323-88499-0.00005-7.
- [39] Wesley Cole, A. Frazier, and Chad Augustine. "Cost projections for utility-scale battery storage: 2021 update". In: (2021). DOI: 10.2172/1786976.
- [40] Agnès Chaumond et al. *Experimental protocols and first results of calendar and/or cycling aging study of lithium-ion batteries – the MOBICUS project*. June 2016. URL: <https://doi.org/10.3390/wevj8020388>.
- [41] Peter Keil et al. "Calendar Aging of Lithium-Ion Batteries I. Impact of the Graphite Anode on Capacity Fade". In: *Journal of The Electrochemical Society* 163 (2016).
- [42] Hayder Ali et al. *Assessment of the calendar aging of lithium-ion batteries for a long-term-space missions*. Jan. 2023. URL: <https://doi.org/10.3389/fenrg.2023.1108269>.
- [43] Simone Barcellona et al. "Analysis of ageing effect on Li-polymer batteries". In: *The Scientific World Journal* 2015 (2015), pp. 1–8. DOI: 10.1155/2015/979321.
- [44] M Safari and C Delacourt. *Aging of a commercial graphite/lifepo4 cell*. Aug. 2011. URL: <https://iopscience.iop.org/article/10.1149/1.3614529>.
- [45] V. Ruiz et al. "Degradation studies on lithium iron phosphate - graphite cells. the effect of dissimilar charging – discharging temperatures". In: *Electrochimica Acta* 240 (2017), pp. 495–505. DOI: 10.1016/j.electacta.2017.03.126.
- [46] Yang Gao et al. "Lithium-ion battery aging mechanisms and life model under different charging stresses". In: *Journal of Power Sources* 356 (2017), pp. 103–114. DOI: 10.1016/j.jpowsour.2017.04.084.
- [47] L. Somerville et al. "The effect of charging rate on the graphite electrode of commercial lithium-ion cells: A post-mortem study". In: *Journal of Power Sources* 335 (Dec. 2016), pp. 189–196. DOI: 10.1016/j.jpowsour.2016.10.002.
- [48] D. Anseán et al. "Fast charging technique for high power lithium iron phosphate batteries: A cycle life analysis". In: *Journal of Power Sources* 239 (2013), pp. 9–15. DOI: 10.1016/j.jpowsour.2013.03.044.
- [49] D. Anseán et al. "Fast charging technique for high power LiFePO4 batteries: A mechanistic analysis of aging". In: *Journal of Power Sources* 321 (2016), pp. 201–209. DOI: 10.1016/j.jpowsour.2016.04.140.
- [50] John Wang et al. "Cycle-life model for graphite-lifepo4 cells". In: *Journal of Power Sources* 196.8 (2011), pp. 3942–3948. DOI: 10.1016/j.jpowsour.2010.11.134.
- [51] *High Energy NMC Battery - Est-Floattech*. Nov. 2021. URL: <https://www.est-floattech.com/products/high-energy-nmc-module/>.
- [52] *High Power NMC Battery System - Est-Floattech*. July 2022. URL: <https://www.est-floattech.com/products/high-power-nmc-battery/>.
- [53] *High energy LFP module - Est-Floattech*. Aug. 2021. URL: <https://www.est-floattech.com/products/high-energy-lfp-module/>.
- [54] *Corvus Orca Energy*. Feb. 2023. URL: <https://corvusenergy.com/products/energy-storage-solutions/corvus-orca-energy/>.
- [55] *Corvus Blue Whale*. Feb. 2023. URL: <https://corvusenergy.com/products/energy-storage-solutions/corvus-blue-whale/>.
- [56] *Corvus Dolphin Energy*. Feb. 2023. URL: <https://corvusenergy.com/products/energy-storage-solutions/corvus-dolphin-energy/>.
- [57] *Ayk Energy. Ayk Energy Products*. Mar. 2023. URL: <https://www.aykenenergy.com/products>.
- [58] *Marine*. Mar. 2023. URL: <https://eas-batteries.com/markets/marine>.

- [59] *Echandia Energy*. Mar. 2023. URL: <https://echandia.se/products/echandia-energy/>.
- [60] Freudenberg. Mar. 2023. URL: <https://indd.adobe.com/view/7000ba20-dc96-4660-b806-93fac64233d5>.
- [61] Lehmann. *Cobra Batteries*. Mar. 2023. URL: <https://www.lehmann-marine.com/en/cobra.html>.
- [62] Super B. *Super - B*. Mar. 2023. URL: <https://www.super-b.com/en/lithium-marine-batteries/commercial-marine>.
- [63] *Spear Power Systems: Marine Battery - Maritime Battery Technology*. Sept. 2021. URL: <https://marine.spearpowersystems.com/technologies/>.
- [64] XMOD 123E. Mar. 2023. URL: <https://www.xaltenergy.com/portfolio/xmod-123e/>.
- [65] Heide Budde-Meiwes et al. "A review of Current Automotive Battery Technology and future prospects". In: *Proceedings of the Institution of Mechanical Engineers, Part D: Journal of Automobile Engineering* 227.5 (2013), pp. 761–776. DOI: 10.1177/0954407013485567.
- [66] Yu Miao et al. "Current Li-ion battery technologies in electric vehicles and opportunities for advancements". In: *Energies* 12.6 (2019), p. 1074. DOI: 10.3390/en12061074.
- [67] Carola Leone et al. "Design and implementation of an electric Skibus line in north Italy". In: *Energies* 14.23 (2021), p. 7925. DOI: 10.3390/en14237925.
- [68] Radhika. *Selecting the right lithium-ion battery for your application*. Apr. 2020. URL: <https://www.ionenergy.co/resources/blogs/lithium-ion-battery-types/>.
- [69] Aug. 2022. URL: <https://corvusenergy.com/products/energy-storage-solutions/>.
- [70] Praxis. URL: https://www.praxis-automation.eu/uploads/default_site/files/brochures/513.01_ESS_Rev1.07.pdf.
- [71] Bruce Dunn, Haresh Kamath, and Jean-Marie Tarascon. "Electrical Energy Storage for the grid: A battery of choices". In: *Science* 334.6058 (2011), pp. 928–935. DOI: 10.1126/science.1212741.
- [72] Lukas Mauler et al. "Battery cost forecasting: A review of methods and results with an outlook to 2050". In: *Energy and Environmental Science* 14.9 (2021), pp. 4712–4739. DOI: 10.1039/d1ee01530c.
- [73] Michael CW Kintner-Meyer et al. "Energy Storage for Power Systems Applications: A Regional Assessment for the Northwest Power Pool (NWPP)". In: 2010.
- [74] Behnam Zakeri and Sanna Syri. "Electrical Energy Storage Systems: A comparative life cycle cost analysis". In: *Renewable and Sustainable Energy Reviews* 42 (2015), pp. 569–596. DOI: 10.1016/j.rser.2014.10.011.
- [75] Bolun Xu et al. "Factoring the Cycle Aging Cost of Batteries Participating in Electricity Markets". In: *IEEE Transactions on Power Systems* 33.2 (2018), pp. 2248–2259. DOI: 10.1109/TPWRS.2017.2733339.
- [76] S. Mashayekh et al. "Optimum sizing of energy storage for an electric ferry ship". In: *2012 IEEE Power and Energy Society General Meeting* (2012). DOI: 10.1109/pesgm.2012.6345228.
- [77] Chuan Yan, Ganesh K. Venayagamoorthy, and Keith A. Corzine. "Optimal location and sizing of energy storage modules for a smart electric ship power system". In: *2011 IEEE Symposium on Computational Intelligence Applications In Smart Grid (CIASG)* (2011). DOI: 10.1109/ciasg.2011.5953336.
- [78] Shui Pang et al. "Multi-objective optimization configuration of electric energy storage capacity of electric propulsion ship". In: *2020 IEEE 4th Information Technology, Networking, Electronic and Automation Control Conference (ITNEC)* (2020). DOI: 10.1109/itnec48623.2020.9084691.
- [79] Armin Letafat et al. "Simultaneous energy management and optimal components sizing of a zero-emission ferry boat". In: *Journal of Energy Storage* 28 (2020), p. 101215. DOI: 10.1016/j.est.2020.101215.
- [80] Mohammad Amini et al. "Optimal sizing of battery energy storage in a microgrid considering capacity degradation and replacement year". In: *Electric Power Systems Research* 195 (2021), p. 107170. DOI: 10.1016/j.epsr.2021.107170.

- [81] Jiageng Ruan et al. "The multi-objective optimization of cost, energy consumption and battery degradation for fuel cell-battery hybrid electric vehicle". In: *2021 11th International Conference on Power, Energy and Electrical Engineering (CPEEE)* (2021). DOI: 10.1109/cpeee51686.2021.9383396.
- [82] Mansour Alramlawi and Pu Li. "Design optimization of a residential PV-battery microgrid with a detailed battery lifetime estimation model". In: *IEEE Transactions on Industry Applications* 56.2 (2020), pp. 2020–2030. DOI: 10.1109/tia.2020.2965894.
- [83] Chiara Bordin et al. "A linear programming approach for battery degradation analysis and optimization in Offgrid Power Systems with Solar Energy Integration". In: *Renewable Energy* 101 (2017), pp. 417–430. DOI: 10.1016/j.renene.2016.08.066.
- [84] Amir Sina Hamed and Abbas Rajabi Ghahnavieh. "Explicit degradation modelling in optimal lead–acid battery use for photovoltaic systems". In: *IET Generation, Transmission and Distribution* 10.4 (2016), pp. 1098–1106. DOI: 10.1049/iet-gtd.2015.0163.
- [85] Shinya Kato et al. "A battery degradation aware optimal power distribution on Decentralized Energy Network". In: *10th IEEE International NEWCAS Conference* (2012). DOI: 10.1109/newcas.2012.6329043.
- [86] Xinda Ke, Ning Lu, and Chunlian Jin. "Control and Size Energy Storage Systems for Managing Energy Imbalance of Variable Generation Resources". In: *IEEE Transactions on Sustainable Energy* 6.1 (2015), pp. 70–78. DOI: 10.1109/TSTE.2014.2355829.
- [87] Iman Naziri Moghaddam, Badrul Chowdhury, and Milad Doostan. "Optimal Sizing and Operation of Battery Energy Storage Systems Connected to Wind Farms Participating in Electricity Markets". In: *IEEE Transactions on Sustainable Energy* 10.3 (2019), pp. 1184–1193. DOI: 10.1109/TSTE.2018.2863272.
- [88] Malek Belouda et al. "Design methodologies for sizing a battery bank devoted to a stand-alone and electronically passive wind turbine system". In: *Renewable and Sustainable Energy Reviews* 60 (2016), pp. 144–154. DOI: 10.1016/j.rser.2016.01.111.
- [89] Meysam Khojasteh, Pedro Faria, and Zita Vale. "Energy-constrained model for scheduling of battery storage systems in joint energy and ancillary service markets based on the Energy Throughput Concept". In: *International Journal of Electrical Power & Energy Systems* 133 (2021), p. 107213. DOI: 10.1016/j.ijepes.2021.107213.
- [90] Carlos Frederico Matt et al. "Optimization of the Operation of Isolated Industrial Diesel Stations". In: *6th World Congress on Structural and Multidisciplinary Optimization* (May 2005).
- [91] MathWorks. *Intlinprog*. URL: <https://nl.mathworks.com/help/optim/ug/intlinprog.html>.
- [92] Ship & Bunker. *Rotterdam bunker prices - MGO Fuel*. URL: <https://shipandbunker.com/prices/emea/nwe/nl-rtm-rotterdam%5C#MGO>.



Definitions

1. **Battery energy storage system (BESS):** Energy storage technology that uses batteries to store electrical energy. The BESS comprises of battery modules, a power conversion system, a bi-directional converter, an energy management system, a thermal management system, monitoring and control system.
2. **Dynamic positioning :** When conducting offshore operations, it is crucial to maintain a vessel's precise position and heading. While anchors were traditionally used for this purpose, Dynamic Positioning (DP) systems have become the preferred option. DP systems employ constantly active thrusters to automatically counteract environmental forces such as wind, waves, and currents that would otherwise displace the vessel. This ensures that the vessel remains in the desired position and heading at all times.
3. **Depth of discharge :** The percentage of battery discharge is relative to the overall capacity.
4. **Energy management system (EMS):** An Energy Management System (EMS) is a software-based system that is used to monitor, control, and optimize the energy consumption and production in a building, facility, or industrial plant. It is designed to help organizations reduce their energy costs, improve energy efficiency, and reduce their carbon footprint.
5. **Energy throughput :** The energy throughput is the total amount of energy that can be charged and discharged within the lifetime of batteries [89].
6. **Global optimization :** Global optimization refers to the process of finding the best possible solution for a given optimization problem within a specified search space. It involves searching for the optimal solution that provides the highest possible objective function value, subject to a set of constraints.
7. **Power management system (PMS):** A power Management System (PMS) is a software or hardware system that monitors, controls, and optimizes the generation, distribution, and consumption of electrical power in a facility or power grid. It enables the management of various power-related parameters, such as voltage, frequency, power factor, and load balancing, to ensure that the power system operates efficiently and reliably.
8. **ROI:** ROI is net income divided by investment costs.
9. **Payback period:** Payback period is how long it takes to recover investment costs or break even.
10. **Calendar aging:** The degradation of a battery cell, which is independent of charge-discharge cycling, is caused by calendar aging.
11. **Cycle aging:** The process of cycling aging takes place when the battery is charged or discharged.

B

Research Paper

Analysis of Potential Hybrid Solutions with Li-ion Battery System for DP-2 Vessels

Sankarshan Durgaprasad^{a,1}, Zoran Malbašić^b, Marjan Popov^a, Aleksandra Lekić^a

^a*Delft University of Technology, Faculty of EEMCS, Delft, The Netherlands*

^b*Alewijnse, Krimpen aan den IJssel, Netherlands*

Abstract

An economical approach for incorporating battery energy storage systems (BESS) onto DP-2 vessels is presented in this research. The study creates the BOOSTER framework for putting research findings into practice by optimizing battery size, technology choice, and power generation scheduling while considering battery deterioration. Twelve battery sizes are analyzed in terms of pricing, fuel costs, and battery technology using mixed integer linear programming (MILP) and load profiles from Taiwan and the North Sea. Findings emphasize the significance of taking battery fuel price and ownership costs into account. In order to promote the use of clean energy and the mitigation of environmental impact in maritime operations, this research develops a method that can be integrated into DP-2 ships at a reasonable cost. As a result of the findings, energy systems may be optimized for a sustainable future, which benefits vessel operators and industry stakeholders.

Keywords: Li-ion, Battery energy storage system (BESS), Cost of ownership, MILP, Optimal sizing

Nomenclature

1. Introduction

1.1. Motivation

As of 2018, the maritime industry is responsible for 1056 million tonnes of CO_2 in greenhouse gas emissions [1]. Compared to the 962 million tons of CO_2 generated in 2012, this is a 9.3% increase. Shipping emissions as a percentage of all anthropogenic emissions have grown from 2.76% in 2012 to 2.89% in 2018. The aim of the worldwide public to minimize greenhouse gas emissions has a significant impact on the design and operation of transportation infrastructure today. To counteract this, the IMO's Marine Environment Protection Committee (mEPC72) adopted the inaugural IMO plan to minimize GHG emissions from international shipping as a resolution in 2018. This IMO strategy describes a broad vision for decarbonization, GHG reduction targets through 2050, a list of short-, mid-, and long-term actions to accomplish these targets, obstacles to attaining the targets and supportive actions to overcome them, and criteria for future assessment. It will be updated in 2023 and reviewed in 2028 [2].

Since the overwhelming success of the first fully electric ferry "The Ampere" in 2015, 70 other such ferries have shown profitability in Norway [3]. Studies show that 127 out of 180 ferries are deemed to be profitable with either battery or

hybrid operation [4]. The successful outcomes in Norway's ferry industry show that electric and hybrid propulsion technologies for maritime transportation are technically feasible and commercially viable. As a result, attempts are being undertaken to investigate how other types of vessels besides ferries may be electrified.

The primary objectives of this paper are to provide a battery system that is appropriately optimized, ensure that the energy system functions effectively, and provide the strongest possible business case. The study focuses on a DP-2 vessel that operates in the North Sea and Taiwan. The paper investigates the prospect of retrofitting the vessel with a battery system to transform it into a hybrid system.

Retrofitting of vessels with BESS is usually performed by electrical system integrators. Therefore it is necessary to analyze different solutions. Optimal sizing of the battery energy storage system is done by considering 12 different battery solutions from 2 different European battery suppliers. These solutions include different battery technologies such as High Power or High Energy Li-ion batteries or a combination of both.

For vessel operators, integrating BESS has several operational benefits. The capacity to operate diesel engines at higher or more efficient points to maximize their performance is a significant advantage, especially for most vessels. Battery systems can also act as "virtual generators" in the case of DP-2 vessels during DP mode, removing the need to operate numerous generators at low or inefficient operating levels. In addition to saving on fuel, this approach lowers on time of diesel engines and the accompanying maintenance costs.

*Corresponding author

Email address: s.durgaprasad@student.tudelft.nl (Sankarshan Durgaprasad)

Hybridization of vessels does not stop at integrating an optimally sized battery system. The existing power management system (PMS) and energy management system (EMS) must also be upgraded to function effectively. A BOOSTER (Battery Optimization for Optimal Sizing and Throughput Energy Regulation) methodology is proposed. The BOOSTER incorporates the operation of an optimized management system functioning based on the fuel price and the throughput energy cost of the battery system.

The following parts of the paper are structured: Section 1.2 provides an overview of the literature reviewed that forms the basis of the work presented. Section 1.3 underlines the critical contribution of the work presented in this paper and the limitations. Section 3 provides the methodology, formulates the MILP problem, and details the simulated cases. The results of the optimization problem for both Taiwan and the North Sea are showcased in section 4. Finally, a Pareto front of optimal solutions and a viable business case with the BOOSTER is presented in section ??.

1.2. Literature review

The literature is reviewed on the implementation and optimization of BESS, battery system degradation, current major BESS technologies available in Europe, and the implementation of battery systems in other industries to seek inspiration from. Section 1.2.1 gives an overview of existing literature on the Optimum operation of vessel management systems, in Section 1.2.2, the available BESS solutions are reviewed, as well as the degradation behavior of NMC and LFP cells, will be delved into. Additionally, the implementation or consideration of degradation in modeling techniques beyond maritime energy systems are explored. The economic implications of operating diesel engine generator set (DG) is discussed in 1.2.3. The section 1.3 offers a comprehensive description of the work's contribution.

1.2.1. Optimum operation of vessel Management system and battery sizing

Vessel management systems have two types of optimization: local and global. Global optimization can be classical or heuristic. This paper focuses on global optimization with a preference for classical techniques.

The authors of [5] use linear and quadratic programming to optimize the sizing of the carbon capture and energy storage system, as well as the vessel energy management system. The importance of combining CC and BESS was highlighted to reduce greenhouse gas emissions by 10% to 60%, with a corresponding increase in operational costs of 6.8%. In [6], nonlinear programming was used to optimize the shipboard BESS, where the authors split the operational profile into various modes and considered reactive power flow. The optimal size of the DE for various operating states was determined using the Branch and Bound technique (BAB)

in [7]. This approach can also be extended to determine the ideal size of a BESS. Comprehensive optimization of the vessel energy management system and BESS sizing was conducted in [8] using the OBLIVION framework, which considers safety constraints, vessel operating modes, sensitivity analysis, and battery degradation. Mixed Integer Nonlinear Programming (MINLP) was used in [9] and [10] to examine effective ship system planning, operation, and battery sizing. Dynamic programming was used in [11] and [12] for fuel savings through the generator, speed, and distance optimization. Finally, [11] achieved optimal power while considering a BESS by varying ship speed, and [12] presented a multi-objective mathematical programming model for optimized energy dispatch considering emissions, energy balance, and technical constraints. Heuristic optimization utilizes several optimization methods, including Particle Swarm Optimization (PSO), Genetic Algorithms (GA), NSGA II, and Improved Sine and Cosine Algorithm (ISCA). PSO is used in [13] to optimize the scheduling of diesel generators in a DC-based off-shore support vessel (OSV), resulting in a reduced fuel consumption of 307 tons annually when compared to an AC architecture. The authors of [14] use a modified fuzzy-based PSO (FPSO) to model a ferry power management system that focuses on reducing emissions and operation costs. In [15]), GA is employed to solve a mixed integer nonlinear problem that minimizes the cost of power generation by optimizing the installed capacity of the vessel and the pump loads. The authors also consider the generator's operational efficiency regarding power factor and loading percentage, which was not done in previous studies. These optimization techniques utilize various power management tactics to fulfill restrictions and reach optimization goals, resulting in improved convergence and optimal solutions. The authors of [16] use the ISCA algorithm that yields more optimal results than other evolutionary algorithms.

A technique described in [17] uses double-layer optimization to improve decision-making for investment and sizing. The inner loop uses MILP, and the outer loop uses NSGA-II. It was applied to retrofit a crew transfer vessel, minimizing investment, operation, and fuel costs. The authors considered different battery and fuel costs, presenting their findings through a Pareto front. A two-layer optimization approach has been proposed in a similar study [18]. The outer layer, utilizing NSGA-II, estimates the capital expenditure (CAPEX) costs incurred. In contrast, the inner layer targets optimizing the energy management system to minimize operational expenditure (OPEX). According to the results, implementing a BESS alone can reduce emissions by 10%, but a fuel cell and shore connection are necessary to achieve further reduction.

Table 1 summarizes other optimization studies considering EMS-PMS optimization and storage sizing.

1.2.2. Battery degradation and optimization

When retrofitting a battery in a vessel, six essential aspects must be considered. These include the price, safety, and phys-

Table 1: Other Vessel Optimization Studies

Reference	Method	Simultaneous	ES Sizing
[16]	ISCA	Yes	FC, BS
[19]	Fmincon	Yes	SC
[20]	MO-PSO	Yes	SC,BS,FW,MES
[21]	MO-DEA	Yes	BS
[22]	ISCA	No	FC,BS
[23]	NLP,MILP	No	BS
[24]	No Info	No	BS
[25]	IO	No	BS
[26]	Rule-Based	No	BS
[27]	MINLP	No	BS

FC - Fuel Cell, BS - Battery System (Chemical), SC- Super Capacitor, FW-Flywheel, Magnetic Energy Storage, MO-Multi Objective, DEA - Differential Evolution Algorithm, Interval Optimization

ical characteristics such as size and weight, as well as the battery's operating performance, encompassing capacity, power, and lifespan. The importance of each factor varies depending on the application. In the maritime industry, the capacity and power rating of the battery affects the ship's range and speed, while the lifespan and cost determine the expenses associated with installation and operation. Table 2 presents a variety of European battery suppliers with varying battery technologies, pricing, and lifespan. There are two primary battery types, nickel manganese cobalt (NMC), and lithium iron phosphate (LFP). NMC batteries offer higher specific energy but come at a higher cost, while LFP batteries have higher specific power, safety, and a longer lifespan [28],[29],[30]. Thus, it is crucial to determine which technology to use and which supplier to choose as it will dictate the constraints in the optimization model. The literature reviewed is limited to LFP and NMC batteries.

Table 2: European Battery Suppliers

Reference	Supplier	Technology
[31],[32]	EST-Floatch	NMC,LFP
[33]	Corvus Energy	NMC,LFP
[34]	Ayk Energy	LFP
[35]	EASy Marine	LFP
[36]	Echandia	LTO
[37]	Freudenberg	NMC
[38]	Lehmann Marine	LFP
[39]	Super-B	LFP
[40]	ZEM Energy	NMC
[41]	Spear Power System	NMC,Nano
[42]	XALT Energy	NMC
[43]	Praxis Autmoation	LFP

NMC - Nickel manganese cobalt, LFP - Lithium iron phosphate, LTO - Lithium titanium oxide

Battery degradation can be categorized into cycle aging and calendar aging. Cycle aging of the battery system refers to the degradation and the subsequent loss of battery capacity

due to repeated cycling of the batteries. Several studies have been performed on modeling battery systems for NMC in [44],[45] and LFP batteries in [46],[47], [48]. Several studies have been conducted on the impact of C-rate and depth of discharge (DoD) on battery lifespan. In particular, the study in [44] looked at 21 batteries and five different C-rates, while [45] examined 12 batteries and 4 C-rates. Both studies found that C-rate severely impacts NMC batteries. On the other hand, [47] and [48] analyzed three batteries with 2 C-rates and 200 batteries with 4 C-rates respectively, and concluded that for LFP batteries, the critical degradation factor is DoD and not C-rate below 4C. The authors of [46] performed a similar analysis on one battery over 4500 cycles at three different C-rates and came to similar conclusions. Considering these variations when modeling the optimization problem or determining the appropriate battery size is essential.

Calendar aging of the battery refers to the degradation that takes place irrespective of the cycling of the battery system. Research on calendar aging has been a major area of focus within the electric vehicle field. This is because their batteries remain inactive for more than 90% of the time, as indicated in [49]. The authors of this study have thoroughly analyzed the impact of cycling and calendar aging on 258 cells of two different types of NMC batteries. The authors of [50] perform tests for calendar aging with 3 different types of cells, i.e., nickel cobalt aluminum (NCA), NMC, and LFP cells. Storage temperature affected calendar aging in 16 SOC levels, but state of charge didn't consistently reduce capacity. Plateau regions were found at 20-30% SOC. NMC and NCA batteries degraded significantly at 60% SOC, while LFP batteries did so at 70%. In maritime industry, DP mode is commonly used, charging batteries to high SOC to act as backup generators during system failure.

There are several methods of incorporating battery degradation into the mathematical optimization model as shown in table 3.

Table 3: Review of existing battery degradation modeling in optimization

Reference	Method	Technique
[51]	MO-PSO	Semi-empirical & arrhenius
[52]	GA	Loss due to cycles
[53]	LP	Cost per kWh, DoD reduction
[54]	LP	Modified Shepherd Equation
[55]	MIP	Limit cycling
[56]	MINLP	DoD and Floatlife
[57]	LR	Incomplete and complete DoD
[58]	RHC	Discharge per cycle
[59]	EA	Cycles to failure
[60]	MILP	RCA

MIP - Mixed Integer Programming, LR - Linear Regression, RHC - Receding Horizon Control, RCA - Rain-flow counting algorithm

Various techniques have been suggested for precise cell/module level modeling in [51], [54], and [52]. However, obtaining the necessary parameters for these models from BESS

Table 4: Other Vessel Optimization Studies

Coefficient	Value
b_0	1040.898
b_1	3.429×10^4
b_2	1.66×10^4
b_3	4.971×10^4
b_4	-3.429×10^4
b_5	-5.504×10^5
b_6	2.803×10^6
b_7	-3.174×10^6

suppliers can be difficult, making it challenging to model for retrofitting during systems integration. In [53], a linear programming method for off-grid power systems is used, considering the cost per kWh in the optimization model and the number of cycles to failure. The authors of [55] limit cycles to the cycles to failure limit while achieving the same amount of renewable energy penetration. In [56], the authors provide a more economic solution over a 10-15 year horizon by considering BESS degradation cost and associated investment costs. The model incorporates a linear approximation of the battery's deterioration per cycle and optimizes the battery system for each time step using Receding Horizon Control (RHC) scheme. Two sources, [57] and [60], introduce the "rain-flow" cycle counting algorithm to distinguish between complete and incomplete cycles. [57] and [60] employ linear regression (LR) and piecewise modeling approaches, respectively, to prevent non-linearity and obtain more optimal solutions in BES sizing models.

1.2.3. Economic implications of diesel engine operation

To the best of the author's knowledge, there has been limited research on the economic impact of enhancing the loading percentage of diesel engine-generator sets. However, by validating the fleet maintenance records of vessel operators and referencing the work of authors in [61], additional maintenance savings can be realized through an extended time before overhauling diesel engines. This is graphically represented in figure 1 and mathematically represented in table

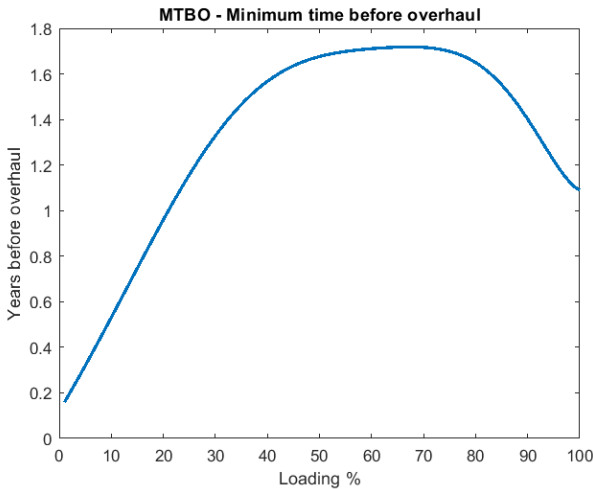


Figure 1: Minimum time before overhaul of diesel engine generator set

The function is the summation of each coefficient b_i multiplied with the loading percentage θ_i^j . The Authors of [61] claim that the costs for overhauling can be as high as 50% of the diesel engine cost, a similar ball park number was provided by the vessel owner.

1.3. Contribution

The work carried out by the authors of this work focuses on contributing towards the analysis of potential Hybrid solutions for DP-2 vessels with Li-ion batteries. The contribution of this work is achieved through the combination of the following,

1. Three different fuel price scenarios are considered for 12 different potential BESS solutions from 2 different European BESS providers
2. BESS option with different depths of discharge (DoD) have been chosen, serving as the foundation for establishing practical technical limitations of the battery system in the optimization model.
3. The operational limitations of the Diesel Engine are taken into account to save maintenance costs by extending the MTBO.
4. Incorporation of power electronic costs for the calculation of total investment costs
5. The BOOSTER considers the operation of BESS when the objective function to be minimized considers the battery degradation costs, and fuel costs with the OPEX of the system. Finally, in the outer optimization calculation, the BOOSTER incorporates the operational savings due to the reduction in the maintenance of DG. The results are discussed in comparison to the optimized results without such a consideration

2. The Vessel

The single-line diagram of the vessel is shown in figure 2. The Vessel comprises of 5 DG's that are connected to a 690 V AC bus. The AC Bus is further separated into 3 segments with the use of 2 bus tie-breakers (TB1 and TB2). DG 1 and DG2 comprise of the DG's present on the port-side (PS) of the vessel that are isolated from other DG's when TB1 is open. Whereas DG3 and DG4 are on the starboard (SB) side of the vessel that is isolated from the system when TB2 is open. DG5 is present in the middle busbar that is isolated from the system when TB1 and TB2 are open. The distribution network is connected to the main AC bus bar.

Based on the status of the Bus Tie breakers, the vessel operates in different modes. I.e, in DP mode both the tie-breakers are open, isolating the PS, SB, and the middle section with DG5. When TB1 is open and TB2 is closed, the vessel is considered to be in Non-Critical DP (NCDP01) mode. The notation NCDP10 applies when TB2 is open and TB1 is closed. When the TB1 and TB2 are closed the vessel is said to be in Auto-Mode. It is expected that there will be redundancy in the number of generators operating during DP mode, in case

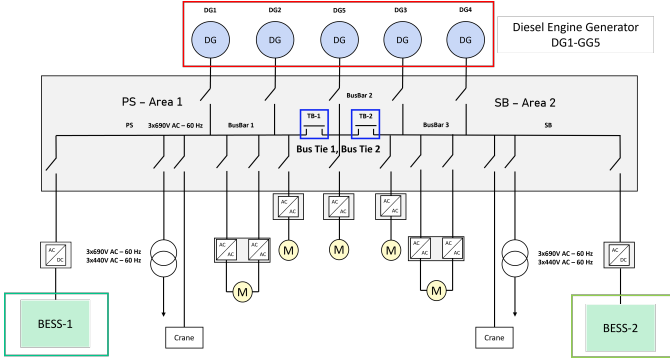


Figure 2: DP-2 Vessel

of failure.

Table 5 displays the power ratings and SFOC of the DGs. The SFOC coefficients are represented by α and β .

Table 5: Review of existing battery degradation modeling in optimization

DG Number	Power Rating (kW)	$\alpha, \frac{L}{kWh}$	$\beta, \frac{L}{h}$
1,4	1912	0.1918	33.778
2,3	2560	0.1869	54.9209
5	1530	0.2351	20.024

Dimension of α, β : $\frac{L}{kWh}, \frac{L}{h}$ respectively

This particular vessel is operational in two separate bodies of water: Taiwan and The North Sea. The recorded data for these two operational profiles span 256 (five minutes sample time) and 286 days (one minute sample time), respectively, as depicted in Figure 3.

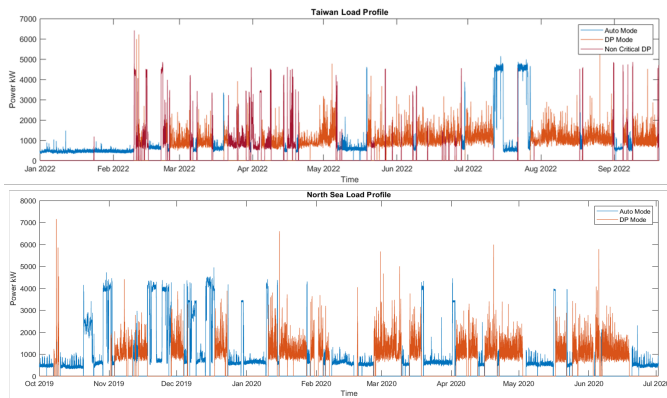


Figure 3: North Sea and Taiwan Load Profile

3. Methodology, solution space and MILP formulation

Within this segment, two sub-sections are presented. The initial sub-section 3.1 provides a detailed explanation of the methodology utilized. The second subsection defines the key performance matrix (KPM) and the solution space described initially in subsection 3.1. Finally, subsection, 3.3, outlines the

formulation of the MILP problem and other pertinent information.

3.1. Methodology

The figure 4 illustrates the methodology used. The process initiates when a request for vessel hybridization is received. The customer's concerns are identified, and a key performance matrix (KPM) is defined, consisting of a list of parameters. In this study, KPM includes return time of investment (ROI), payback period, and years of profitability, as discussed in later sections. The data is pre-processed in the next stage to ensure its usability. This is followed by developing a solution space of n ($n=12$) possible solutions. These solutions are then implemented on the vessel and their power system is optimized using MILP. After obtaining the results, they are presented in a Pareto front and discussed with the customer. The KPM is then fine-tuned according to their specific requirements. The BOOSTER is implemented for the best solution and its impact is analysed.

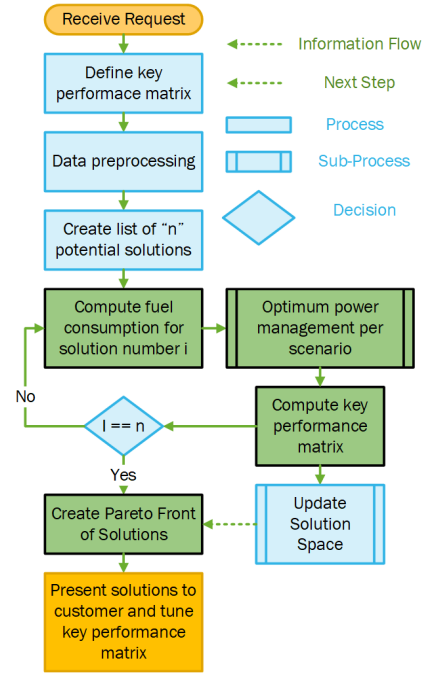


Figure 4: Methodology

3.2. KPM and solution space

The KPM used in this paper to evaluate the performance of each solution are ROI, payback period, and the years of profitability (YOP). These are explained by the equations (1)-(3).

$$ROI = \frac{Profit - Initial\ investment}{Initial\ investment} \quad (1)$$

$$Payback\ period\ (years) = \frac{Initial\ investment}{Profit\ per\ year} \quad (2)$$

$$YOP(years) = Battery\ lifetime - Payback\ period \quad (3)$$

The values of the following performance indicators are set to

$$\begin{aligned} \text{Payback Time} &\leq 6 \text{ years,} \\ \text{Years of Profitability Time} &\geq 4 \text{ years,} \\ \text{ROI} &\geq 0.9 \end{aligned}$$

Where the battery lifetime and profit are provided by equations (4) and (5). The profit is divided into two parts, fuel savings and maintenance savings.

$$\frac{\text{Total number of cycles}}{\text{Cycles per year} + \text{calendar aging(cycles equivalent)}} \quad (4)$$

$$\text{Profit (Euro)} = \text{Fuel Savings} + \text{Maintenance Saving} \quad (5)$$

The equation (6) illustrates how maintenance savings are calculated. Here, Cdg_n denotes the cost of the generator, T represents the total number of time periods, Θ_{im}^i indicates the current loading percentage of generator n at time t , and i refers to the exponential power. On the other hand, θ_{im}^i represents the optimized loading percentage of generator n at time t , where i is the exponential power. The coefficient b_i can be obtained from table 4. At any given time, the loading percentage of a generator can be calculated by dividing the power it is currently producing by its rated power. The method for calculation of fuel savings is discussed in subsection 3.3.

$$\sum_{n=1}^5 (0.5 \times Cdg_n \left(\frac{\sum_{t=1}^T (\sum_{i=1}^7 (\Theta_{im}^i - \theta_{im}^i) \times b_i)}{T} \right)) \quad (6)$$

The equations in this subsection are not included in the optimization process. Instead, they are solved using the results from the optimized PMS-EMS system outlined in subsection 3.3.

Table 6: Review of existing battery degradation modeling in optimization

No.	Capacity (Netto)	DoD (%)	Cost (Million)	Cycles	TC ($\frac{\text{Cost}}{\text{kWh}}$)
1	1530 x2	70	2.18	10000	0.05
2	1530 x2	75	2.04	7500	0.0667
3	1530 x2	80	1.91	5000	0.1
4	510 x2	70	1.16	12133	0.0659
5	510 x2	75	1.08	9166	0.0873
6	510 x2	80	1.02	6200	0.129
7	1000+175 x2	70	1.56	10000	0.0548
8	1000+175 x2	75	1.6	7500	0.0803
9	1000+175 x2	80	1.52	5000	0.121
10	1000 x1	70	0.7	10000	0.05
11	1000 x1	75	0.6	7500	0.0667
12	1000 x1	80	0.62	5000	0.1

Cost represented in Euros, cycles represent the number of cycles the can endure till 80 % of capacity remaining, TC - Throughput cost

3.3. MILP Formulation

A MILP approach is chosen, due to the availability of efficient algorithms that enable faster problem-solving compared to the MINLP method. The linearity of both the objective function and constraints allows for the use of this optimization technique. Furthermore, MILP problems have a more structured form, which is advantageous for modeling, analysis, and interpretation. The decision variables and constants used in the optimization are depicted in tables 7 and 8.

Table 7: Decision variables used

Notation	Description	Variable
u_{it}	DG_i Status	Integer
PG_{it}	DG_i Power N	Continuous
$Ebat_t$	Energy stored in battery	Continuous
Ton_{it}	Minimum on time of DG_i	Integer
$Ebatcharging_t$	Charging Energy of Battery	Continuous
Uon_{it}	DG_i Turn-On	Integer
δ_{it}	Parallel Loading of DG	Integer
M_t	Battery Charging	Integer

UC - Unit commitment

Table 8: Constants used

Notation	Description
C_i	DG_i SC
PG_{min}	DG minimum power
PG_{max}	DG max power
C_{rate}	Maximum C-rate
PG_{irated}	DG rated power (table 5)
R_i	Ramp rate of DG_i
TC	Throughput cost of BS
M	Big M integer
X	Big M integer
Max_{NC}	Maximum number of cycles
η	One way efficiency

SC - Startup cost

The subsection is further divided into 3 parts, section 3.3.1 provides the function to be minimized. The second section 3.3.2 provides the constraints defined for the system.

3.3.1. Objective Function

The objective function's goal is to minimize operational costs (OC). The operational costs are represented in the equations below

$$\text{OC} = \text{Fuel Consumption} \times \text{Fuel Price} + \text{ETC} \quad (7)$$

The fuel consumption can be split into fuel consumed due to power generation (F_{PG}) and fuel consumed due to starting up the DG (F_{SG}). The fuel consumed due to power generation is shown in equation (8),

$$F_{pg} = \text{Price of Fuel} \times \sum_{t=1}^T \left(\sum_{i=1}^{DG_n} (\alpha_i \times PG_{it} + \beta_i) \right) \times \Delta t \quad (8)$$

The F_{SG} can be linearly modelled using the big M integer method as shown in equations (9)-(11)

$$u_{it} - u_{i(t-1)} \geq 1 + 0.001 - M(1 - U_{on_{it}}) \quad (9)$$

$$u_{it} - u_{i(t-1)} \leq 1 + M(U_{on_{it}}) \quad (10)$$

$$F_{SG} = C_i \times \sum_i^T \left(\sum_{i=1}^{DG_n} (U_{on_{it}}) \right) \quad (11)$$

where C_{it} is the startup and shutdown cost of DG_i . The value of $U_{on_{it}}$ holds the value of 1 every time DG_i goes from on-state to off-state and 0 otherwise. The ETC can be modelled by adding up total amount of charging the battery goes through during each cycle / partial cycles

$$ETC = TC \times \sum_i^T E_{batching_t} \quad (12)$$

3.3.2. Constraints

The generators have upper limit (80% of rated power) and lower limit constraints (40% of rated power). These limits are based on the SFOC and diesel engine maintenance curves. The constraints are modeled as per (13), (14). The values of PG_{min} and PG_{max} are 0.4 and 08 respectively.

$$PG_{it} \geq PG_{min} \times PG_{irated} \cdot \quad (13)$$

$$PG_{it} \leq PG_{max} \times PG_{irated} \cdot \quad (14)$$

The DG's must also be associated with unit commitment (U_{it}) (ON-OFF state). These constraints are modelled through equations (15), (16)

$$PG_{it} \geq U_{it} \times PG_{irated} \times PG_{min} \quad (15)$$

$$PG_{it} \leq U_{it} \times PG_{irated} \times PG_{max} \quad (16)$$

The DG set is also constrained with ramp-up and ramp-down limits. The ramp limits are considered as 20 percent of the maximum allowable power. Turning ON and OFF the generators have no ramping limits. This is incorporated by adding an additional unit commitment term. Ramping up and ramping down limits are presented in (17),(18), respectively. In equation (17), the variable $u_{it}(t-1)$ is 0 if the DG is turned on at time t, it is similarly done in equation 18. This the conditions stated above.

$$PG_{it} - PG_{i(t-1)} \leq ((0.3 \times (1 - u_{i(t-1)})) + Ri_{rate}) \times PG_{irated}, \quad (17)$$

$$PG_{i(t-1)} - PG_{it} \leq ((0.3 \times (1 - u_{it})) + Ri_{rate}) \times PG_{irated}, \quad (18)$$

When two or more DG are ON they are parallel loaded, i.e., the load is shared between the DG's proportional to their rated power. For example, parallel loading of DG1 - DG3 are modelled as shown in equations (19)-(22).

$$u_{2t} + u_{3t} \geq 1 + 0.001 - M \times (1 - \delta_{1t}), \quad (19)$$

$$u_{2t} + u_{3t} \leq 1 + M \times \delta_{1t}, \quad (20)$$

$$\frac{PG_{3t}}{PG_{3rated}} - M \times (1 - \delta_{1t}) \leq \frac{PG_{2t}}{PG_{2rated}} \quad (21)$$

$$\frac{PG_{2t}}{PG_{2rated}} \leq \frac{PG_{3t}}{PG_{3rated}} + M \times (1 - \delta_{1t}) \quad (22)$$

When both DG1 and DG3 are switched on, the value of δ_{1t} is set to 1. In this context, the variable M is a large integer with a value of 8000. To minimize the number of constraints and variables, parallel loading of only a few selected DGs is done due to the similarities between $DG_{1,4}$ and $DG_{2,3}$, and also because the power demand in the load profiles do not require the full installed capacity on board.

The minimum ON-time ensures that the generators are on for a minimum specific duration. This is described by the equation:

$$\sum_{t=1}^{Min\ Time} (U_{it}) = Min\ Time \times Ton_i \quad \forall T. \quad (23)$$

Here Ton_i is a Boolean decision variable that ensures that the sum of the unit commitment variable U_{it} is either ON for the minimum specified duration or OFF. The value of minimum ON-time is set to 20 minutes.

The net capacity of the battery system serves as the basis for its modeling. When in Auto mode, the ESS can be represented by the combined net capacity of the BESS on both the PS and SB sides, denoted as E_{max} . The stored energy (E_{bat_t}) that can be utilized at any given time cannot exceed the net capacity of the combined BESS, and it cannot go below zero. These parameters are mathematically modeled according to equations (24),(25)

$$E_{bat_t} \geq 0 \quad (24)$$

$$E_{bat_t} \leq E_{max} \quad (25)$$

The minimum C-rate restriction ensures that the battery system charges and discharges within its technical capabilities. A single charging and discharging C-rate is considered. Charging and discharging equations are represented in equations (26) and (27) respectively.

$$E_{bat_t} - E_{bat_{t-1}} \leq C_{rate} \times E_{max} \times \Delta t, \quad (26)$$

$$E_{bat_{t-1}} - E_{bat_t} \leq C_{rate} \times E_{max} \times \Delta t. \quad (27)$$

In order to determine the number of complete or partial charge cycles a battery goes through, it is necessary to calculate the total charge energy. This can be achieved using the big M integer method, as previously done. The variable M_t is an integer that equals 1 when the battery is charging and 0 otherwise.

Equations (28)-(31) outline the formulation of the decision variable $Ebatcharging_t$, which only includes the charged values of the battery.

$$Ebatcharging_t \geq 0, \quad (28)$$

$$Ebatcharging_t \geq Ebat_t - Ebat_{t-1}, \quad (29)$$

$$Ebatcharging_t \leq 0 + M \times M_t, \quad (30)$$

$$Ebatcharging_t \leq Ebat_t - Ebat_{t-1} + M \times (1 - M_t). \quad (31)$$

The battery charging variable can only take values greater than 0 (equation (28)) and the maximum possible amount of charge (kWh) for a given time period, this is represented by equation (32).

$$Ebatcharging_t \leq C_{rate} \times E_{max} \Delta t \quad (32)$$

Based on this the number of cycles for a given time period T can be approximated/computed as

$$Number\ of\ Cycles = \frac{\sum_{t=1}^T Ebatcharging_t}{E_{max}} \quad (33)$$

Battery degradation or cycle limitation can be limited per time segment using inequality constraints as shown in the equation

$$\sum_{t=1}^T Ebatcharging_t \leq E_{max} \times Max_{NC} \quad (34)$$

The energy flow or load balance equation is modeled by considering the round trip efficiency of the system η . There are two main equations, i.e. Charging and discharging. While charging the battery it is already established that the value of $M_t = 1$ and 0 otherwise. Therefore, the energy balance equations for charging ((35),(36)) and discharging ((37),(38)) can be modeled as,

$$Ebat_t \geq Ebat_{t-1} + \eta \times \Delta t \left(\sum_{i=1}^T PG_{it} - Pdemand_t \right) - X \times (1 - M_t) \quad (35)$$

$$Ebat_t \leq Ebat_{t-1} + \eta \times \Delta t \left(\sum_{i=1}^T PG_{it} - Pdemand_t \right) + X \times (1 - M_t) \quad (36)$$

$$Ebat_t \geq Ebat_{t-1} - \frac{\Delta t \left(Pdemand_t - \sum_{i=1}^T PG_{it} \right)}{\eta} - X \times M_t \quad (37)$$

$$Ebat_t \leq Ebat_{t-1} - \frac{\Delta t \left(Pdemand_t - \sum_{i=1}^T PG_{it} \right)}{\eta} + X \times M_t \quad (38)$$

Here X is a big integer equal to 8×10^3 . A round trip efficiency of 96 % is considered, hence the value of $\eta = 0.98$.

3.4. Modes of optimization

The optimization is performed on 3 modes of operations. I.e, auto mode, non-critical DP (NCDP) mode and DP mode. The values of constants in the MILP formulation are listed for each mode in table 9.

Optimization is done separately for each mode of operation to ensure optimal performance. After each AUTO mode, the battery charge $Ebat_{it}$ is set to its maximum for use in DP and NCDP modes. In AUTO mode, power demand combines SB and PS demand, while in DP and NCDP mode, SB and PS sides are treated separately. Results are combined for each mode to produce overall optimization. The value of Δt is 1/12 (5mins) for Taiwan and Δt is 1/60 (1min) for The North Sea.

In addition to the three different optimization modes, three different fuel price scenarios are also considered as shown in table 10. Therefore finally, we obtain results for twelve different solutions as per table 6 for three different scenarios as per table 10.

Table 9: Mode dependent constants values

Notation	Auto	DP & NCDP
C_i	Rated SC	Rated SC
PG_{min}	0.4	0.2
PG_{max}	0.8	0.8
C_{rate}	Rated C-rate	0
PG_{irated}	Table 5	Table 5
Ri	0.5 NS ; NA Taiwan	0.5 NS ; NA Taiwan
TC	Table 6	NA
M	8000	8000
X	8×10^6	8×10^6
Max_{NC}	Table 6	0
η	0.98	0.98
$Pdemand_t$	PS+SB	PS,SB

NA - Not applicable where the value is 0 or the constraint is disabled. PS+SB indicates the power demand of PS + SB combined; it is separate for DP/NCDP

Table 10: table: Fuel price per scenario

Scenario Number	Percentage of time		
	450 Euro/ton	650 Euro/ton	850 Euro/ton
1	33	50	17
2	50	33	17
3	50	50	0

4. Results

The combined optimized fuel savings per solution without considering the ETC costs are shown in table 11. The optimized solutions also yield an increase in the MTBO of DG as shown in table 12 and a subsequent decrease in the running time of DG as shown in table 13. It is important to note that these results are a consequence of the MILP optimization.

Table 11: Fuel savings per scenario

Solution Number	Fuel Savings (tons)	Number of Cycles
Taiwan		
1-3	425.08	289.7
4-6	424.9	644.7
7-9	416.3	400
10-12	98.3	652.2
North Sea		
1-3	470.9	357.1
4-6	467.3	900.9
7-9	459.6	554.1
10-12	152.6	925.5

Table 12: Minimum time before overhaul (days)

Solution Number	MTBO (days)				
	DG1	DG2	DG3	DG4	DG5
Taiwan					
1-3	442.6	463.4	464.7	398.3	124.8
4-6	443.5	498.4	436.9	398.3	124.8
7-9	443.5	494.8	436.9	398.3	124.8
10-12	354.7	297.9	228.8	296.2	125.1
Current Scenario	326.9	298.8	250.4	326.2	130.4
North Sea					
1-3	486.7	603.3	619.6	414.7	151.3
4-6	505	603.1	619.2	414.7	151.3
7-9	495.2	603.0	619.2	414.7	151.3
10-12	452.1	440.1	369.7	378.4	151.1
Current Scenario	378.9	393.6	339.7	406.3	303.8

Table 13: DG running time

Solution Number	Running time (days)				
	DG1	DG2	DG3	DG4	DG5
Taiwan					
1-3	174.3	56.3	58.2	169.3	134.2
4-6	175.3	72.5	48.4	169.3	134.2
7-9	175.3	70.4	48.4	169.3	134.2
10-12	185	122.2	116.9	147.3	134.4
Current Scenario	187.4	123.5	124.4	188.5	136.1
North Sea					
1-3	145.4	57.5	34.4	127.5	115.6
4-6	168.5	67.3	21.1	127.5	115.6
7-9	155.4	77.7	21.1	127.5	115.6
10-12	140.9	111.3	87.6	79.9	115.7
Current Scenario	145.3	91.6	100.2	107.2	183.4

In order to determine the maintenance savings, we utilize equation (6). Additionally, we calculate the expected lifespan of the battery using equation (4). The results of this analysis

are presented in table 14, which shows the annualized figures. Based on the fuel prices per scenario (table 10) payback period of each solution and the ROI is calculated from equations (3),(1) and presented in table 16.

Table 14: Annualised result of fuel saving maintenance savings battery life time

Annualised average result (Taiwan + North Sea)			
Solution number	Fuel savings	Maintenance savings (Euros)	BS life time (years)
1	604.5	101863	13.6
2	604.5	101863	11.36
3	604.5	101863	8.54
4	601.5	100472	8.67
5	601.5	100472	6.99
6	601.5	100472	5.07
7	590	100706	10.64
8	590	100706	8.67
9	590	100706	6.33
10	167.5	16000	7.37
11	167.5	16000	5.85
12	167.5	16000	4.14

Table 15: Payback period

Solution number	Capital investment (Million Euros)	Payback period (years) per scenario		
		1	2	3
1	2.68	6.5	6.8	6.3
2	2.54	6.1	6.4	5.9
3	2.41	5.8	6.1	5.6
4	1.66	4.1	4.2	3.9
5	1.58	3.9	4	3.7
6	1.52	3.7	3.9	3.6
7	2.06	5.1	5.3	4.9
8	2.10	5.2	5.4	5
9	2.02	5.0	5.2	4.8
10	0.88	8.6	9	8.3
11	0.82	8.1	8.5	7.8
12	2.06	7.7	8.1	7.4

It is important to note that the payback period, years of profitability, and ROI is calculated in the outer loop of the MILP optimization. Based on these results, solution seven offers the best performance based on the KPM parameters set in section 3.2. Therefore, the booster methodology with the inclusion of ETC costs is implemented for the seventh solution for the three scenarios. Therefore, the booster methodology with the inclusion of ETC costs is implemented for the seventh solution for the three scenarios. The KPM performance of booster 7 is presented in table 17.

Figure 5 provides a visual representation of the comparison between Solution 7 with and without the BOOSTER. The BOOSTER optimization resulted in a significant increase of 21.88%, 81.63%, and 32.67% in ROI for Solution 7. This

Table 16: Years of profitability and ROI

Solution number	Years of profitability per scenario			ROI per scenario		
	1	2	3	1	2	3
1	7.1	6.8	7.3	1.26	0.99	1.19
2	5.2	5	5.4	0.98	0.76	0.93
3	2.7	2.5	2.9	0.54	0.4	0.52
4	4.6	4.4	4.8	1.31	1.03	0.85
5	3.1	3.0	3.3	0.93	0.72	0.58
6	1.4	1.2	1.5	0.43	0.31	0.27
7	5.5	5.3	5.7	1.25	0.98	1.01
8	3.5	3.3	3.6	0.77	0.59	0.64
9	1.3	1.1	1.5	0.31	0.21	0.27
10	-1.2	-1.6	-0.9	-0.17	-0.18	-0.04
11	-2.3	-2.7	-2.0	-0.33	-0.31	-0.09
12	-3.6	-4	-3.3	-0.54	-0.48	-0.15

Table 17: Solution 7 BOOSTER performance

Key performance index	Scenario number		
	1	2	3
Payback period	5.2	5.5	5.7
Years of profitability	8.3	9.6	9.7
ROI	1.6	1.78	1.5

was made possible by the EMS-PMS’s mindful operation, incorporating energy throughput cost and purchasing fuel price. Although the overall fuel savings per year were reduced in the BOOSTER method, the number of years of profitability increased, leading to a higher lifetime fuel savings. This is due to disproportional fuel savings seen in DP mode. For Scenario 1, there was a 9% increase in fuel savings, corresponding to 594.2 tons of fuel. For Scenario 2, there was a 17% increase in fuel savings, corresponding to 1039.02 tons of fuel. Lastly, for Scenario 3, there was a 21% fuel savings, corresponding to 1316 tons of fuel saved. Another benefit of extending the battery lifetime is the annual savings on maintenance costs for a greater number of years.

Figure 6 shows the operational matrix of the BESS for the given power system network. The fuel cost and power demand are taken into account when deciding whether to use the battery system. Batteries with 70% DoD have a higher operational region as compared to others. It is advisable to opt for solution 7 due to its low ETC to mitigate the risks linked with unstable fuel prices.

A Pareto front of all the solutions is provided in figure 7. However, not all these solutions are in line with the key performance indicators set in section 3.2. Therefore, on applying the KPM boundaries the solutions are presented in figure 8 and these solutions are known as lucrative solutions. The Pareto front with lucrative solutions clearly shown the increase in the ROI with the implementation of the BOOSTER. In addition,

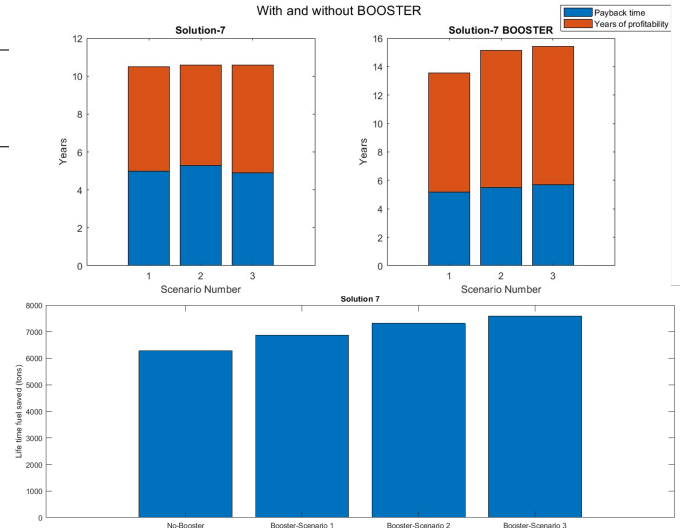


Figure 5: Payback period and years of profitability with and without BOOSTER

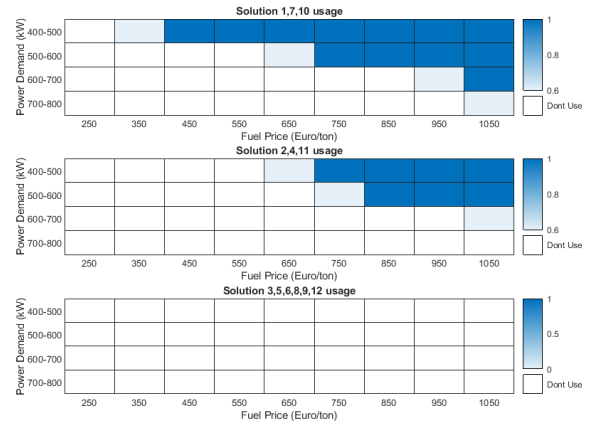


Figure 6: BESS operation matrix

high-power solution four is also feasible in the case of fuel price scenario one and scenario two. Solution two is only feasible in the case of fuel price scenario 3.

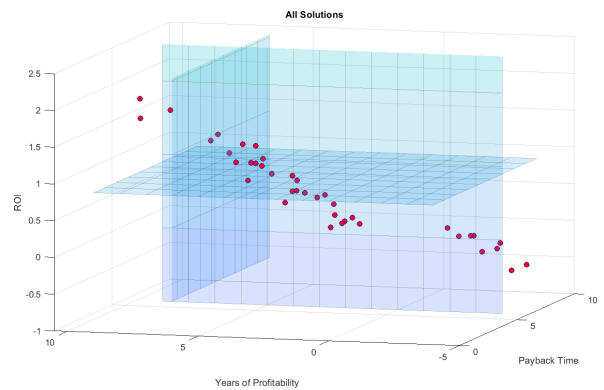


Figure 7: Pareto front of all solutions for all scenarios

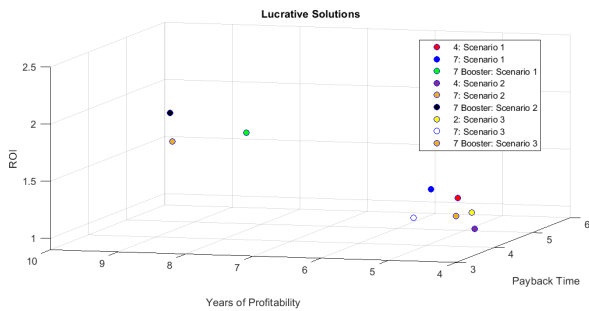


Figure 8: Pareto front only lucrative solutions

5. Conclusions

The research presented in this paper highlights the importance of a smart EMS-PMS system that incorporates the BOOSTER methodology. Rather than relying on a static average fuel price, the BOOSTER methodology considers fuel prices as a function of time, allowing the EMS-PMS to operate realistically in real-world vessel functioning. This includes knowledge of fuel prices, power requirements for various tasks, and the ETC of the battery or a decision to invest. There is also a disparity in the fuel savings per cycle observed between the results in the North Sea and Taiwan due to the higher power requirements in the North Sea. This further strengthens the need for a smarter management system.

For vessel owners, a combination of HP and HE batteries is a cost-effective solution. HE batteries are cheaper per kWh than HP batteries, but their large size to meet DP class requirements can be expensive. Therefore, the combination of HP + HE batteries is a better option as it requires a smaller battery size to meet class requirements. Additionally, the power electronic costs of the HP+HE system are the same as HP or HE systems, and lower-powered power electronic converters are cheaper than one large high-power converter. Considerable amounts of fuel savings can also be observed due to overhaul maintenance savings of the DG. This is often overlooked while calculating or estimating the feasibility of an investment.

This work has its limitations, it's important to note that the current battery system experiences a three percent calendar aging (year on year). However, research on how SOC, temperature, and cycling affect on calendar aging is limited. Proper cycling of the battery can help reduce calendar aging, which is essential for the BOOSTER solution's longevity, particularly if it will be used for more than 10 years. To ensure future developments of this model are successful, calendar aging must be considered in relation to cycles, idle time, and SOC state. The costs of implementing the BESS consider the power electronic costs and the battery system costs. Another crucial consideration in calculating investment costs is the expense of system integration. Due to the numerous factors that affect it, such as the number of hours required to upgrade the current PMS-EMS and space limitations on board, this has

been deliberately excluded it from the analysis. Additionally, the first author acknowledges their lack of knowledge regarding future interest rates, inflation rates, and fuel prices as of July 3, 2023 due to ongoing geopolitical and financial changes. As a result, these factors were excluded from calculating the payback period and ROI to maintain simplicity.

To summarize, the paper proposes a methodology for fleet owners and systems integrators to make decisions and implement investments in BESS. The results recommend implementing either solution four or solution seven and strongly advocate for the implementation of the smart BOOSTER EMS-PMS system.

References

- [1] J. Faber, S. Hanayama, S. Zhang, P. Pereda, B. Comer, International Maritime Organization, 2021.
- [2] C. D. Association, Energy efficiency considerations for dredging projects and equipment (2022).
URL <https://dredging.org/resources/ceda-publications-online/position-and-information-papers>
- [3] BELLONA, Siemens, Decarbonizing maritime transport - a study on the electrification of the european ferry fleet (Sep 2022).
URL <https://network.bellona.org/content/uploads/sites/3/2022/09/Decarbonizing-maritime-transport.pdf>
- [4] BELLONA, Siemens, Electric operation makes seven out of ten ferries more profitable – a feasibility study (2015).
- [5] S. Fang, Y. Xu, Z. Li, Z. Ding, L. Liu, H. Wang, Optimal sizing of shipboard carbon capture system for maritime greenhouse emission control, *IEEE Transactions on Industry Applications* 55 (6) (2019) 5543–5553. doi:10.1109/tia.2019.2934088.
- [6] F. Balsamo, P. De Falco, F. Mottola, M. Pagano, Power flow approach for modeling shipboard power system in presence of energy storage and energy management systems, *IEEE Transactions on Energy Conversion* 35 (4) (2020) 1944–1953. doi:10.1109/tec.2020.2997307.
- [7] S. Solem, K. Fagerholt, S. O. Erikstad, N. y. Patricksson, Optimization of diesel electric machinery system configuration in conceptual ship design, *Journal of Marine Science and Technology* 20 (3) (2015) 406–416. doi:10.1007/s00773-015-0307-4.
- [8] C. Bordin, O. Mo, Including power management strategies and load profiles in the mathematical optimization of energy storage sizing for fuel consumption reduction in maritime vessels, *Journal of Energy Storage* 23 (2019) 425–441. doi:10.1016/j.est.2019.03.021.
- [9] A. Anvari-Moghaddam, T. Dragicevic, L. Meng, B. Sun, J. M. Guerrero, Optimal planning and operation management of a ship electrical power system with energy storage system, *IECON 2016 - 42nd Annual Conference of the IEEE Industrial Electronics Society* (2016). doi:10.1109/iecon.2016.7793272.
- [10] S. Fang, Y. Xu, Z. Li, T. Zhao, H. Wang, Two-step multi-objective management of hybrid energy storage system in all-electric ship microgrids, *IEEE Transactions on Vehicular Technology* 68 (4) (2019) 3361–3373. doi:10.1109/tvt.2019.2898461.
- [11] F. D. Kanellos, G. J. Tsekouras, N. D. Hatziazgyriou, Optimal demand-side management and power generation scheduling in an all-electric ship, *IEEE Transactions on Sustainable Energy* 5 (4) (2014) 1166–1175. doi:10.1109/tste.2014.2336973.
- [12] Y. Yan, H. Zhang, Y. Long, Y. Wang, Y. Liang, X. Song, J. J. Yu, Multi-objective design optimization of combined cooling, heating and power system for cruise ship application, *Journal of Cleaner Production* 233 (2019) 264–279. doi:10.1016/j.jclepro.2019.06.047.
- [13] P. J. Chauhan, K. S. Rao, S. K. Panda, G. Wilson, X. Liu, A. K. Gupta, Fuel efficiency improvement by optimal scheduling of diesel generators using pso in offshore support vessel with dc power system architecture, *2015 IEEE PES Asia-Pacific Power and Energy Engineering Conference (APPEEC)* (2015). doi:10.1109/appeec.2015.7380963.

- [14] F. D. Kanellos, A. Anvari-Moghaddam, J. M. Guerrero, A cost-effective and emission-aware power management system for ships with integrated full electric propulsion, *Electric Power Systems Research* 150 (2017) 63–75. doi:10.1016/j.epsr.2017.05.003.
- [15] H.-M. Chin, C.-L. Su, C.-H. Liao, Estimating power pump loads and sizing generators for ship electrical load analysis, *IEEE Transactions on Industry Applications* 52 (6) (2016) 4619–4627. doi:10.1109/tia.2016.2600653.
- [16] A. Letafat, M. Rafiei, M. Sheikh, M. Afshari-Igder, M. Banaei, J. Boudjadar, M. H. Khooban, Simultaneous energy management and optimal components sizing of a zero-emission ferry boat, *Journal of Energy Storage* 28 (2020) 101215. doi:10.1016/j.est.2020.101215.
- [17] S. Karagiorgis, S. Nasiri, H. Polinder, Implementation of ship hybridisation: Sizing a hybrid crew transfer vessel considering uncertainties, *Proceedings of the International Naval Engineering Conference 16, 16th International Naval Engineering Conference and Exhibition incorporating the International Ship Control Systems Symposium, INEC/iSCSS 2022, INEC/iSCSS 2022*; Conference date: 08-11-2022 Through 10-11-2022 (2022). doi:10.24868/10643. URL <https://www.imarest.org/events/category/categories/imarest-event/international-naval-engineering-conference-and-exhibition-2022>
- [18] X. Wang, U. Shipurkar, A. Haseltalab, H. Polinder, F. Claeys, R. R. Negenborn, Sizing and control of a hybrid ship propulsion system using multi-objective double-layer optimization, *IEEE Access* 9 (2021) 72587–72601. doi:10.1109/access.2021.3080195.
- [19] S. Mashayekh, Z. Wang, L. Qi, J. Lindtjorn, T. Myklebust, Optimum sizing of energy storage for an electric ferry ship, *2012 IEEE Power and Energy Society General Meeting* (2012). doi:10.1109/pesgm.2012.6345228.
- [20] C. Yan, G. K. Venayagamoorthy, K. A. Corzine, Optimal location and sizing of energy storage modules for a smart electric ship power system, *2011 IEEE Symposium on Computational Intelligence Applications In Smart Grid (CIASG)* (2011). doi:10.1109/ciasg.2011.5953336.
- [21] S. Pang, Y. Lin, G. Liu, D. Ren, Multi-objective optimization configuration of electric energy storage capacity of electric propulsion ship, *2020 IEEE 4th Information Technology, Networking, Electronic and Automation Control Conference (ITNEC)* (2020). doi:10.1109/itnec48623.2020.9084691.
- [22] A. Letafat, M. Rafiei, M. Sheikh, M. Afshari-Igder, M. Banaei, J. Boudjadar, M. H. Khooban, Simultaneous energy management and optimal components sizing of a zero-emission ferry boat, *Journal of Energy Storage* 28 (2020) 101215. doi:https://doi.org/10.1016/j.est.2020.101215. URL <https://www.sciencedirect.com/science/article/pii/S2352152X19317177>
- [23] A. Boveri, F. Silvestro, M. Molinas, E. Skjong, Optimal sizing of energy storage systems for shipboard applications, *IEEE Transactions on Energy Conversion* 34 (2) (2019) 801–811. doi:10.1109/TEC.2018.2882147.
- [24] S.-Y. Kim, S. Choe, S. Ko, S.-K. Sul, A naval integrated power system with a battery energy storage system: Fuel efficiency, reliability, and quality of power, *IEEE Electrification Magazine* 3 (2) (2015) 22–33. doi:10.1109/MELE.2015.2413435.
- [25] S. Wen, H. Lan, Y.-Y. Hong, D. C. Yu, L. Zhang, P. Cheng, Allocation of ess by interval optimization method considering impact of ship swinging on hybrid pv/diesel ship power system, *Applied Energy* 175 (2016) 158–167. doi:https://doi.org/10.1016/j.apenergy.2016.05.003. URL <https://www.sciencedirect.com/science/article/pii/S0306261916305852>
- [26] K. Kim, K. Park, J. Lee, K. Chun, S.-H. Lee, Analysis of battery/generator hybrid container ship for co2 reduction, *IEEE Access* 6 (2018) 14537–14543. doi:10.1109/ACCESS.2018.2814635.
- [27] A. Anvari-Moghaddam, T. Dragicevic, L. Meng, B. Sun, J. M. Guerrero, Optimal planning and operation management of a ship electrical power system with energy storage system, in: *IECON 2016 - 42nd Annual Conference of the IEEE Industrial Electronics Society*, 2016, pp. 2095–2099. doi:10.1109/IECON.2016.7793272.
- [28] A. Eddahech, O. Briat, J.-M. Vinassa, Performance comparison of four lithium-ion battery technologies under calendar aging, *Energy* 84 (2015) 542–550. doi:https://doi.org/10.1016/j.energy.2015.03.019. URL <https://www.sciencedirect.com/science/article/pii/S03060544215003138>
- [29] G. Patry, A. Romagny, S. Martinet, D. Froelich, Cost modeling of lithium-ion battery cells for automotive applications, *Energy Science and Engineering* 3 (1) (2014) 71–82. doi:10.1002/ese3.47.
- [30] M. Brand, S. Gläser, J. Geder, S. Menacher, S. Obpacher, A. Jossen, D. Quinger, Electrical safety of commercial li-ion cells based on nmc and nca technology compared to lfp technology, in: *2013 World Electric Vehicle Symposium and Exhibition (EVS27)*, 2013, pp. 1–9. doi:10.1109/EVS.2013.6914893.
- [31] EST-Floattech, Octopus High Power, [Online; accessed July 3, 2023] (Mar 2023). URL <https://www.est-floattech.com/products/octopus-high-power/>
- [32] EST-Floattech, Octopus High Power, [Online; accessed July 3, 2023] (Mar 2023). URL <https://www.est-floattech.com/products/octopus-high-power/>
- [33] Corvus-Energy, Corvus Energy Products, [Online; accessed July 3, 2023] (Mar 2023). URL <https://corvusenergy.com/products/>
- [34] AYK-Energy, AYK Energy Products, [Online; accessed July 3, 2023] (Mar 2023). URL <https://www.aykenenergy.com/products>
- [35] EAS-Batteries, EAS Marine Batteries, [Online; accessed July 3, 2023] (Mar 2023). URL <https://eas-batteries.com/markets/marine>
- [36] Echandia, Echandia Energy, [Online; accessed July 3, 2023] (Mar 2023). URL <https://echandia.se/products/echandia-energy/>
- [37] Freudenberg, XPAND Battery Bank Solution, [Online; accessed July 3, 2023] (Mar 2023). URL <https://indd.adobe.com/view/7000ba20-dc96-4660-b806-93fac64233d5>
- [38] Lehmann-Marine, Lehmann Marine Cobra, [Online; accessed July 3, 2023] (Mar 2023). URL <https://www.lehmann-marine.com/en/cobra.html>
- [39] SuperB, Commercial Marine Batteries, [Online; accessed July 3, 2023] (Mar 2023). URL <https://www.super-b.com/en/lithium-marine-batteries/commercial-marine>
- [40] ZEM-Energy, Batteries ZEM Energy, [Online; accessed July 3, 2023] (Mar 2023). URL <https://www.zemenergy.com/batteries>
- [41] S. P. Systems, Technologies, [Online; accessed July 3, 2023] (Mar 2023). URL <https://marine.spearpowersystems.com/technologies/>
- [42] XALT-Energy, Xmod XALT Energy, [Online; accessed July 3, 2023] (Mar 2023). URL <https://www.xaltenergy.com/portfolio/xmod-123e/>
- [43] Praxis-Automation, Green Battery, [Online; accessed July 3, 2023] (Mar 2023). URL https://www.praxis-automation.eu/uploads/default_site/files/brochures/513.01.GreenBattery_Rev1.12.A4.pdf
- [44] Y. Gao, J. Jiang, C. Zhang, W. Zhang, Z. Ma, Y. Jiang, Lithium-ion battery aging mechanisms and life model under different charging stresses, *Journal of Power Sources* 356 (2017) 103–114. doi:10.1016/j.jpowsour.2017.04.084.
- [45] L. Somerville, J. Bareño, S. Trask, P. Jennings, A. McGordon, C. Lyness, I. Bloom, The effect of charging rate on the graphite electrode of commercial lithium-ion cells: A post-mortem study, *Journal of Power Sources* 335 (2016) 189–196. doi:10.1016/j.jpowsour.2016.10.002.
- [46] D. Anseán, M. González, J. Viera, V. García, C. Blanco, M. Valledor, Fast charging technique for high power lithium iron phosphate batteries: A cycle life analysis, *Journal of Power Sources* 239 (2013) 9–15. doi:10.1016/j.jpowsour.2013.03.044.
- [47] D. Anseán, M. Dubarry, A. Devie, B. Liaw, V. García, J. Viera, M. González, Fast charging technique for high power lifepo4 batteries: A mechanistic analysis of aging, *Journal of Power Sources* 321 (2016) 201–209. doi:10.1016/j.jpowsour.2016.04.140.
- [48] J. Wang, P. Liu, J. Hicks-Garner, E. Sherman, S. Soukiazian, M. Verbrugge, H. Tataria, J. Musser, P. Finamore, Cycle-life model for graphite-lifepo4 cells, *Journal of Power Sources* 196 (8) (2011) 3942–3948. doi:10.1016/j.jpowsour.2010.11.134.
- [49] M. Ben-Marzouk, A. Chaumond, E. Redondo-Iglesias, M. Montaru, S. Pélissier, Experimental protocols and first results of calendar and/or

- cycling aging study of lithium-ion batteries – the mobicus project, *World Electric Vehicle Journal* 8 (2) (2016) 388–397. doi:10.3390/wevj8020388.
- [50] P. Keil, S. F. Schuster, J. Wilhelm, J. Travi, A. Hauser, R. C. Karl, A. Jossen, Calendar aging of lithium-ion batteries, *Journal of The Electrochemical Society* 163 (9) (2016). doi:10.1149/2.0411609jes.
- [51] J. Ruan, B. Zhang, B. Liu, S. Wang, The multi-objective optimization of cost, energy consumption and battery degradation for fuel cell-battery hybrid electric vehicle, 2021 11th International Conference on Power, Energy and Electrical Engineering (CPEEE) (2021). doi:10.1109/cpeee51686.2021.9383396.
- [52] M. Alramlawi, P. Li, Design optimization of a residential pv-battery microgrid with a detailed battery lifetime estimation model, *IEEE Transactions on Industry Applications* 56 (2) (2020) 2020–2030. doi:10.1109/TIA.2020.2965894.
- [53] C. Bordin, H. O. Anuta, A. Crossland, I. L. Gutierrez, C. J. Dent, D. Vigo, A linear programming approach for battery degradation analysis and optimization in offgrid power systems with solar energy integration, *Renewable Energy* 101 (2017) 417–430. doi:10.1016/j.renene.2016.08.066.
- [54] A. Hamed, A. Rajabi-Ghahnavieh, Explicit degradation modelling in optimal lead-acid battery use for photovoltaic systems, *IET Generation, Transmission and Distribution* 10 (4) (2016) 1098–1106. doi:10.1049/iet-gtd.2015.0163.
- [55] S. Kato, I. Taniguchi, M. Fukui, K. Sakakibara, A battery degradation aware optimal power distribution on decentralized energy network, in: 10th IEEE International NEWCAS Conference, 2012, pp. 409–412. doi:10.1109/NEWCAS.2012.6329043.
- [56] M. Amini, A. Khorsandi, B. Vahidi, S. H. Hosseini, A. Malakmahmoudi, Optimal sizing of battery energy storage in a microgrid considering capacity degradation and replacement year, *Electric Power Systems Research* 195 (2021) 107170. doi:https://doi.org/10.1016/j.epsr.2021.107170.
URL <https://www.sciencedirect.com/science/article/pii/S0378779621001516>
- [57] X. Ke, N. Lu, C. Jin, Control and size energy storage for managing energy balance of variable generation resources, 2014 IEEE PES General Meeting — Conference and Exposition (Oct 2014). doi:10.1109/pesgm.2014.6939484.
- [58] I. N. Moghaddam, B. Chowdhury, M. Doostan, Optimal sizing and operation of battery energy storage systems connected to wind farms participating in electricity markets, *IEEE Transactions on Sustainable Energy* 10 (3) (2019) 1184–1193. doi:10.1109/TSTE.2018.2863272.
- [59] M. Belouda, A. Jaafar, B. Sareni, X. Roboam, J. Belhadj, Design methodologies for sizing a battery bank devoted to a stand-alone and electronically passive wind turbine system, *Renewable and Sustainable Energy Reviews* 60 (2016) 144–154. doi:10.1016/j.rser.2016.01.111.
- [60] J.-O. Lee, Y.-S. Kim, Novel battery degradation cost formulation for optimal scheduling of battery energy storage systems, *International Journal of Electrical Power and Energy Systems* 137 (2022) 107795. doi:10.1016/j.ijepes.2021.107795.
- [61] C. F. Matt, L. Vieira, G. Soares, P. Faria, Optimization of the operation of isolated industrial diesel stations, 6th World Congress on Structural and Multidisciplinary Optimization (05 2005).